THE PIPELINE DESIGN OF SETTLING SLURRY WITH ANALYTICAL MODELS

A Thesis

Submitted to the Graduate School of Engineering and Resource Science in Partial Fulfilment of the Requirements for the Degree of Doctor of Engineering in the Department of Geosciences, Geotechnology and Materials Engineering for Resources

Akita University

---

by

Itumeleng Tshoganetso Seitshiro

July 2013

Akita University

CONTENTS

Akita University

Akita University

Akita University

Akita University

List of Symbols

A	Cross-sectional area of pipe	[m^2]
C	Delivered concentration in volume	[−]
C_D	Drag coefficient of solid particles	[−]
D	Pipe diameter	[m]
d	Particle diameter	[m]
d_a	Arbitrary particle diameter of solids in mixed-sized slurry	[m]
d_c	Critical particle diameter	[m]
d_e	Equivalent particle diameter	[m]
d_m	Average particle diameter	[m]
f	Friction factor	[−]
g	Gravitational constant	[m/s^2]
i	Hydraulic gradient of slurry	[mAq/m]
i_s	Hydraulic gradient of solids	[mAq/m]
i_w	Hydraulic gradient of water flowing alone at the same velocity as slurry	[mAq/m]
k	Condition factor	[−]
n	Index depending on particle Reynolds number	[−]
q	In-situ concentration in volume	[−]
$\overline{q}$	Mean value of the in-situ concentrations for whole cross-section of pipe	[−]
q_a	Reference concentration at the bottom of pipes	[−]

Q	Slurry flow rate	[m^3/s]
Re	Reynolds number	[−]
Re_p	Particle Reynolds number	[−]
V_h	Hindered settling velocity of solids	[m/s]
V_m	Mean velocity of slurry flow	[m/s]
V_s ,V_w	Velocities of solids and water	[m/s]
V_t	Terminal velocity of single solid particle	[m/s]
V_*	Friction velocity	[m/s]
z	Distance from the bottom of pipe	[m]
α,β	Swanson's shape factors	[−]
δ	Specific gravity of water	[−]
δ_s	Specific gravity of solids	[−]
θ	Vertex of the geometrical plane of concentration profiles	[rad]
ρ	Density of water	[kg/m^3]
μ	Viscosity of water	[Pa·s]
λ	Coefficient of friction of water flow in pipe	[−]
φ	Head loss parameter	[−]
Ψ	Householder-Goldschmidt particle parameter	[−]
ψ	Modified Froude number	[−]
ε_m	Diffusion coefficient of water flow	[−]
γ	Specific weight of water or vehicle	[N/m^3]
γ_s	Specific weight of solids	[N/m^3]
ξ	Turbulent Schmidt number	[−]

Akita University

Main subscripts:

H	refers to heterogeneous
m	refers to average
s	refers to solids
sl	refers to slurry
v	refers to vehicle
w	refers to water

Akita University

List of Figures

Akita University

Akita University

Akita University

Akita University

Akita University

List of Tables

Akita University

CHAPTER 1

Introduction

Slurry transport technology has been employed to pump solid-liquid mixtures through pipelines in dredging operations, mining and waste-disposal applications. The technology has been developed for decades, although most research reports do not cover major pipelines over long distances. For pipeline designers it is important to determine the flow velocity and hydraulic gradient of slurry transport systems, based on the transport conditions such as pipe diameter, density and size of solids, and concentration. It is worth noting that, due to the complex behaviour of mixed-sized slurry flows, most correlations have been inclined to develop models for single size slurries. However, in commercial slurries the single-sized slurries are seldom encountered. It results in inaccurate predictions [1]. Moreover, the correlations are empirical and restricted to the range of transport conditions, as summarised by Kazanskij [2].

The object of this study is to develop analytical models of hydraulic gradient for mixed-sized slurry flows in pipes, confirming the applicability of the model with extensive experimental data.

Akita University

The study covers three main aspects: (1) database of slurry flow[3], (2) single size model of settling slurry flow [4], and (3) innovated models for mixed-sized slurry flows [5].

The researchers of pipeline design over the years have performed experimental work to analyse the behaviour of slurries. However, some experimental data are not readily available in reports, or lack crucial information of temperature, density, and viscosity of fluids. The focus of the database in chapter 2 was, therefore, aimed at developing a program for slurry transport database: the functions are; to accumulate, input, edit, sort, store the data, and display the results in graphical forms for comparison with predictions.

The information of data includes transport conditions of pipe diameter, particle size, flow velocity, concentrations, fluid temperature, and hydraulic gradient. The database consisted of the representative data of Shook et al. [6], Gillies [7], and others [3]. Also contained is experimentals from the author's laboratory, conducted in small pipelines over decades [8]-[10], as shown in Figure 1.1.

In chapter 3, an analytical model [4] was proposed and then verified by using the slurry flow database. The model was established for single size settling slurry flows through the analysis of energy components needed to transport solids in pipes. The design procedure for the optimum operation of the pipeline was also discussed, based on the parameter of specific energy consumption.

Figure 1. 1 Experimental pipeline apparatus

Akita University

Chapter 4 covered two types of innovated models [5] developed for predicting hydraulic gradient *i* of mixed-sized slurry flows. The deviations of predicted hydraulic gradients from the experimentals was highlighted when the single size model was applied to the data of multi-sized slurry flow. The innovated models depend on particle size distribution: for coarse-coarse and coarse-fine slurries. The models were confirmed by using experimental data from various slurry transport systems. Since the Wasp et al. method [11],[12] has held great promise in the prediction of *i*, comparison was drawn with the analytical models, as well as the correlation of Condolios-Chapus [13]. Limitations of all the prediction methods were also discussed.

It was concluded that, the innovated models could be useful for predicting pressure drop in practical pipeline systems. The accumulated data in the database, which covered vast transport conditions, was vital for verifying the agreement of the models with the experimentals discussed in this study.

Akita University

1.1 References

[1] Kao, D. T. Y. and Hwang, A. L. Y.: Determination of Particle Settling Velocity in Heterogeneous Suspensions and its Effects on Energy Loss Prediction in Solid-Liquid Freight Pipelines, *J. of Powder and Bulk Solids Technology*, **4**, No. 1, 31-40, (1980).

[2] Kazanskij, I.: Scale-up Effects in Hydraulic Transport Theory and Practice, Hydrotransport 5, 5th Int. Conf. on the Hydraulic Transport of Solids in Pipes, Paper B3, 47–79, (1978).

[3] Seitshiro, I. Sato, I., and Sato, H.: Development and Application of Slurry Transport Database, *J. of Min. and Metall. Inst. of Japan*, **127**, 77-81, (2011).

[4] Seitshiro, I., Sato, I., and Sato, H.: Verification and Application of Design Model for Settling Slurry Transport in Pipes, *Int. J. Soc. Mater. Eng. Resour.*, **18**, No. 2, 44-50, (2012).

[5] Seitshiro, I., Fujii, S., Yokoyama, N., Sato, I., and Sato, H.: Data Analysis of Mixed-sized Flows in Pipes with Innovated Models, Proc. MMIJ Fall Meeting, 161-162, (2012).

[6] Shook, C. A., Schriek, W., Smith, L. G., Haas, D. B., and Husband, W. H. W.: Experimental Studies on the Transport of Sands in Liquids of Varying Properties in 2 and 4 inch Pipelines, Saskatchewan Research Council, **VI**, 1-158, (1973).

[7] Gillies, R. G.: PhD Thesis, University of Saskatchewan, (1993).

Akita University

[8] Sato, H., and Kawahara, M.: Critical Deposit Velocity of Slurry Flow Including Single-size Solid Particles, Proc. 2nd Int. Conf. on Multiphase Flow, Kyoto, Japan, 23-30, (1995).

[9] Sato, H., Takemura, S., Takamatsu, H., and Cui, Y.: An Improved Wasp Method for the Hydraulic Gradient of Slurry Flow with Size Distribution in a Horizontal Pipe, Proc. ASME Fluids Engng. Div. Summer Meeting FEDSM'97, Vancouver, British Columbia, Canada, 1-11, (1997).

[10] Sato, H., Cui, Y., Sugimoto, F., and Tozawa, Y.: Determination of Distributions of Velocity and Concentration of Solids in a Horizontal Slurry Pipeline with a Digital Video Camera System, *Int. Society of Offshore and Polar Engineers*, **1**, 44-51, (1998).

[11] Wasp, E.J., Kenny, J.P., and Gandhi, R.L.: Solid-Liquid Flow, Slurry Pipeline Transportation, Trans Tech Publications, Germany, pp. 93–95, (1977).

[12] Liu, H.: Pipeline Engineering, Lewis Publishers, USA, pp. 131-143, (2003).

[13] Condolios, E. and Chapus, E. E.: Designing Solids-Handling Pipelines, Solids Pipelines 2, *J. Chemical Eng.*, 131-138, (1963).

Akita University

CHAPTER 2

Development and Application of Slurry Transport Database

The transport conditions of solids in slurry pipelines cause the flow behaviours of solid-liquid mixture to vary strongly and affect the hydraulic gradients in the systems. Since any transport design correlations of slurry should be confirmed by a wide range of data, experiments in various flow regimes have been carried out over the years by many researchers.

The study in this chapter was, therefore, aimed at developing a slurry transport database for accumulation, input, editing, sorting, storing of the data available in literature, and displaying the results in graphical form for comparison. A basic processing procedure was adopted for the design of the program. Then a flowchart of the program was developed to analyse the data. The flowchart consisted of three sub-flowcharts: (1) input – for the input and addition of data; (2) editing – for modifying and standardising all the data into the Excel CSV form; and (3) graph displays of the data – for comparison of the researchers' data on log-log graphs. In addition Star graphs were used to give a clear description of the transport conditions for the researchers. The database was applied for the verification of proposed correlations.

Akita University

2.1 Introduction

For the slurry flow, the optimal transport conditions of pipe diameter, flow velocity, concentration, and pressure loss should be evaluated based on transport capacity and maximum particle diameter. The selection of the pump and the pipeline design, and evaluation of the operating cost were pushed forward by using these parameters. The proposed correlations of pressure loss in reported studies do not guarantee the accuracy of the prediction in the practical pipelines of mixed-sized slurries.

Although the pressure loss analysis by numerical simulations gives a clear calculation result, it has not widely been used in the practical design; there is limited access to special software and super computers, as pointed out by Jacobs [1]. Whether designers estimate the hydraulic gradient with the correlations or the numerical simulations, the evaluated results should be confirmed with the specific experimental data of slurry pipelines. It is expected that the data of the slurry transport conducted by universities and institutes would be extensive. However, there is great concern about the scatter and loss of the data when the researchers leave or the slurry transport project reaches completion. Therefore, it is valuable to accumulate, arrange, and store the data in the unified form.

This chapter explores the database software developed not only for the input, editing, and sorting of the data, but also the comparison of

Akita University

calculated results with graphical representations. In addition, the data characterisation of researchers was performed. The database is vital for the verification of proposed correlations.

2.2 The Database Management System (DBMS)

In this study, the database management system (DBMS) was constructed by using the Visual Basic 6.0. The programming language was developed for computers operating on Microsoft Windows. Before Visual Basic was created, the popular languages for developing a user-friendly interface were C or C++. However, they usually require lots of lines of code. Microsoft introduced Visual Basic in 1991, as Visual Basic 1.0 [2]. It became instantly popular as a programming language that was easy to learn and quickly led to a whole new generation of Windows software. Over the years, Microsoft continued to enhance the Visual Basic, with support systems for databases, ActiveX, COM, and so on.

The two main features that make Visual Basic different from the traditional programming tools are:

(1) The user interface is literally drawn-similar to using the paint program.

(2) The sequence of procedures is controlled by users' initiated actions, e.g., buttons, text boxes, and others, instead of a predetermined sequence of procedures in the program.

Akita University

Once the interface has been drawn on the monitor, the programming can start. However, unlike traditional languages where a program runs sequentially from first line of commands to bottom, Visual Basic actions respond to specific instructions written by the programmer. These instructions, which are called Event Procedures in Visual Basic, instructs the program to respond to different events, such as mouse click. A combination of the Event Procedures is called a “Project” in Visual Basic. In summary, designing a Visual Basic application follows this procedure:

a) Design the window for the user.

b) Choose the events for the window, which the project will follow.

c) Write the instructions, which the events will follow.

A complete set of these steps should enable the program to run according to the event procedures, which makes it more user-friendly.

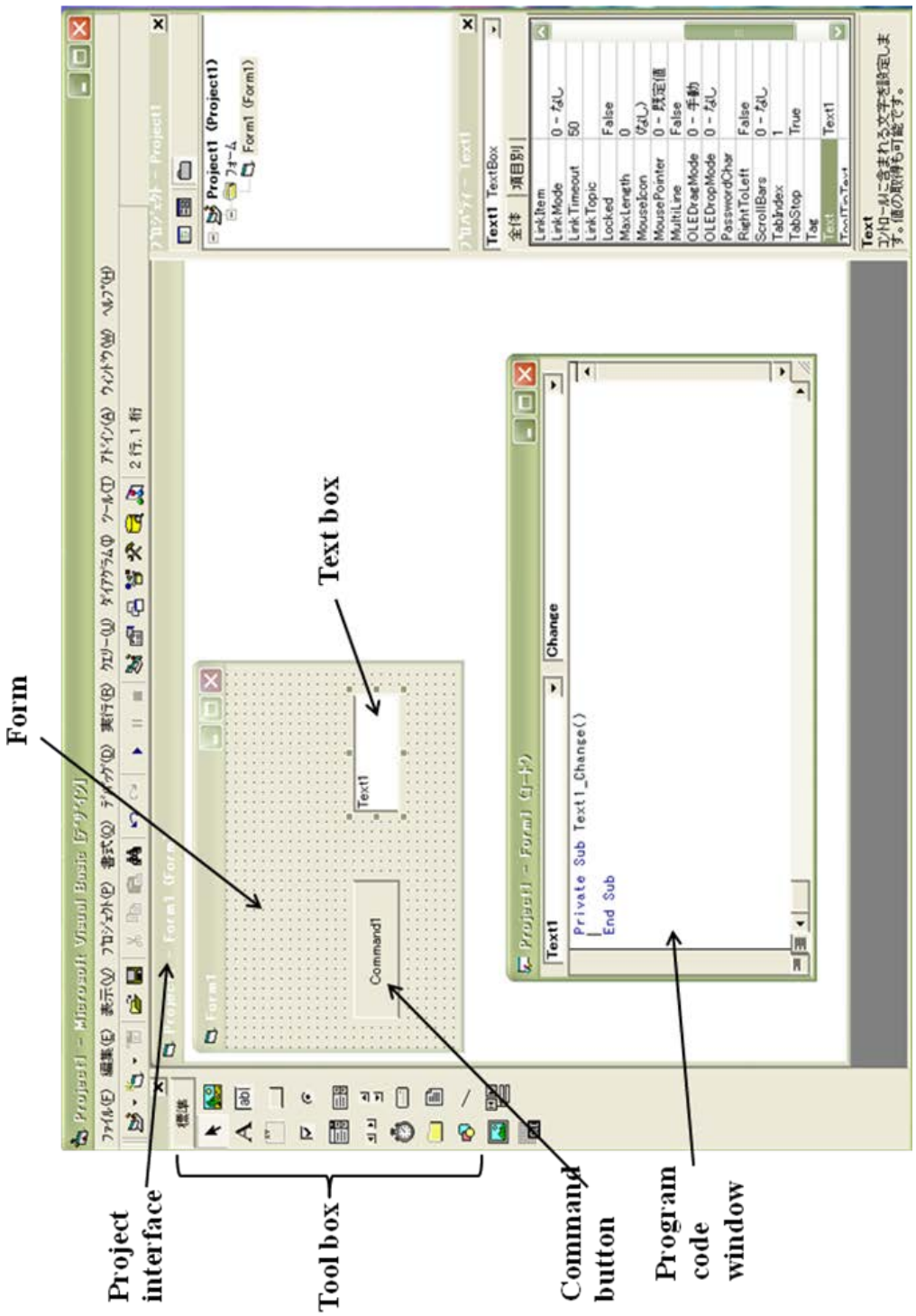

Figure 2. 1 Concept of Visual Basic 6.0

Akita University

2.3 The Design and Functions of the Database Management System

2.3.1 Designs of the database program

The database management system (DBMS) in this study was constructed by using the Visual Basic 2006, which allows users not only to input data and edit existing information with the Microsoft Windows operating system, but also represent graphical display on the monitor. The most important aspect of database design is not its complexity but instead a simple design, which includes careful focus on the information, that is most important. The design must also allow for accurate data capture and effective long term management and maintenance of the data, as indicated by Morris [3]. The design for the slurry transport database was based on the warehouse-type of database, which puts emphasis on the function of storing data in unified format.

2.3.2 Database items entry

For constructing the database in this study the data was accumulated, input by Microsoft Excel, and saved in the CSV format (*.csv). Although experimental conditions of slurry transport have been thoroughly described in some reports, there is often little known about the information: water temperature, settling velocity of the solids, friction factor of the pipe, and so on. Moreover, all data should be

Akita University

unified by unit conversion, especially for U.S. customary units. The items used to characterise transport conditions are shown in Table 2. 1.

Table 2. 1 Input items for transport conditions in the database

Cell	Input item	Representation	Units
A	No.	Data number	(–)
B	Data name	Researcher's name	(–)
C	Sample	Kinds of solids	(–)
D	D	Pipe diameter	(cm)
E	d	Particle diameter	(cm)
F	κ	Area index	(–)
G	V_t	Terminal velocity	(cm/s)
H	C_d	Drag coefficient	(–)
I	ρ_s	Solids density	(g/cm^3)
J	t	Temperature	(°C)
K	V_m	Mean flow velocity	(cm/s)
L	C	Delivered concentration	(%)
M	i	Hydraulic gradient of slurry flow	(mmAq/m)
N	Index	Index of λ-Re Equation	(–)
O	Coefficient	Coefficient of λ-Re Equation	(–)

Akita University

2.3.3 Functions of the database program

For constructing the database the data was accumulated through three kinds of methods: 1) making standardised table of Excel format transferred from original data, 2) digitisation of plotted experimental results in graphical form by using scanning software, 3) direct input of data into the unique table on the monitor. According to the design concept by Fujita [4], the simplified processing procedure of the data is required, as shown in Figure 2.2.

Figure 2.3 shows the flowchart of the DBMS, which was used for collection of programs that enables users to create and maintain the database, as defined by Elmasri and Navathe [5]. It consists of three subprograms: input, editing, and graphical representation of the data. The subflowchart of the direct input function in the database program is shown in Figure 2.4.

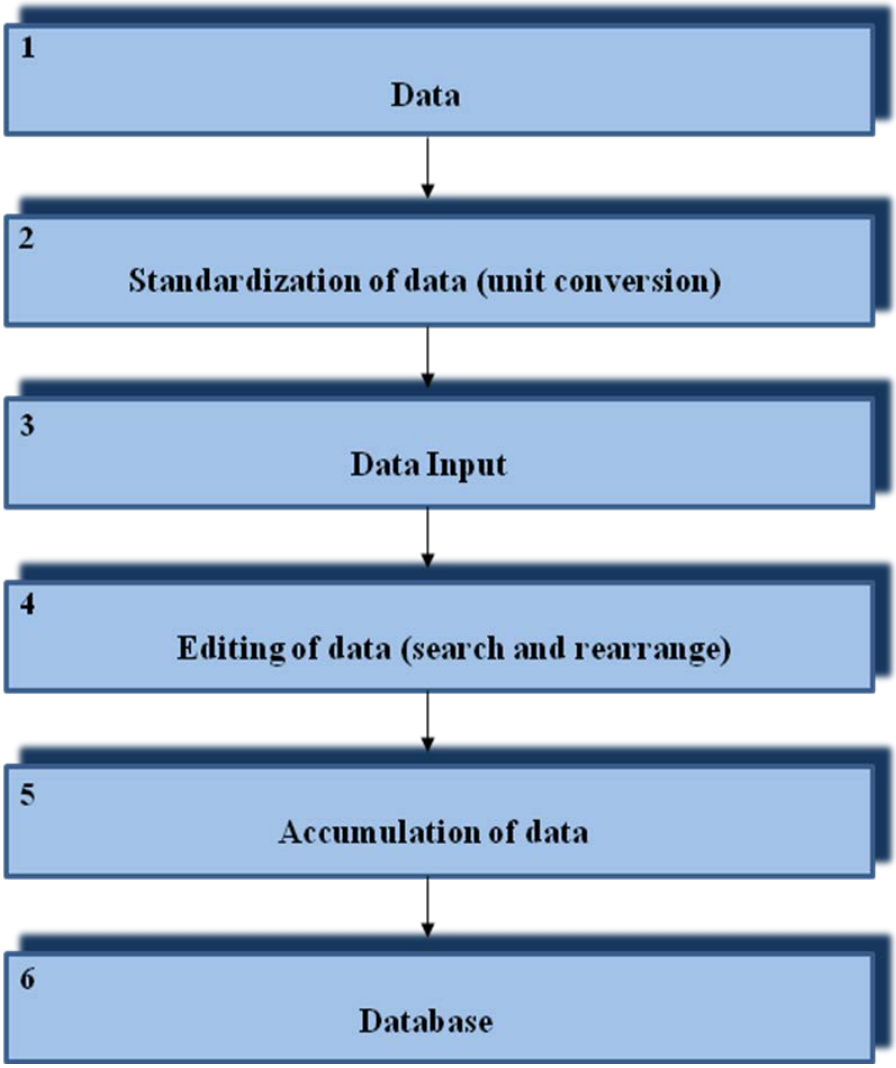

Figure 2. 2 Data processing procedure

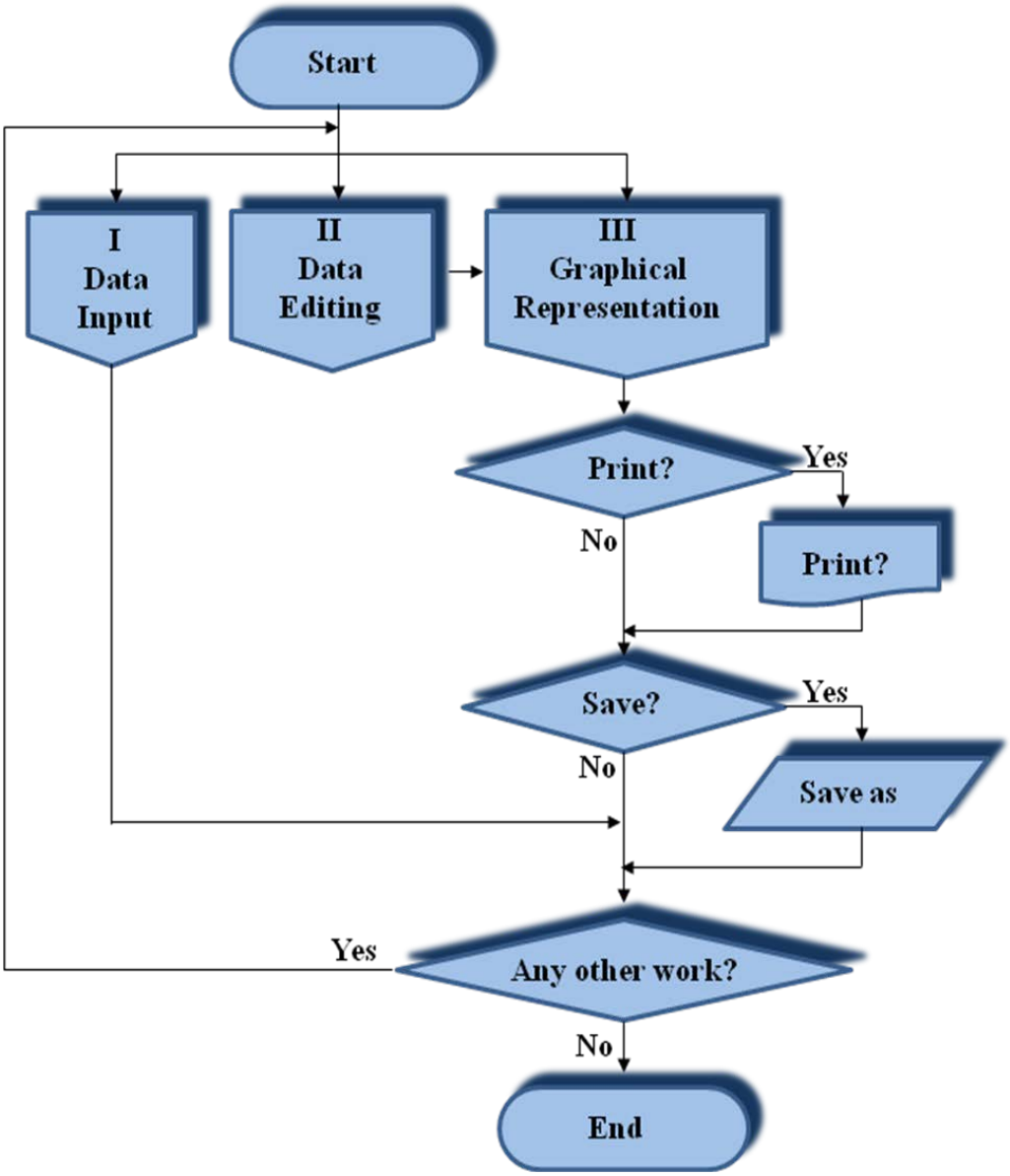

Figure 2. 3 Flowchart of database management system

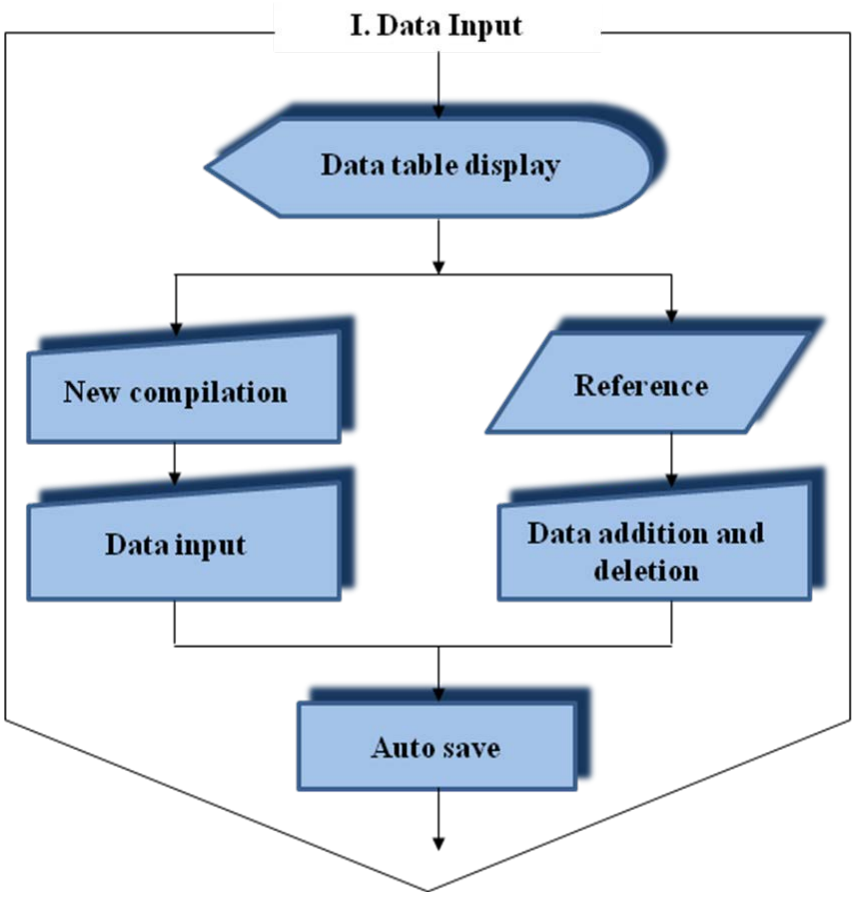

Figure 2. 4 Subflowchart of input and addition of data

Akita University

The input of data table shown in Figure 2.5 ensures accurate processing for users. The vital information against the input should be limited for the design of slurry transport. The data box of “Area Index” on the table represents the shape factor [6] of irregular-shaped solids: sand, 1.5; coal, 1.7 [7]. The data boxes of “Index of Power Function” and “Coefficient of Power Function” were prepared for representing the λ-Re relationship in the form of power function, which indicates the characteristics of water flow in pipelines. The input procedure on the monitor should be repeated until no further experimental data remain. If some reports lack the experimental results of water flowing alone, the λ-Re relationship should be approximated by the Blasius equation;

$$\lambda = 0.3164\, Re^{-1/4} \qquad \text{.....(2. 1)}$$

Table 2.2 shows a sample of the standardized data in the Excel CSV format used to construct the database. Each data item in the three thousand more data used in this study has 66 different types of data elements stored in it. That is, for each of the 10 items of data in the sample, they correspond with records of 13 data elements that include; data name, researcher name, pipe diameter, particle diameter, and others.

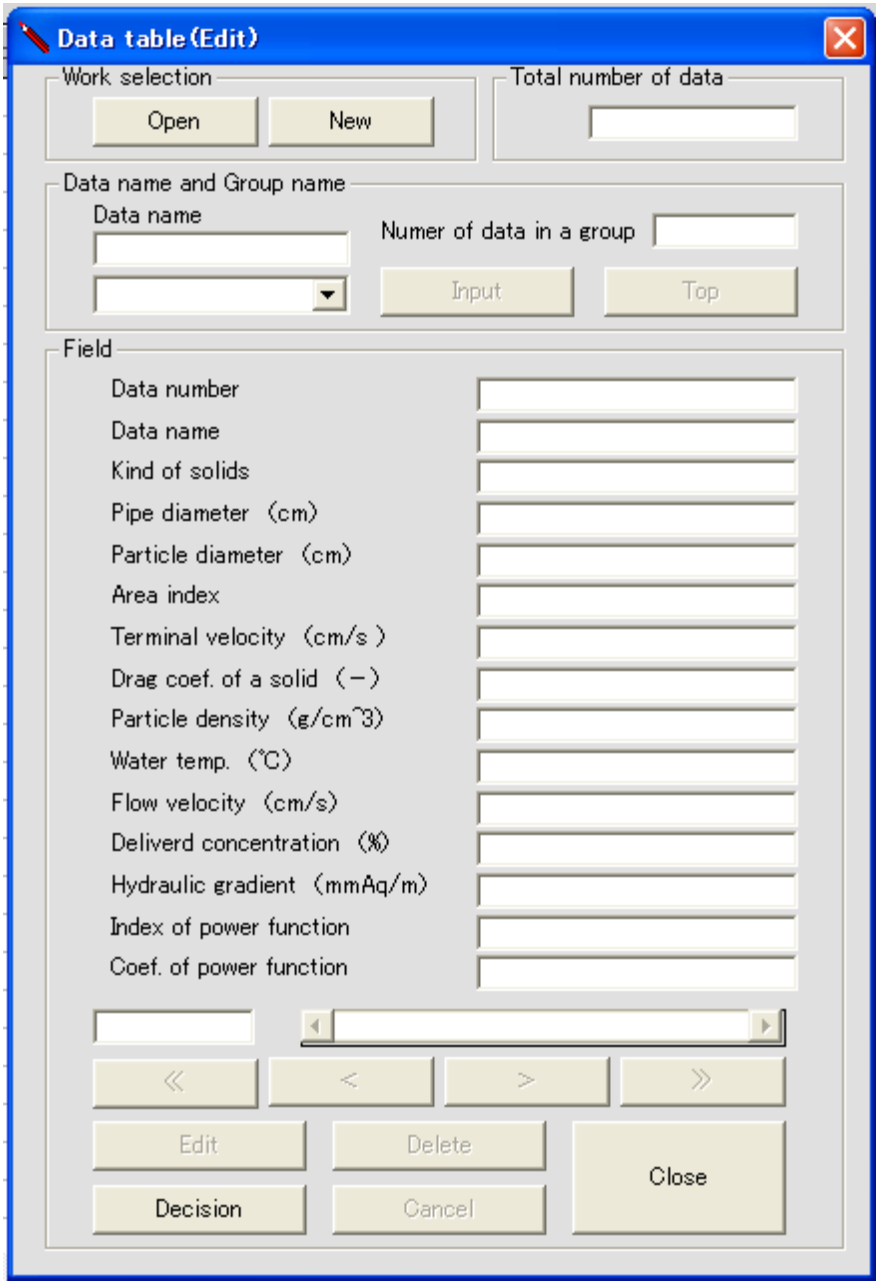

Figure 2. 5 Data Table (Edit) for input of data

Table 2. 2: A sample of the data items and elements in the database

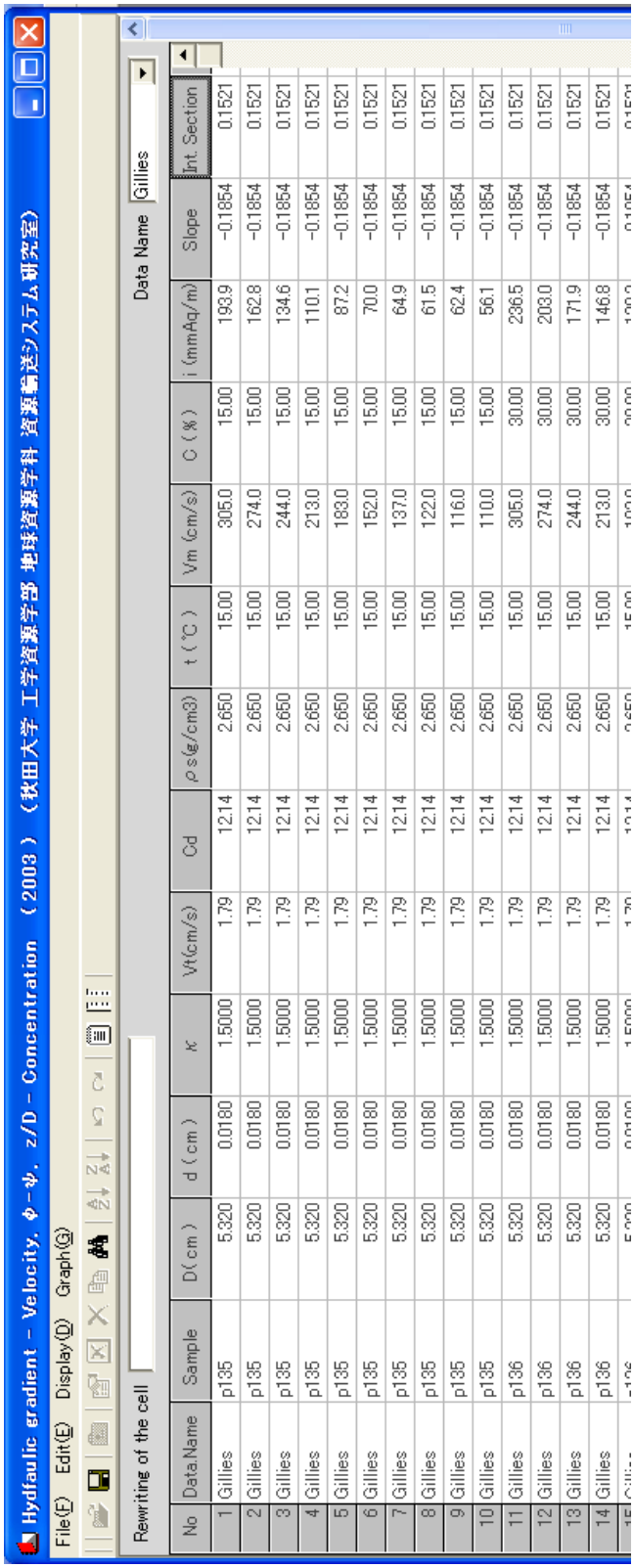

No	Data Name	Sample	D(cm)	d (cm)	κ	Vt(cm/s)	Cd	ρs(g/cm3)	t (℃)	Vm (cm/s)	C (%)	i (mmAq/m)	Slope	Int. Section
1	Gillies	p135	5.320	0.0180	1.5000	1.79	12.14	2.650	15.00	305.0	15.00	193.9	-0.1854	0.1521
2	Gillies	p135	5.320	0.0180	1.5000	1.79	12.14	2.650	15.00	274.0	15.00	162.8	-0.1854	0.1521
3	Gillies	p135	5.320	0.0180	1.5000	1.79	12.14	2.650	15.00	244.0	15.00	134.6	-0.1854	0.1521
4	Gillies	p135	5.320	0.0180	1.5000	1.79	12.14	2.650	15.00	213.0	15.00	110.1	-0.1854	0.1521
5	Gillies	p135	5.320	0.0180	1.5000	1.79	12.14	2.650	15.00	183.0	15.00	87.2	-0.1854	0.1521
6	Gillies	p135	5.320	0.0180	1.5000	1.79	12.14	2.650	15.00	152.0	15.00	70.0	-0.1854	0.1521
7	Gillies	p135	5.320	0.0180	1.5000	1.79	12.14	2.650	15.00	137.0	15.00	64.9	-0.1854	0.1521
8	Gillies	p135	5.320	0.0180	1.5000	1.79	12.14	2.650	15.00	122.0	15.00	61.5	-0.1854	0.1521
9	Gillies	p135	5.320	0.0180	1.5000	1.79	12.14	2.650	15.00	116.0	15.00	62.4	-0.1854	0.1521
10	Gillies	p135	5.320	0.0180	1.5000	1.79	12.14	2.650	15.00	110.0	15.00	56.1	-0.1854	0.1521
11	Gillies	p136	5.320	0.0180	1.5000	1.79	12.14	2.650	15.00	305.0	30.00	236.5	-0.1854	0.1521
12	Gillies	p136	5.320	0.0180	1.5000	1.79	12.14	2.650	15.00	274.0	30.00	203.0	-0.1854	0.1521
13	Gillies	p136	5.320	0.0180	1.5000	1.79	12.14	2.650	15.00	244.0	30.00	171.9	-0.1854	0.1521
14	Gillies	p136	5.320	0.0180	1.5000	1.79	12.14	2.650	15.00	213.0	30.00	146.8	-0.1854	0.1521

Akita University

Figure 2.6 shows the subflowchart of the editing function, which enables to search for specified range of data, make rearrangement, and save it after accessing reference files in the CSV format. If some ranges of flow velocity, delivered concentration, and hydraulic gradient could be fixed on the specification table of the monitor screen, as shown in Figure 2.7, the only data required would be displayed. It should be further developed such that particle size, pipe diameter and researcher's name can be specified on the table.

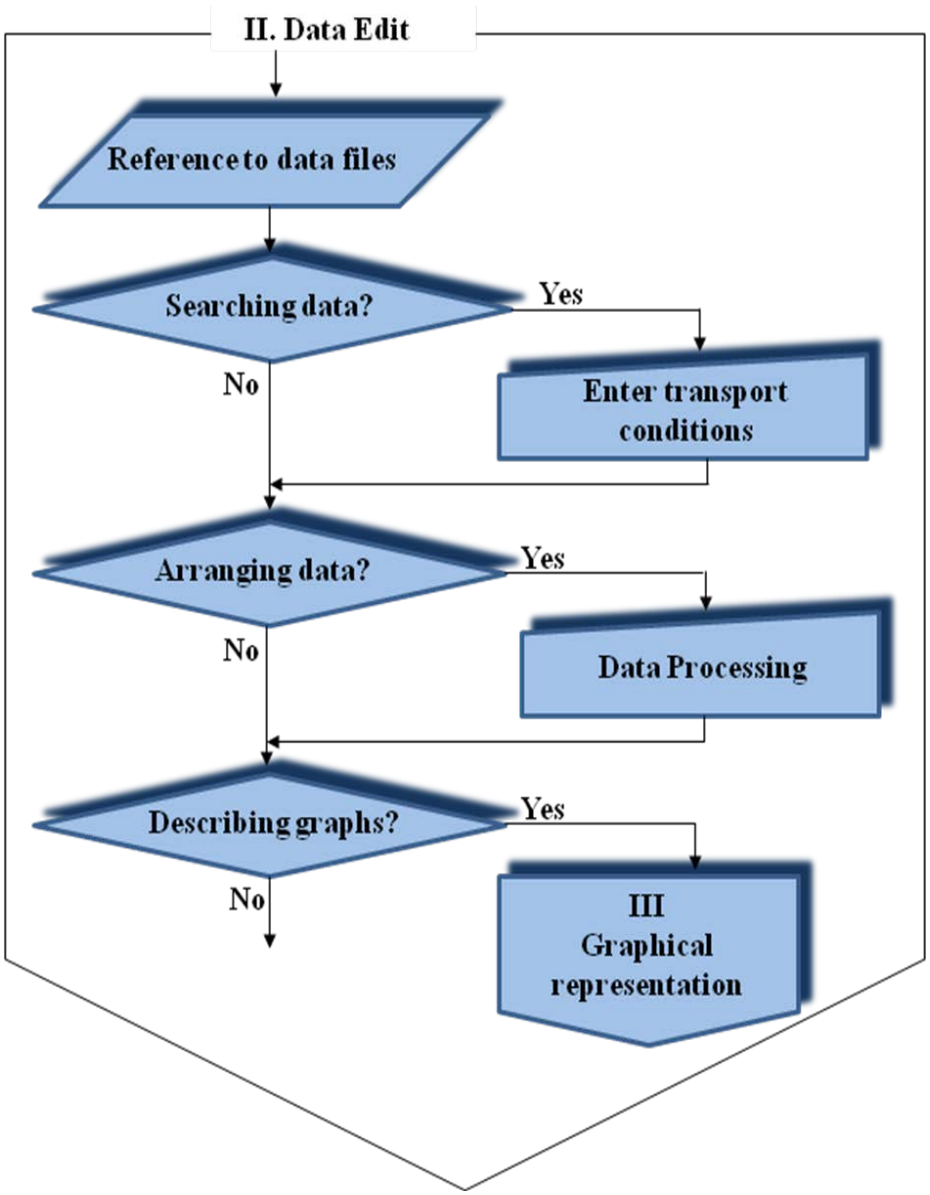

Figure 2. 6 Data edit sub flowchart

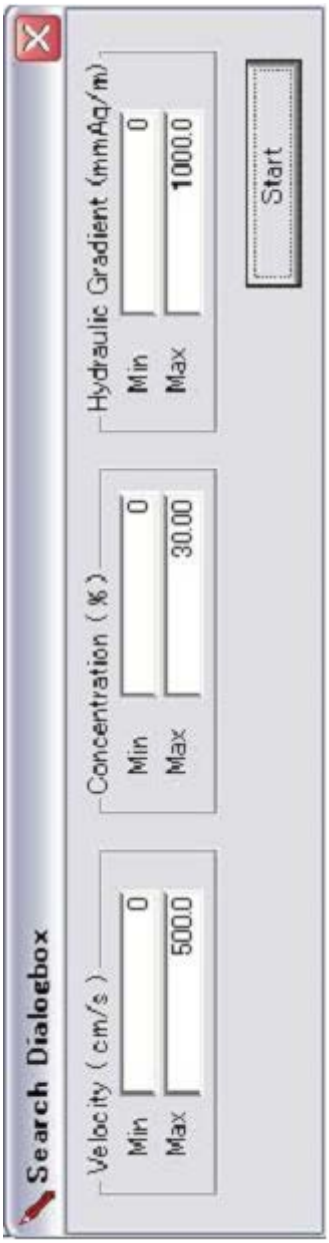

Figure 2. 7 Range specification table

Akita University

For graphical representation of results calculated with desired correlations of hydraulic gradient, two options are prepared as shown in Figure 2.8. If the process box of “reference to data files” is chosen, the ranges of transport conditions should be entered by mouse operations. It allows, on the monitor, the confirmation of the reference data in the files before the calculating hydraulic gradients. The calculated results could be automatically registered and displayed in graphs. The other option of the subflowchart has possibility to compare calculated results with the saved data, and display the graphs on the monitor. When the Durand-Condolios correlation [8];

$$\varphi = 82\psi^{-1.5} \qquad \text{….....(2.2)}$$

where;

$$\phi = \frac{i - i_w}{i_w \cdot C} \qquad \text{….....(2.3)}$$

and

$$\psi = \frac{V_m{}^2 \sqrt{C_{Dm}}}{gD(\delta - 1)} \qquad \text{….....(2.4)}$$

is selected, the results give typical i-V_m and φ-ψ relationships with the experimental data, as shown in Figures 2. 9 and 2. 10.

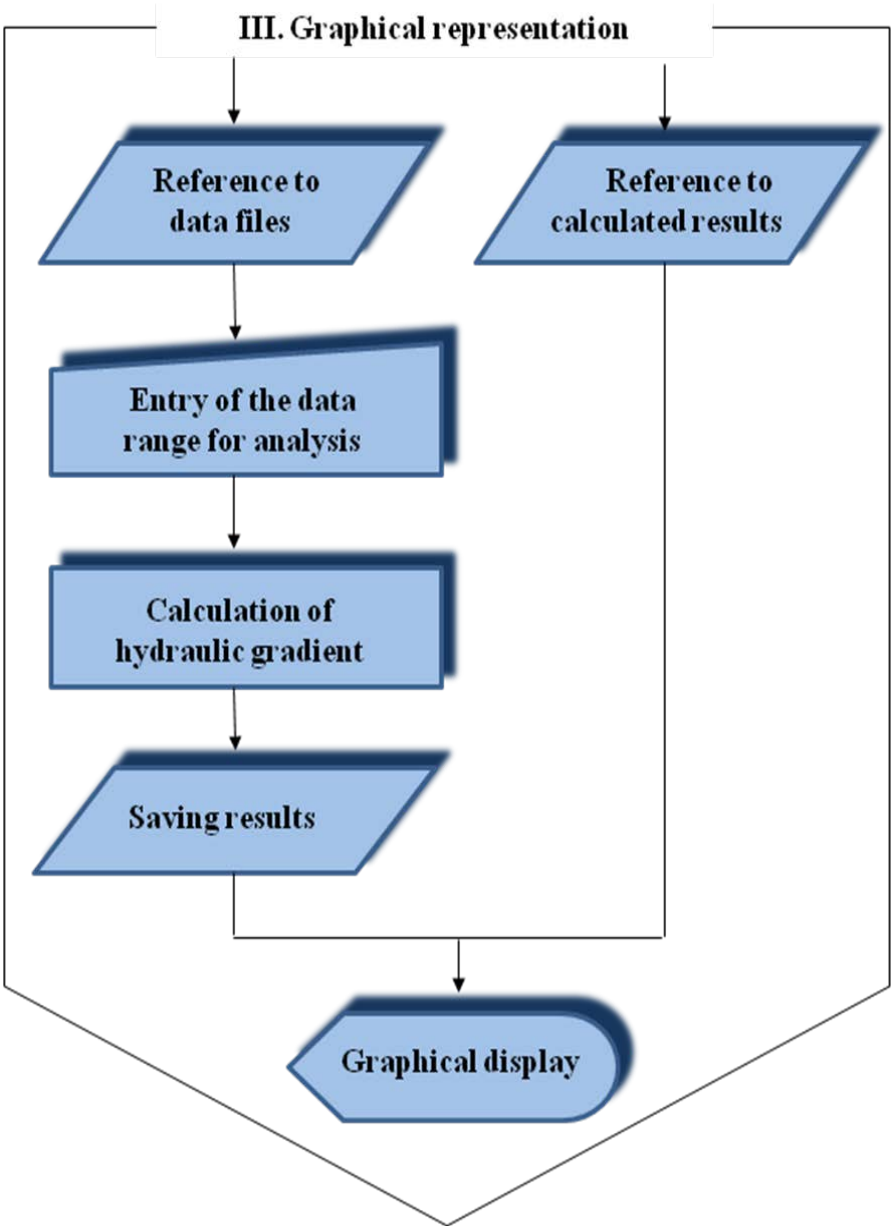

Figure 2. 8 Sub flowchart of graphical representation

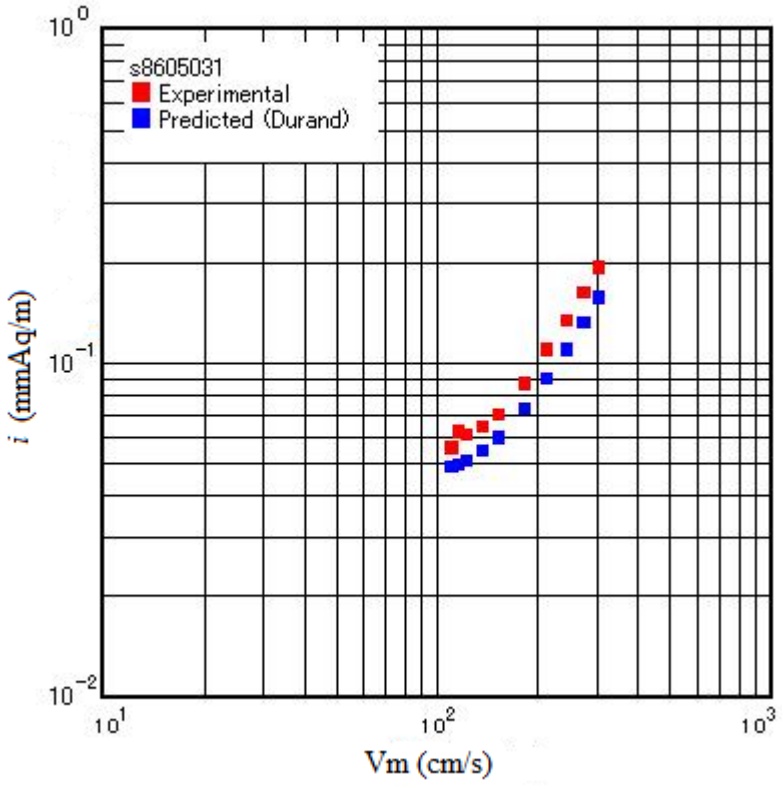

Figure 2. 9 Representative *i* - *Vm* graph

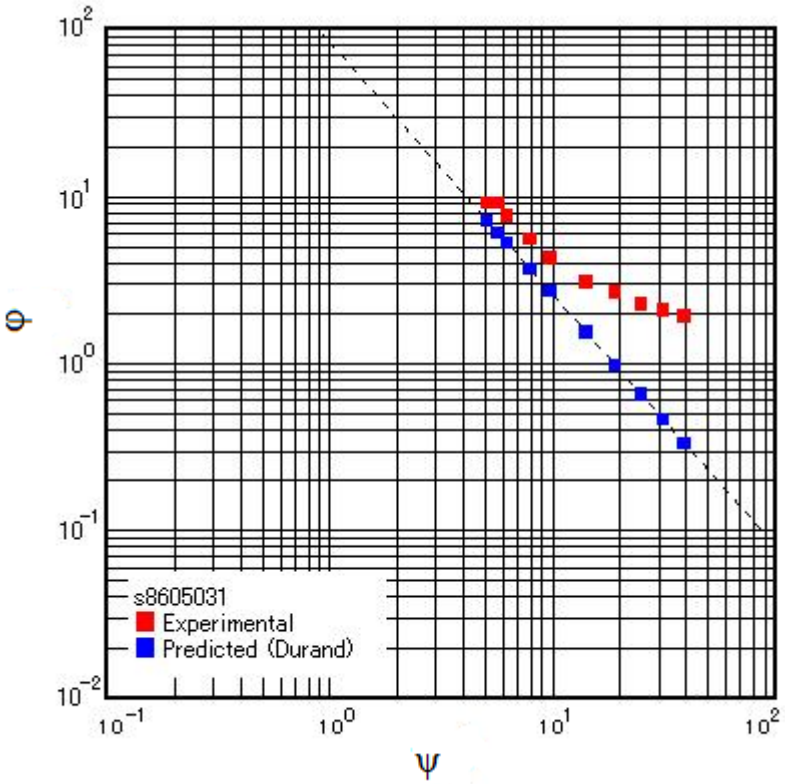

Figure 2. 10 Representative φ - ψ graph

Akita University

2.4 Characterisation of researchers' data

In this study, over 3,000 data including experimental results by Sato et al. [6], [9] – [11] were collected from references with clear transport conditions. The ranges of experimental data of slurry flow are dependent on the researchers. The database for verifying correlations of hydraulic gradient should cover wide range of data. The characterisations of researchers' data could be summarised in the form of star graphs.

2.4.1 Laboratory data

Some of the experimental data used in the database were collected from the Hydraulic Transport laboratory in Akita University. The experiments have been conducted over decades since the 1960s.

(1) Experimental conditions

Although a 1-inch transparent perspex pipeline is currently being used, previous tests were carried out in various sizes of pipes. The diameters ranged from 25.9 mm to 31. 9 mm. Depending on the scope of research, the solids of diameters in the range of 0.565 mm to 2.18 mm were used: sand solids; average specific gravity of 2.65, and Bakelite (polyoxybenzyl methylene glycol anhydride); specific gravity 1.4. The slurries were transported through the pipeline at mean velocities between

Akita University

70 cm/s ~ 230 cm/s, and lower volume concentrations of C < 20 %. Transport conditions of the experiments are summarised in Table 2.3.

(2) Experimental apparatus and procedure

The pipeline system used in the experiment was closed loop system, as shown in Figure 1.1. In this system, discharged slurry is returned back into the mixing tank and re-circulated.

The experimental equipment was consists of the following items:

Pipeline: A transparent acrylic resin pipe of 25.7 m length, set on the support approximately 1.85 m above the ground. The diameter of the pipe was 26.15 mm. The inlet and outlet of pipeline loops fed and discharged slurry in a mixing tank of 260 L capacity in volume.

Pump: A Warman pump (a centrifugal-type pump) was installed in the experimental system. The pump, shown in Figure 2.11, can handle slurry in capacities of 0.02 – 14 m^3/min, with solids size range of 20 mm – 200 mm. It was driven by a 3.7 kW electric motor. The rotational speed of maximum 2,200 revolutions per minute was adjusted from a control panel to change flow velocities.

Table 2. 3 Summarised transport conditions of laboratory data

Pipe diameter, D (mm)	Solids	Particle diameter, d (mm)	Specific gravity, δ_s (-)	Mean flow velocity, V_m (cm/s)	Concentration, C (%)	Temperature, t (°C)
25.9	Sand	0.565	2.69	84.5 ~153.4	1.27 ~ 20.24	7.32 ~ 12.87
		1.205	2.66	86.7 ~ 152.5		
		1.705	2.66	88.5 ~ 209.7		
26.15	Sand	0.855	2.65	93.9 ~ 219.1	1.7 ~ 9.86	9.3 ~ 20
		1.205				
		1.705				
	Bakelite	1.705	1.40	73.2 ~ 236.5	2.06 ~ 7.48	13.6 ~ 29.6
		2.18		58.5 ~ 210.3	0.55 ~ 9.98	14.0 ~ 28.4
27.92	Sand	0.855	2.67	97.1 ~ 169.6	1.13 ~ 12.5	8 ~ 25
		1.205	2.66			
		1.705	2.66			
31.9	Sand	0.565	2.69	89 ~ 188	0.61 ~ 10.24	6.8 ~ 13.7

Figure 2. 11 Warman pump

Akita University

Flowmeter: An electromagnetic flowmeter with detector and converter provide continuous flow measurements. In this system, the devices were installed separately and connected together via cables, as shown in Figure 2.12. The converter changes electromotive force from the detector to the flow rate signal. The flowmeter sends the instantaneous flow rate to the computer.

Pressure transducer: Pressure drops were measured by using a Differential Pressure Transducer, as shown in Figure 2.13. The pressure transducer functions at the output power of 1.5 mV/V ±1 %, and can be operated in the safe temperature range of -10 to 70 °C. It can make highly accurate measurements in the maximum range of 10 kPa working pressure with maximum line pressure of 2.94 MPa (30 kg/cm^2). The distance of pressure taps on the pipe, connected to the transducer, was 1.89 m. The taps were also used for bleeding air bubbles before commencing the experiments.

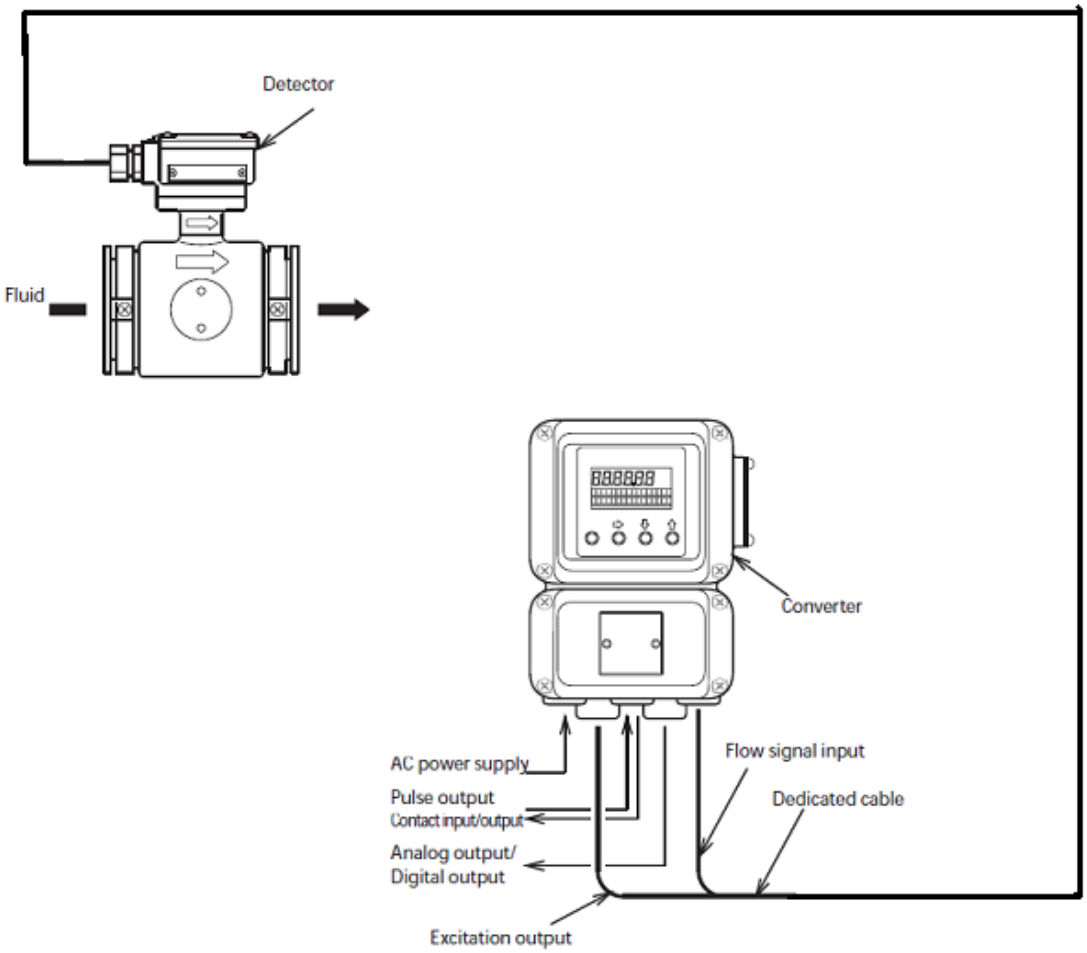

Figure 2. 12 Schematic composition of devices for measurement of flow rate (Referred: Yamatake Corporation Smart Electromagnetic Flowmeter Converter User's Manual)

Akita University

Figure 2. 13 Differential pressure transducer

Akita University

The experimental procedure followed the following steps:

(a) After ensuring that the water outlet valve is closed, water is filled into the mixing tank. Then the pump is started to circulate the water through pipeline. By using the flow control panel, the velocity of the water was increased to the maximum, usually 200 m/s. The flow was monitored until the velocity and pressure drop readings reached stabilised values on the computer.

(b) By using the pressure taps located on the return loop, the air bubbles were removed from the pipeline. Water measurements were then recorded.

(c) Solids, which have previously been weighed, were fed into the mixing tank gradually to avoid chocking the pipeline.

(d) The flow velocity was manually controlled and varied by the dial on the flow control panel. After the desired velocity was selected and slurry flow stabilised, mean velocity and hydraulic gradient measurements displayed on the monitor were recorded.

(e) The weighing cage was used to collect discharged solids. The solids were weighed and used to determine delivered concentration of solids.

(f) The process was repeated at regular time intervals of approximately 10 ~ 15 minutes, in the velocity range of 70 cm/s to 200 cm/s. Water temperature was monitored and measured throughout the experiment, although no attempt is made to control it.

Akita University

(g) At the section, which is located between the pressure taps on the pipeline, flow behaviour was observed. With the sections illuminated by LED lamps, a digital camera was installed to take images of flow patterns and a video camera captured the movement of solids. During the experiments with sand, the water was regularly replaced with fresh water to ensure visibility at the observation section.

2.4.2 Other researchers' data

2.4.2.1 Shook et al. data

The main purpose of the experimental research of Shook et al. was to investigate the effects of the factors – size distribution of particles and the physical properties of the fluid, which are frequently neglected by many researchers – on flow behaviour. In the experiment, silica sands were used as a representative of fine solids instead of the commonly-used clay, which has a tendency of non-Newtonian behaviour. Fluid properties, terminal velocity and drag coefficient were considered, as well as discussion of Newtonian carrier fluids of high viscosity.

(1) Experimental conditions

Two pipeline systems of 2-inch-closed and 4-inch-open loops were used in the Shook et al. research. The 2-inch loop tests were carried out after experiments in the open loop showed air bubbles for viscosity $\mu > 2$

Akita University

cp. Three different kinds of carrier fluids of water, Ethylene glycol, and Brine were used.

However, only experimental data restricted to carrier fluid of water was analysed. The temperature of the fluids was varied between 10, 21.11 and 60 °C for the 2-inch pipeline, but kept at a constant 21.11 °C for tests in the 4-inch pipeline. The range of solids size of density ρ = 2.65 g/cm^3 was from 0.198 mm to 0.54 mm. The slurries in both pipelines were conveyed at mean velocities of about 55.8 cm/s to 378 cm/s. Measurements were made in a wide range of concentrations of 5, 12, 18, 24, 30, 36, and 42 % for closed loop, but varied from 1.4 % to 41.9 % for the open loop pipeline. Summary of the experimental data can be shown in Table 2.4.

(2) Experimental apparatus and procedure

The experiment procedure for both the 2-inch and 4-inch sand tests were as follows.

Solids were fed into a mixing tank, and conveyed through the pipe by a centrifugal pump. A magnetic flow meter was equipped to measure flow velocity. For pressure drop readings, a Meriam U-tube manometer was applied. Different sampling methods were used for determination of particle distribution and concentration. For the 2-inch pipe, a circular instrument of half-inch diameter and 1-inch long was used to sample half a kilogram of slurry approximately on the return leg. Diversion method was used in the 4-inch pipe, where 0.91 kg of slurry was collected as it

Akita University

drained back into the mixing tank. Fluid viscosity was measured with a Brookfield viscometer – a rotational viscometer that uses torque to determine viscosity. Extensive information can be found in the cited report of Shook et el. [12]

Table 2. 4 Summary of experimental conditions for data of Shook et al.

Carrier	Water								Ethylene glycol				Brine ($CaCl_2$)	
D (mm)	52.5 Closed loop				103.0 Open loop				52.5 Closed loop				52.5 Closed loop	
d (mm)	0.198	0.21	0.297	0.54	0.198	0.21	0.54		0.198		0.54		0.198	0.54
V_m (cm/s)	55.8 ~ 361.5	72.5 ~ 361.5	74.4 ~ 339.5	70.4 ~ 378.0	86.0 ~ 338.9	129.9 ~ 367.6	166.7 ~ 374.0		33.2 ~ 339.5				55.8 ~ 339.5	47.9 ~ 333.1
C (%)	5 ~ 42				1.4 ~ 41.9				5 ~ 42		5 ~ 30		5 ~ 42	
t (°C)	60.0	21.1		10.0	21.1				63.3	32.2	21.1	10.0	21.1	

Akita University

2.4.2.2 Gillies data

(1) Experimental conditions

Experiments by Gillies were carried out in pipelines of varying sizes of 2, 6, 10, and 20 inches. In the 2-inch pipeline, three different sizes of particles were used, with diameters of; 0.18, 0.29, and 0.55 mm. The slurries were transported at mean velocities of 110 cm/s ~ 305 cm/s, in the concentration of 15 % ~ 45 %. The tests were conducted with water of temperature of 15 °C.

For tests in the 6-inch pipe, only solids of 0.19 mm diameter were used at a concentration of 16 %. Water temperature was kept at 13 °C, and the slurry transported at a relatively small range of velocities of 213 cm/s to 296 cm/s.

Two different solids with particle sizes of 0.29 mm and 0.55 mm were used in the experiments of the 10-inch pipe system. The slurries were carried through the pipe at high velocities of 288 cm/s ~ 530 cm/s. Transport behaviours were studied with three different concentrations of between 15 % to 34 % at carrier fluid temperatures of 15 °C and 40 °C.

In the largest pipe, the slurry consisted of solids of diameter 0.18 mm and water with the temperature varied from 9 °C to 15 °C. The concentration range was from 10 % to 34 %. Mean velocities was increased from 265 cm/s to 428 cm/s.

Akita University

(2) Experimental apparatus and procedure

All the four pipelines used in the research were closed loop systems, where the slurry inlet and discharge points are at the same place. The experiment procedures for the loops was as follows:

(a) After filling the pipeline with water, a chilled or heated mixture of water and ethylene glycol was used to determine a desirable operating temperature. Then at steady flow, measurements of pressure difference and flow rate were made by using a differential pressure transducer and an electromagnetic flow meter respectively.

(b) At the feed tank, solids were added to the system, and the centrifugal pump was used to transport the slurry through the pipe – different kind of pump for each of the loops.

(c) After stable flow and selected temperatures are reached, pressure drop and flow rate were measured. Reducing the flow rate gradually, the same measurements were determined until the onset of solids deposition at the bottom of the pipe.

(d) Electric probes were used to measure the solids velocities and a gamma ray-density meter determined in-situ concentrations during transport. A transparent observation section was equipped to determine flow regimes as well as monitor the presence of air bubbles.

(e) Last, samples were taken to determine viscosity and density of the carrier fluid.

Akita University

During the experiment process, a digital converter and a personal computer were used to compile and store data. The summary of transport conditions of Gillies [13] from the study are shown in Table 2.5.

Akita University

Table 2. 5 Summary of transport conditions of Gillies

Pipe diameter, D (mm)	Particle diameter, d (mm)	Mean flow velocity, V_m (cm/s)	Concentration, C (%)	Temperature, t (°C)
53.2	0.18	110 ~ 305	15, 30, 45	15
	0.29	122 ~ 305	15, 30 ,40	
	0.55	116 ~ 305	15, 30, 40	
159	0.19	213 ~ 296	16	13
263.1	0.29	288 ~ 527	16, 25, 34	15, 40
	0.55	312 ~ 520	16, 25, 30	
495.3	0.18	265 ~ 428	10, 15, 20,25, 29, 34	9, 10, 13, 14,15

Akita University

2.4.2.3 Acaroglu data

(1) Experimental conditions

Acaroglu conducted experiments using medium size particles of 2 mm and 2.78 mm in a pipeline of diameter 7.6 cm. The solids were transported through the pipe in concentrations of between 1 % ~ 15 %, with high velocities ranges of approximately 160 cm/s to 650 cm/s. The experiment can be characterised as a medium particle, and high speed slurry transport.

(2) Experimental apparatus and procedure

The pipeline in the research consisted of aluminium pipes joined with couplings, as well as a 1.85 m observation section all in a closed-loop system. The sands were transported in different flow patterns: suspension flow with the 2 mm solids, and stationary bed flow with the 2.78 mm solids. The experimental procedures were as follows:

(a) By using the solid-liquid slurry-type pump, water was injected into the pipeline at a low velocity. Then air bubbles are removed by bleeding the water-air manometers.

(b) Sand solids were fed into the pipe at a constant rate to ensure uniform flow of the solids.

(c) After solids feeding was completed, and stable flow was achieved, water valves were closed to take measurements of parameters: pressure drop by using the manometers; mean velocities by a pitot-static tube for suspension flow, and brine

Akita University

injection method for flows with stationary bed; and concentration profiles by a the sampler.

(d) The measurements were repeated with gradual change of mean velocity.

(e) After each sampling, the materials were re-fed into the system, except at the end of the experiment.

Throughout the experiment, water temperature was monitored and recorded. For further details on the exact experimental procedures and the measurements, refer to the report of Acaroglu [14]. Representative transport conditions used in this chapter are summarised in Table 2.6.

Akita University

Table 2. 6 Representative transport conditions of Acaroglu

Pipe diameter, D (mm)	76	
Particle diameter, d (mm)	2	2.78
Mean flow velocity, V_m (cm/s)	191 ~ 594	159 ~ 650
Concentration, C (%)	0.94 ~ 14.57	0.97 ~ 8.49
Temperature, t (° C)	20 ~ 35	19 ~ 21

Akita University

2.4.2.4 Daniel data

(1) Experimental conditions

Medium sized sand solids were used in the experiment by Daniel [15]. The solids of diameters ranging from 0.15 mm to 1.57 mm were conveyed in a small pipeline with inside diameter of 5.08 cm, at velocities of roughly 70 cm/s for the larger solids to 370 cm/s for the finer solids. Flow behaviours were monitored at lower concentrations of up to maximum 26 %.

(2) Experimental apparatus and procedure

The approximately 27 m long-closed loop horizontal pipeline consisted of two sections: a 2-inch diameter-steel inlet pipe section, and a 1-by-4 inches (height x width) rectangular return section. A 45.7 cm long-transparent section was set on the circular loop for observing flow behaviour. An Allis Chalmers rubber lined pump, a centrifugal-type pump, was used to circulate the sand slurry at fixed speeds. To vary flow velocity, a portion of the slurry was diverted on the return flow section.

Two different pressure transducers were equipped to measure pressure differences: an inclined Mercury-manometer for the 2-inch section, and a Meriam fluid manometer for the rectangular section. Concentrations were determined by using a gamma-ray density gauge. Summary of the transport conditions are shown in Table 2.7, and full experimental procedures can be referred to the report of Daniel [15].

Table 2. 7 Summary of transport conditions of Daniel

Pipe diameter, D (mm)	Particle diameter, d (mm)	Mean flow velocity, V_m (cm/s)	Concentration, C (%)	Temperature, t (°C)
50.8	0.15	32.0 ~ 370.3	1.2 ~ 21.8	24.2
	0.35	59.1 ~ 381.3	2.5 ~ 25.7	22.5
	0.53	15.2 ~ 378.9	1.3 ~ 26.1	23.9
	1.03	32.3 ~ 89.6	0.5 ~ 7.8	23.3
	1.57	39.9 ~ 68.9	2.9 ~ 12.3	23.6

Akita University

2.4.2.5 Yagi et al. data

(1) Experimental conditions

The data was extracted from two different sized transparent pipeline systems. For the experiment in the 155-mm-diameter pipe, sand particles of the size 0.91 mm and specific gravity 2.63 were transported. Flow velocities were changed from 173.4 cm/s to maximum values of 546.0 cm/s. Concentration was varied between 5 % to 25 % at regular intervals.

Coarser solids, gravel of 8 mm size were carried in the pipe of diameter 80 mm. Similarly, at higher range of velocities between 107.2 cm/s ~ 519.6 cm/s the slurries were transported through the pipe at concentrations of 5 % ~ 30 %. For both pipeline systems, water temperature was kept at 20 °C.

(2) Experimental apparatus and procedure

The brief explanation of the experimental apparatus and procedure is as follows:

(a) As in most experiments, first, measurements of flow rate and pressure drop were made with water flowing alone to determine the characteristics of pipes.

(b) A gate was opened to discharge the sand solids into the pipeline after measuring the weight and volume. The solids were sucked up the pipeline through a centrifugal pump, and the flow rate

Akita University

was adjusted by controlling the revolutions of the pump. Solids concentration was controlled by opening the feeder gate.

(c) Once the slurry flow stabilised: the in-situ concentration was determined by density-meter; Mercury-manometer pressure transducer measured pressure drop; and flow rate recorded by using the magnetic flow-meter. Simultaneously, delivered concentration was also evaluated.

The data was collated and stored in computer files. The experimental results were analysed to discuss the behaviour of slurry flows containing coarse particles. A summary of transport conditions of the representative data is shown in Table 2.8. Refer to Yagi et al. [16] for details of the researchers' work.

Akita University

Table 2. 8 Summary of transport conditions of representative data of Yagi et al.

Pipe diameter, D (mm)	80.7	155.2
Particle diameter, d (mm)	8.0	0.91
Specific gravity of solids, δ_s (-)	2.61	2.63
Mean Velocity, V_m (cm/s)	107.2 ~ 519.6	173.4 ~ 546.0
Concentration, C (%)	5 ~ 30	5 ~ 25
Temperature, t (°C)	20	

Akita University

2.4.2.6 Link et al. data

(1) Experimental conditions

Tests in the report were carried out in different sizes of steel pipelines with solids of wide size distributions, to investigate the behaviour of water and oil shale mixtures flows. Although the researchers used both horizontal and vertical pipelines, only data from the horizontal pipes was contributed to the database.

Different types of oil shale were transported: Shale-A (residue) at 0.03 mm, Shale-B (residue) at 0.03 mm ~ 0.48 mm, and Shale-C (raw) at a wide range of coarse solids of approximately 2 mm ~ 12 mm. In pipelines of 6-inch and 8-inch, solids were conveyed at varying velocities of maximums 540 cm/s and 390 cm/s respectively. Solids concentrations were measured in weight percentage, varied with each type of shale: 45 % ~ 62 % for Shale-A, up to 45 % for Shale-B, and maximum of 32 % for Shale-C. Recorded water temperatures were in the range of 20 °C to 38 °C. Table 2.9 shows the summarised transport conditions.

(2) Experimental apparatus and procedure

The research was developed by Link et al. on behalf of U.S. Bureau of Mines, to handle tailings disposal from mining of oil shale. High carbon content-fine waste, lower carbon content-coarse waste, and unrefined oil shale were transported in the pipelines. Both the pipelines used the recirculating loop systems, with a centrifugal pump used to

Akita University

carry the solids. Slurry temperature was not controlled, although its effect on the fluid density and viscosity was observed. The flow diversion sampling method was employed to determine delivered concentrations, which were compared with feed concentrations. For each test run, pressure losses were measured at various velocities to correlate head loss against velocity. Full contents of the research can be found in U.S. Bureau of Mines Report [17].

Table 2. 9 Summarised transport conditions of Link et al.

Pipe diameter, D \ Sample		Shale A	Shale B	Shale C
6-inch	Particle diameter, d (mm)	0.03	0.03 / 0.04 / 0.48	2.06 ~ 12.7
	Specific gravity, δ_s (-)	2.602	2.670	2.183
	Mean flow velocity, V_m (cm/s)	27.43 ~ 539.50	54.86 ~ 499.87	54.86 ~ 469.39
	Concentration, C (%)	22.8 ~ 34.28	8.12 / 14.46 / 15.4	0.12 ~ 28.19
	Temperature, t (°C)	30.4 / 30.8	21.9 ~ 28	14.3 ~ 37.7
8-inch	Particle diameter, d (mm)	0.03	0.04 / 0.11 / 0.15	12.7
	Specific gravity, δ_s (-)	2.602	2.670	2.183
	Mean flow velocity, V_m (cm/s)	45.72 ~ 390.14	79.25 ~ 381.0	155.45 ~ 368.81
	Concentration, C (%)	19.74 ~ 36.86	11.38 / 14.77 / 21.14	5.8 ~ 14.65
	Temperature, t (°C)	31.2 ~ 36.4	25.9 ~ 28.9	23.1 ~ 30.5

Akita University

2.4.3 Summary of researchers' data

The researchers' data [6], [9], [11] – [16] can also be characterised through the star graphs with six axes as shown in Figures 2. 14. A Star graph is generally constructed by choosing one special vertex, then drawing edges from the special vertex to every other vertex of the power *n*. In this study a Star S_7 was applied, with the six outer vertices representing the following: particle size as *d* (cm); pipe diameter, *D* (cm); flow velocity, V_m (cm/s); delivered concentration, *C* (%); hydraulic gradient, *i* (mmAq/m); and water temperature, *t* (°C).

The features of researchers' data can be summarised as follows:

(1) Sato et al.: Low concentration, low-speed transport

(2) Shook et al.: High concentrations, fine particle transport

(3) Gillies: Fine particle, high concentration, high-speed transport

(4) Acaroglu: Medium particle, low concentration, high-speed transport

(5) Daniel: Medium particle, medium-speed transport

(6) Yagi et al.: Coarse particle, high-speed transport

(7) Link et al.: High concentration, high-speed transport

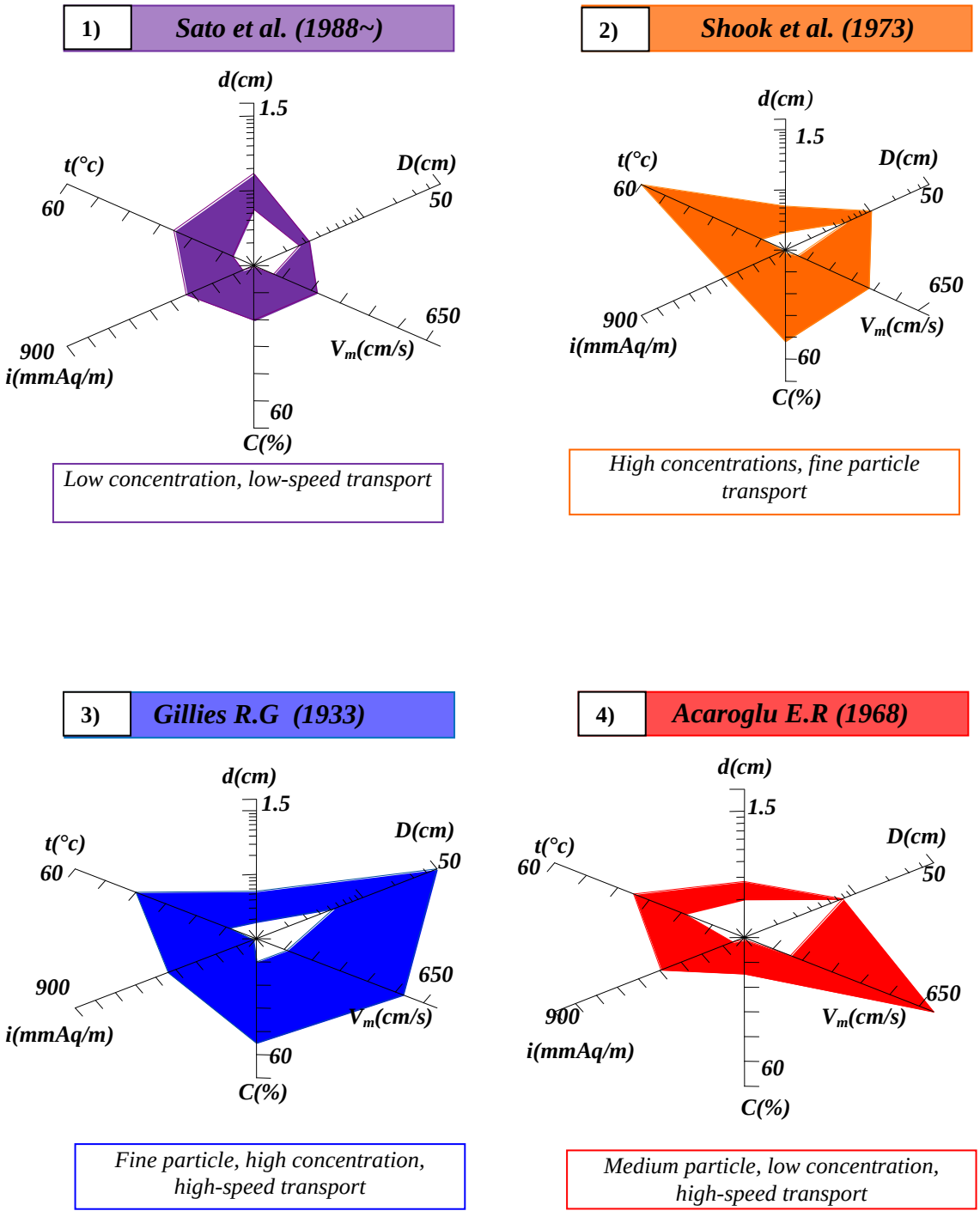

Figure 2. 14 Representative star graphs

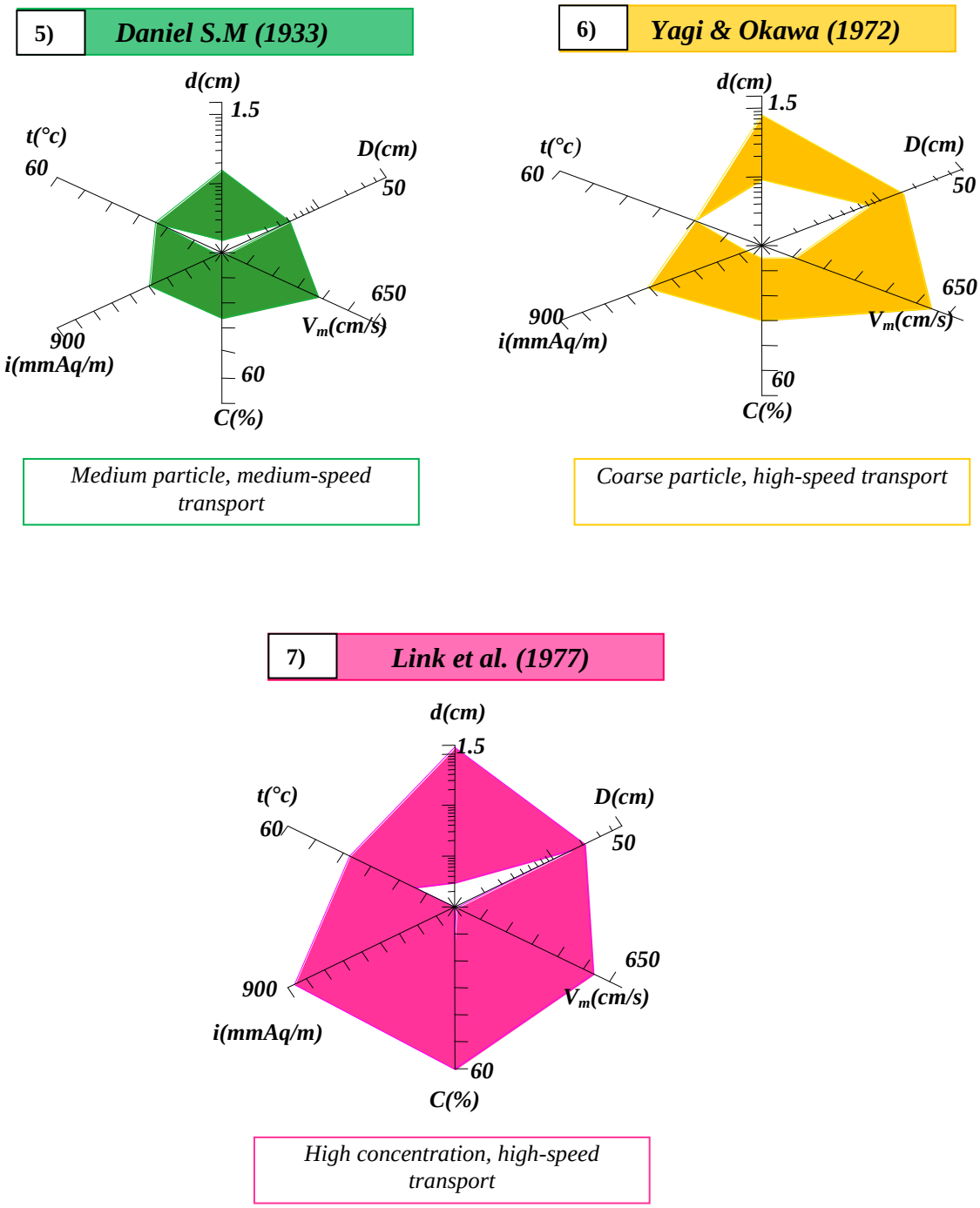

Figure 2. 14 Representative star graphs (continued from previous page)

Akita University

2.5 The application of the database program

In this chapter, analytical procedure of data should be explained with the database program. The following section could be useful for designers of pipeline systems using the monitor displays.

2.5.1 Starting the program

Double clicking the shortcut of the Database program on the computer desktop starts the program. The clicking produces the interface on which the program is written. After activating the “RUN” action of the program, a blank table is produced as shown in Figure 2.15. At the top of the interface, there is a tool bar with buttons of File (F), Edit (E), Display (D), and Graph (G). Each has a function on the program: File (F); opens a new or existing file. The display of this blank table signals that the program has started and the functions of: I. Data input, II. Data Edit and III. The graphical representation on the flowchart in Figure 2.3 can be attained.

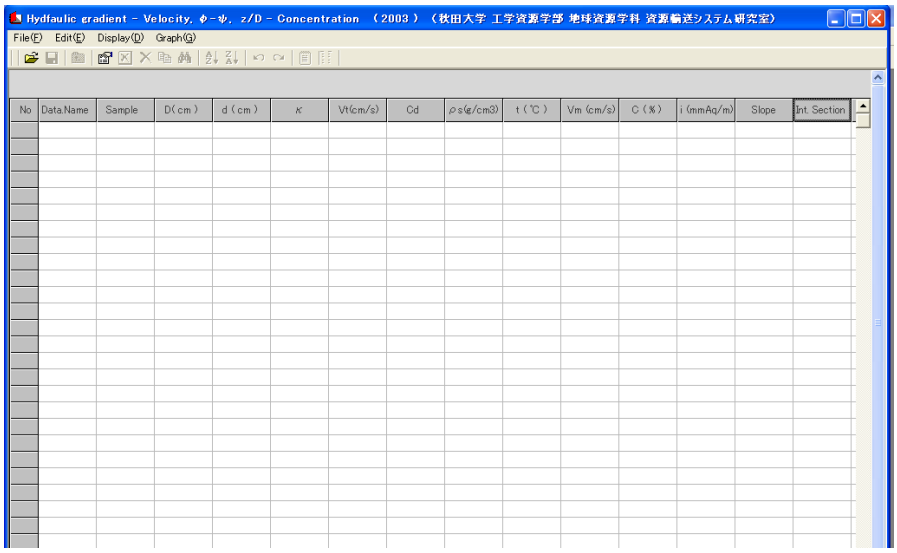

Figure 2. 15 Starting the program

Akita University

2.5.2 Data Input – Subprogram I

On the toolbar at the top, under Edit (E), clicking the button “Data table (T)” produces a blank table for input of data, as shown in Figure 2.5. The following actions should be taken by using the mouse selection:

(1) Under Work selection, click “Open” – the action opens a window from which to choose the data, as shown in Figure 2.16.

(2) Choose the type of data needed by selecting the data and clicking Open (O). The action generates a Data Table (Edit) filled with the characteristics of the selected data, as shown in Figure 2.17.

(3) Click “Input”, to submit the data for processing. Then, click “Close” to quit the table. The screen will display a table with the submitted data, as shown in Figure 2.18.

(4) To process the selected data and display analytical results, on the toolbar, click “Graph (G)” and then “Calculation (C)” in the dropdown menu select to start the calculations based on the program codes. The calculation process, shown in Figure 2.19, takes a few seconds to analyse the data.

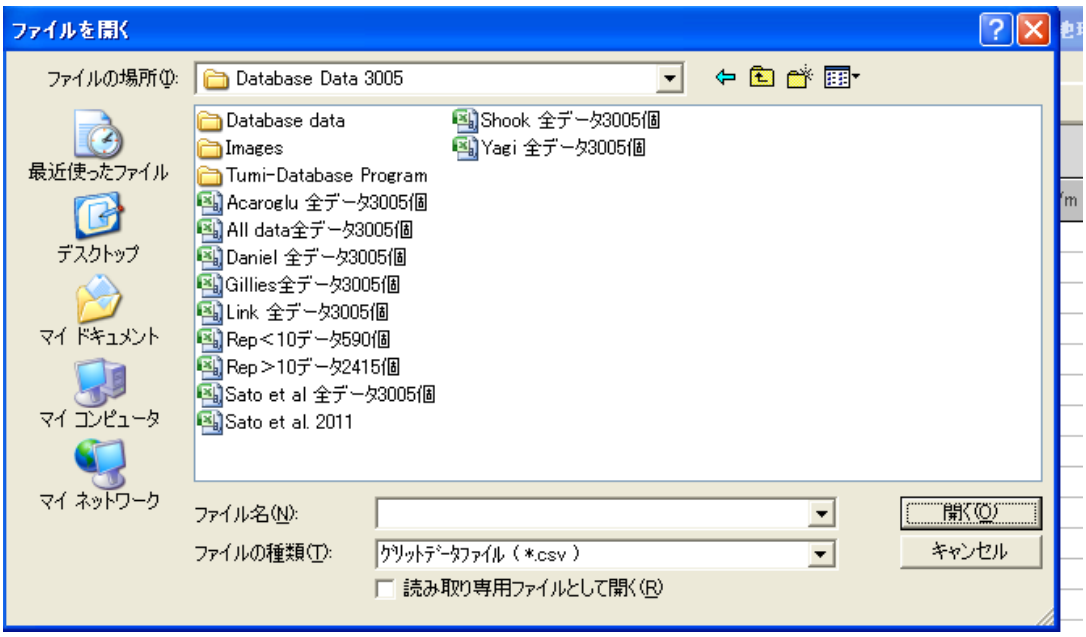

Figure 2. 16 Selection of data for analysis

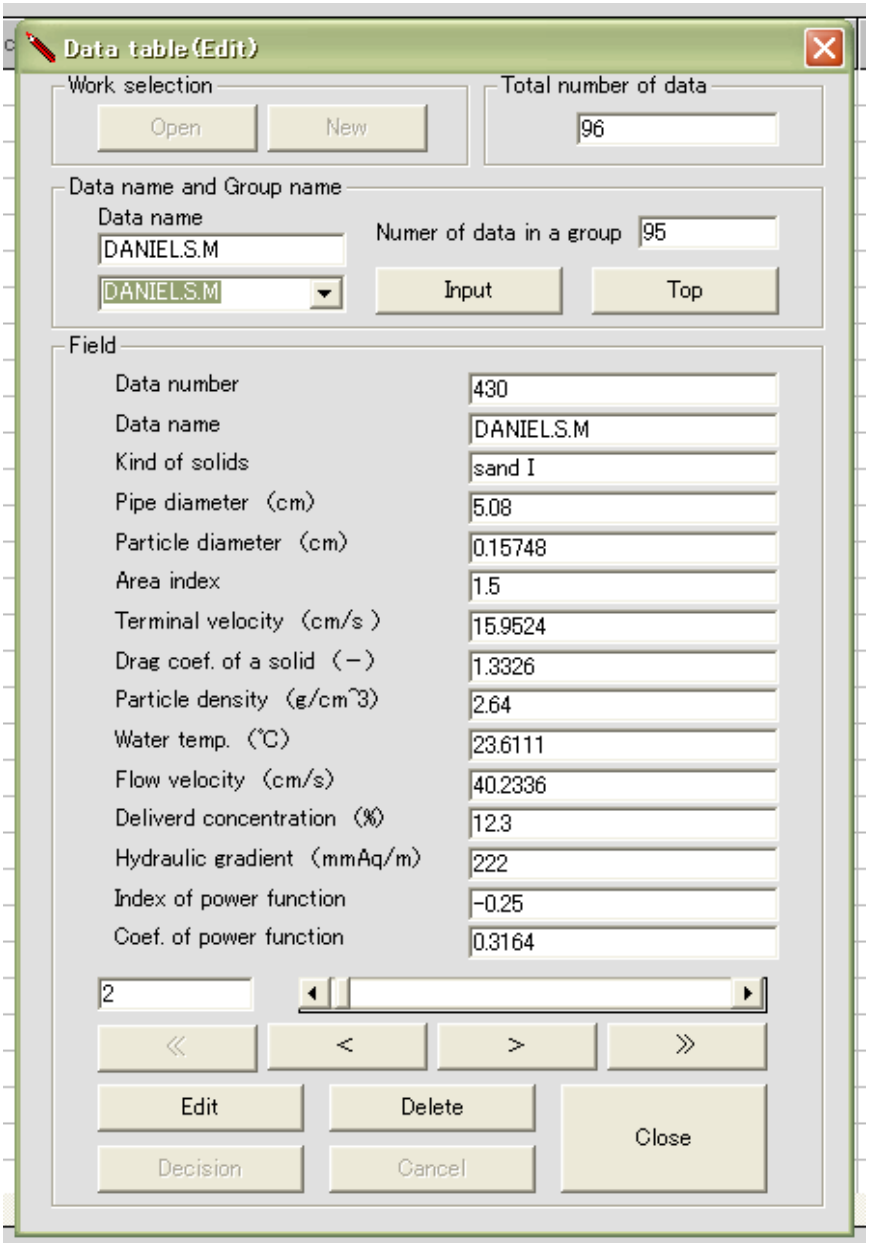

Figure 2. 17 Data Table (Edit) showing characteristics of the selected data

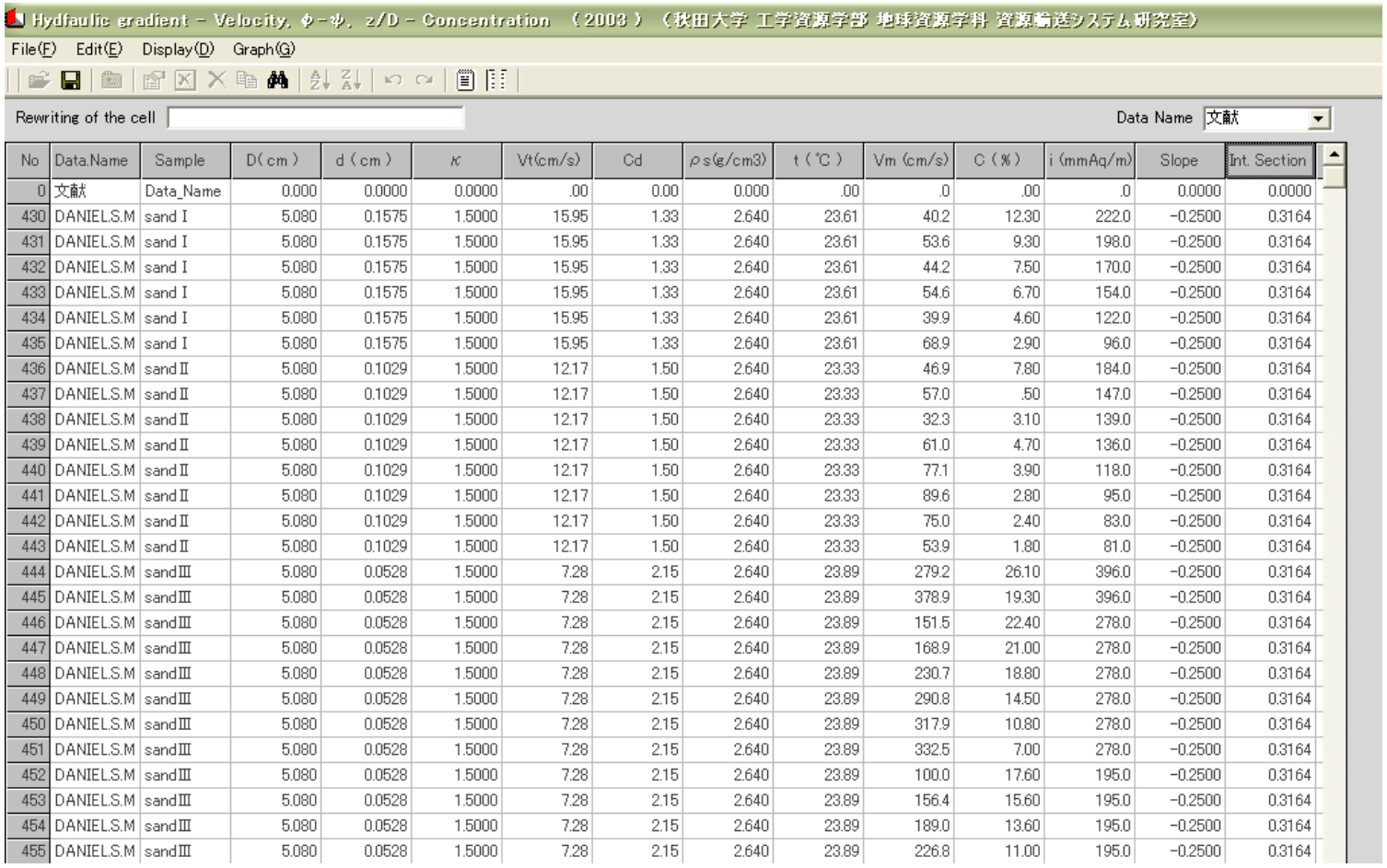

No	Data.Name	Sample	D(cm)	d(cm)	κ	Vt(cm/s)	Cd	ρs(g/cm3)	t(℃)	Vm(cm/s)	C(%)	i(mmAq/m)	Slope	Int. Section
0	文献	Data_Name	0.000	0.0000	0.0000	.00	0.00	0.000	.00	.0	.00	.0	0.0000	0.0000
430	DANIELS.M	sand I	5.080	0.1575	1.5000	15.95	1.33	2.640	23.61	40.2	12.30	222.0	-0.2500	0.3164
431	DANIELS.M	sand I	5.080	0.1575	1.5000	15.95	1.33	2.640	23.61	53.6	9.30	198.0	-0.2500	0.3164
432	DANIELS.M	sand I	5.080	0.1575	1.5000	15.95	1.33	2.640	23.61	44.2	7.50	170.0	-0.2500	0.3164
433	DANIELS.M	sand I	5.080	0.1575	1.5000	15.95	1.33	2.640	23.61	54.6	6.70	154.0	-0.2500	0.3164
434	DANIELS.M	sand I	5.080	0.1575	1.5000	15.95	1.33	2.640	23.61	39.9	4.60	122.0	-0.2500	0.3164
435	DANIELS.M	sand I	5.080	0.1575	1.5000	15.95	1.33	2.640	23.61	68.9	2.90	96.0	-0.2500	0.3164
436	DANIELS.M	sandⅡ	5.080	0.1029	1.5000	12.17	1.50	2.640	23.33	46.9	7.80	184.0	-0.2500	0.3164
437	DANIELS.M	sandⅡ	5.080	0.1029	1.5000	12.17	1.50	2.640	23.33	57.0	.50	147.0	-0.2500	0.3164
438	DANIELS.M	sandⅡ	5.080	0.1029	1.5000	12.17	1.50	2.640	23.33	32.3	3.10	139.0	-0.2500	0.3164
439	DANIELS.M	sandⅡ	5.080	0.1029	1.5000	12.17	1.50	2.640	23.33	61.0	4.70	136.0	-0.2500	0.3164
440	DANIELS.M	sandⅡ	5.080	0.1029	1.5000	12.17	1.50	2.640	23.33	77.1	3.90	118.0	-0.2500	0.3164
441	DANIELS.M	sandⅡ	5.080	0.1029	1.5000	12.17	1.50	2.640	23.33	89.6	2.80	95.0	-0.2500	0.3164
442	DANIELS.M	sandⅡ	5.080	0.1029	1.5000	12.17	1.50	2.640	23.33	75.0	2.40	83.0	-0.2500	0.3164
443	DANIELS.M	sandⅡ	5.080	0.1029	1.5000	12.17	1.50	2.640	23.33	53.9	1.80	81.0	-0.2500	0.3164
444	DANIELS.M	sandⅢ	5.080	0.0528	1.5000	7.28	2.15	2.640	23.89	279.2	26.10	396.0	-0.2500	0.3164
445	DANIELS.M	sandⅢ	5.080	0.0528	1.5000	7.28	2.15	2.640	23.89	378.9	19.30	396.0	-0.2500	0.3164
446	DANIELS.M	sandⅢ	5.080	0.0528	1.5000	7.28	2.15	2.640	23.89	151.5	22.40	278.0	-0.2500	0.3164
447	DANIELS.M	sandⅢ	5.080	0.0528	1.5000	7.28	2.15	2.640	23.89	168.9	21.00	278.0	-0.2500	0.3164
448	DANIELS.M	sandⅢ	5.080	0.0528	1.5000	7.28	2.15	2.640	23.89	230.7	18.80	278.0	-0.2500	0.3164
449	DANIELS.M	sandⅢ	5.080	0.0528	1.5000	7.28	2.15	2.640	23.89	290.8	14.50	278.0	-0.2500	0.3164
450	DANIELS.M	sandⅢ	5.080	0.0528	1.5000	7.28	2.15	2.640	23.89	317.9	10.80	278.0	-0.2500	0.3164
451	DANIELS.M	sandⅢ	5.080	0.0528	1.5000	7.28	2.15	2.640	23.89	332.5	7.00	278.0	-0.2500	0.3164
452	DANIELS.M	sandⅢ	5.080	0.0528	1.5000	7.28	2.15	2.640	23.89	100.0	17.60	195.0	-0.2500	0.3164
453	DANIELS.M	sandⅢ	5.080	0.0528	1.5000	7.28	2.15	2.640	23.89	156.4	15.60	195.0	-0.2500	0.3164
454	DANIELS.M	sandⅢ	5.080	0.0528	1.5000	7.28	2.15	2.640	23.89	189.0	13.60	195.0	-0.2500	0.3164
455	DANIELS.M	sandⅢ	5.080	0.0528	1.5000	7.28	2.15	2.640	23.89	226.8	11.00	195.0	-0.2500	0.3164

Figure 2. 18　Representative table of submitted data

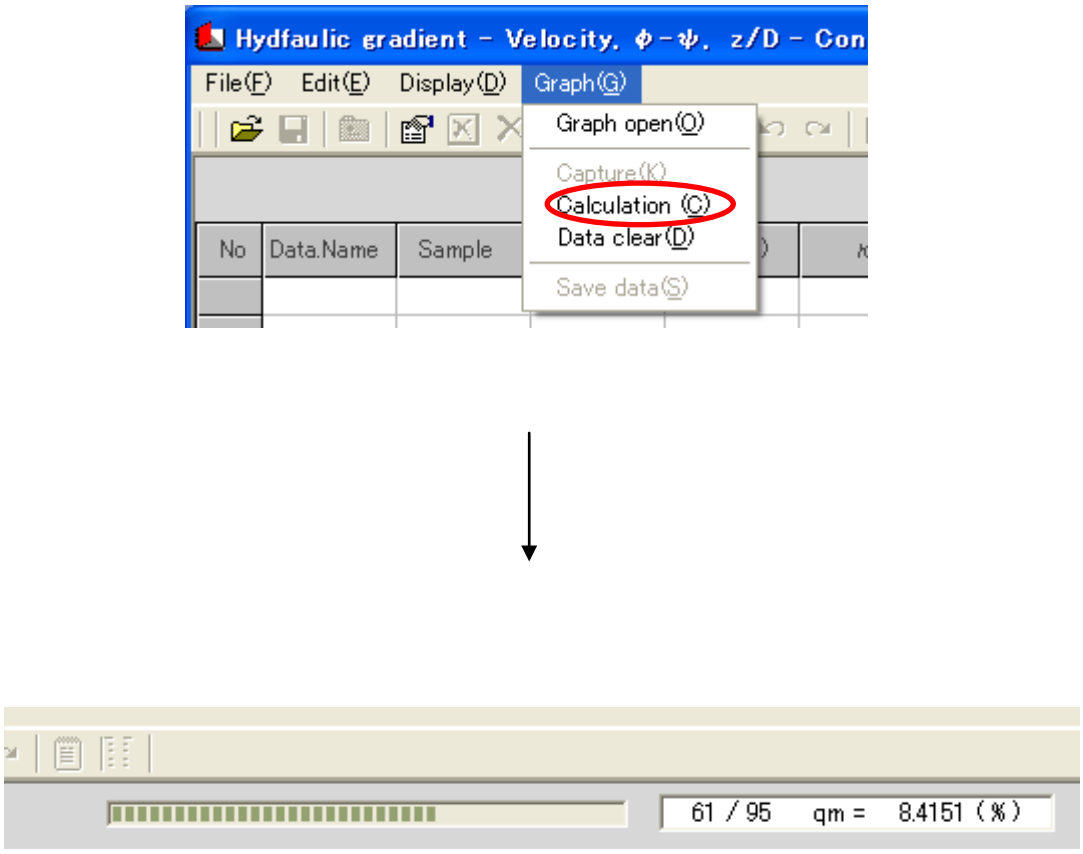

Figure 2. 19 Calculation process of the submitted data

Akita University

After analysis is completed, monitor display would show calculation results, as illustrated in Figure 2.20. The Dialog box is prepared for the selection of the graphical representation.

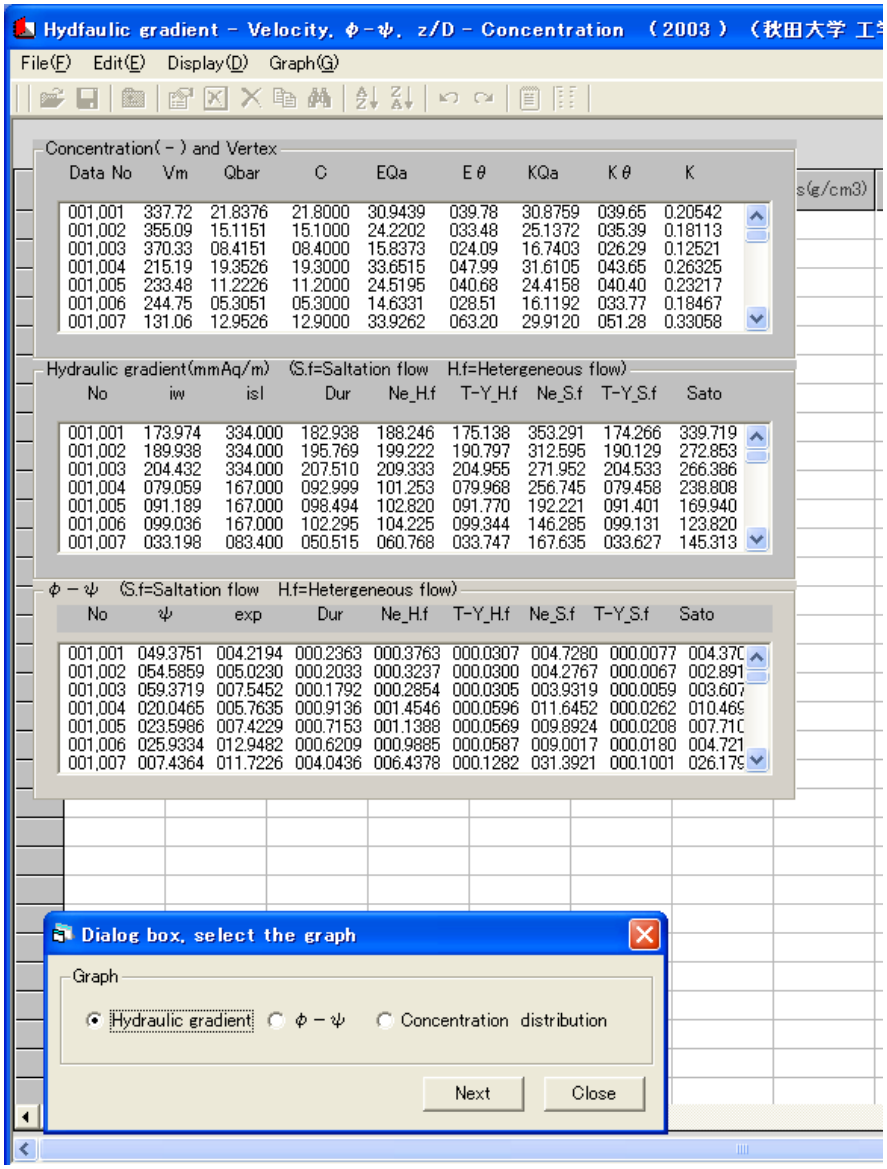

Figure 2. 20 Calculation results tables for the selected data and dialog box for graphical display options

Akita University

2.5.3 Data Edit – Subprogram II

When carrying out “Data Edit” function, as shown in Figure 2.6, reference data files are used. This allows users to specify analytical data for processing, based on the desired transport conditions. Data edit can be progressed as follows:

(1) Open a reference file by using the “File (F)” button, which will display table with analytical data as shown in Figure 2.18.

(2) In the table, the data could be specified by clicking either the “Edit (E)” then “Search” or “Binoculars”, shown in Figure 2.21. Both options will result in a Search dialog box, as shown in Figure 2.21.

(3) As mentioned in Sect. 2.3.3, the box can be used to fix the ranges of flow velocity, delivered concentration, and hydraulic gradient.

(4) After transport conditions are chosen, the users have option to proceed or delete and re-arrange specified data.

(5) To process the specified data, the calculation procedures discussed in Sect. 2.5.2 should be repeated. Figure 2.22 shows representative processing specified data, as compared with Figure 2.19.

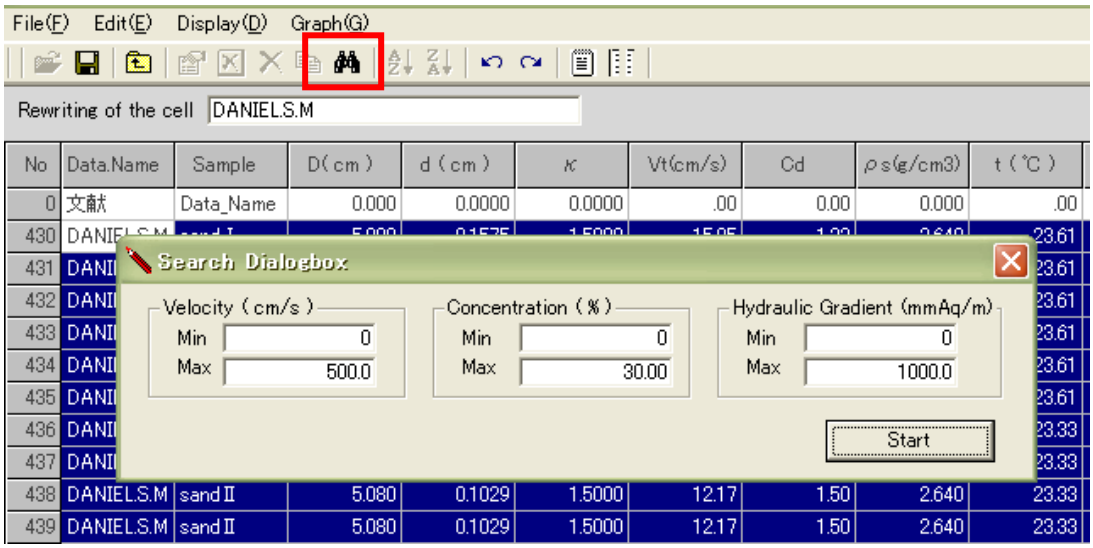

Figure 2. 21 Search dialog box for selecting specified data

Rewriting of the cell DANIELS.M

8 / 23 qm = .5067 (%)

No	Data.Name	Sample	D(cm)	d (cm)	κ	Vt(cm/s)	Cd	ρ s(g/cm3)	t (°C)	Vm (cm/s)	C (%)	i (mmAq/
0	文献	Data_Name	0.000	0.0000	0.0000	.00	0.00	0.000	.00	.0	.00	
430	DANIELS.M	sand I	5.080	0.1575	1.5000	15.95	1.33	2.640	23.61	40.2	12.30	222
431	DANIELS.M	sand I	5.080	0.1575	1.5000	15.95	1.33	2.640	23.61	53.6	9.30	198
432	DANIELS.M	sand I	5.080	0.1575	1.5000	15.95	1.33	2.640	23.61	44.2	7.50	170
433	DANIELS.M	sand I	5.080	0.1575	1.5000	15.95	1.33	2.640	23.61	54.6	6.70	154

Figure 2. 22 Calculation procedure for a specified set of data

Akita University

2.5.4 Graphical representation – Subprogram III

In Figure 2.20, the dialog box at the bottom displays three kinds of graphs to display: hydraulic gradient, φ-ψ relationship, and concentration distribution curve. Representative analytical results for each option are as follows:

(1) *Hydraulic gradient* Choosing the option of hydraulic gradient results gives another dialog box, shown in Figure 2.23. The box has two options: Selection 1; for data-group numbers, and Selection 2; for correlations. After this processing, a representative i-V_m graph would be displayed, as shown in Figure 2.24.

(2) *φ-ψ graph* Choosing the φ-ψ relationship provides selection options of data-group numbers and correlations. Figure 2.25 shows representative results of the φ-ψ relationship.

(3) *Concentration distribution curve* By the option of concentration distribution, the monitor shows the calculated results of in-situ concentration of solids in pipes, shown in Figure 2.26. The profile informs the flow patterns of slurry flow.

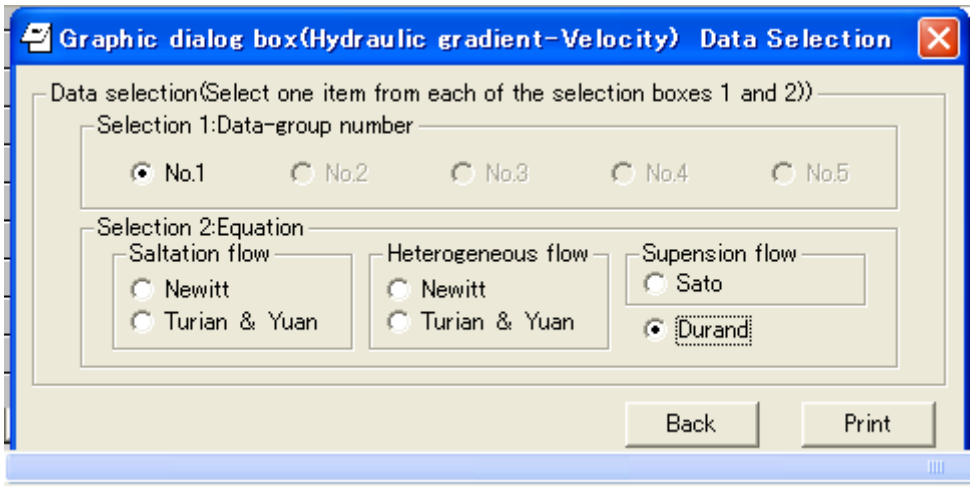

Figure 2. 23 Dialog box for data group numbers and *i-Vm* correlations

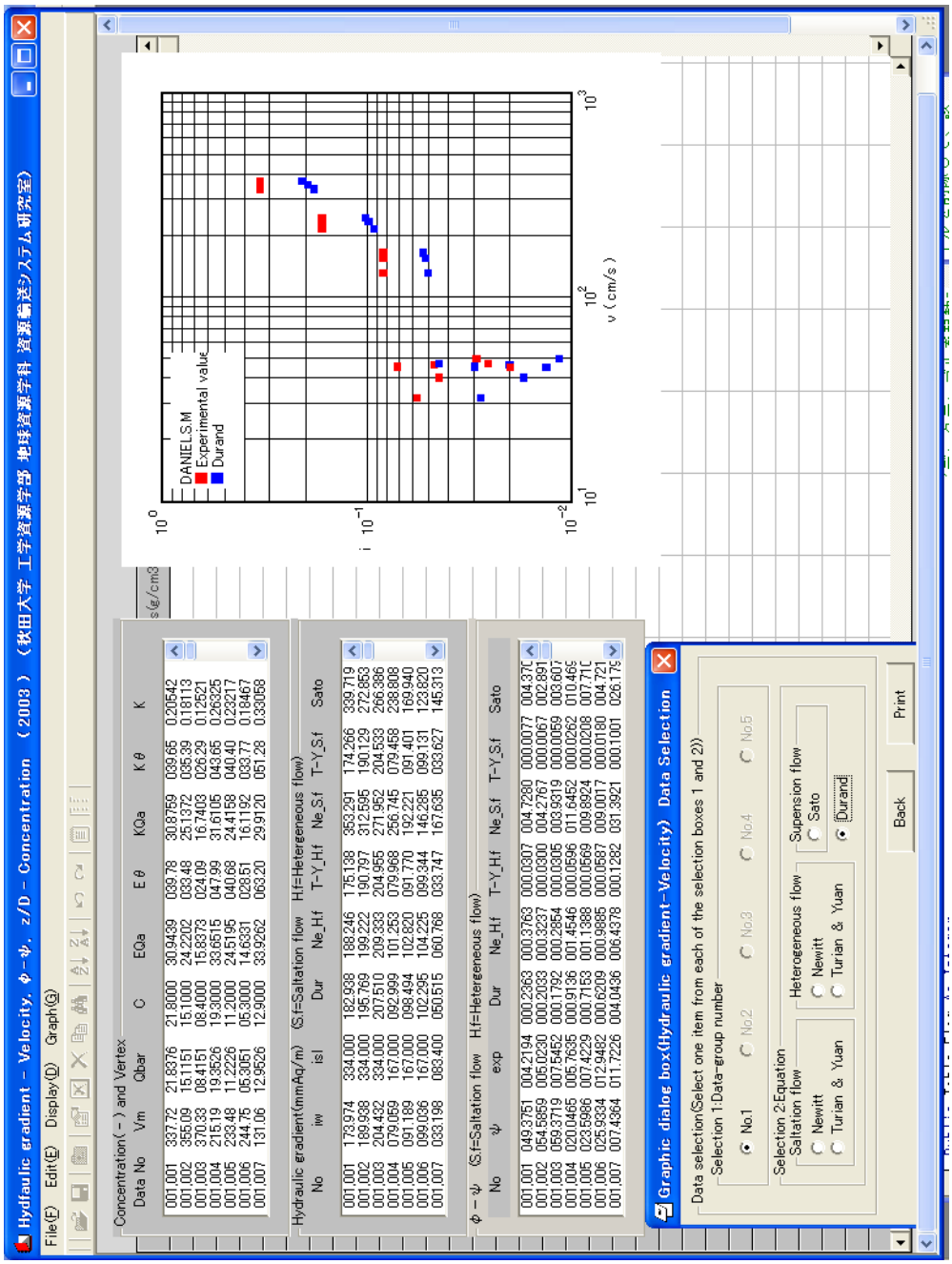

Figure 2. 24 Representative presentation of analytical *i-Vm* results

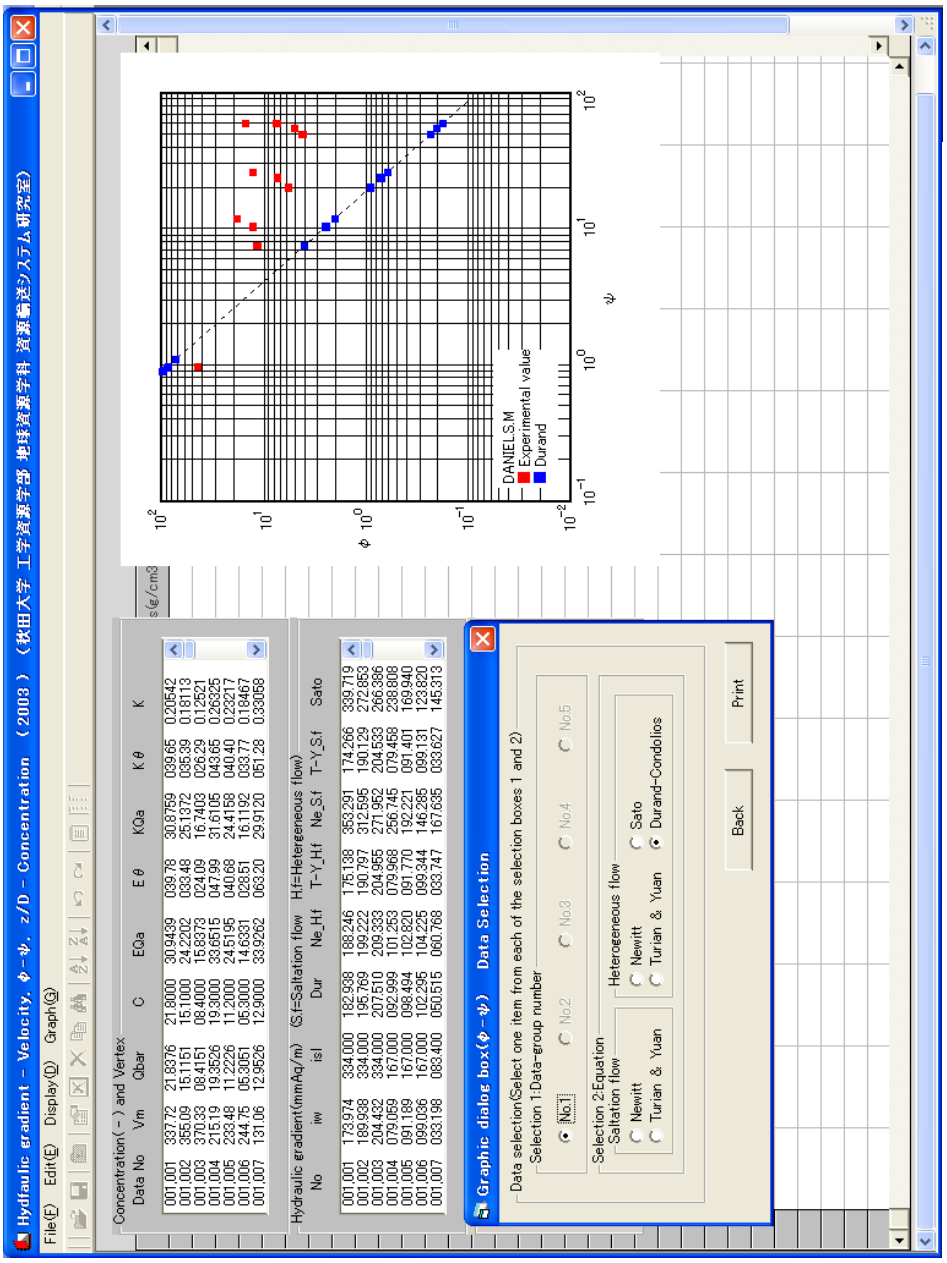

Figure 2. 25 Representative φ - ψ graph with the Durand-Condolios correlation

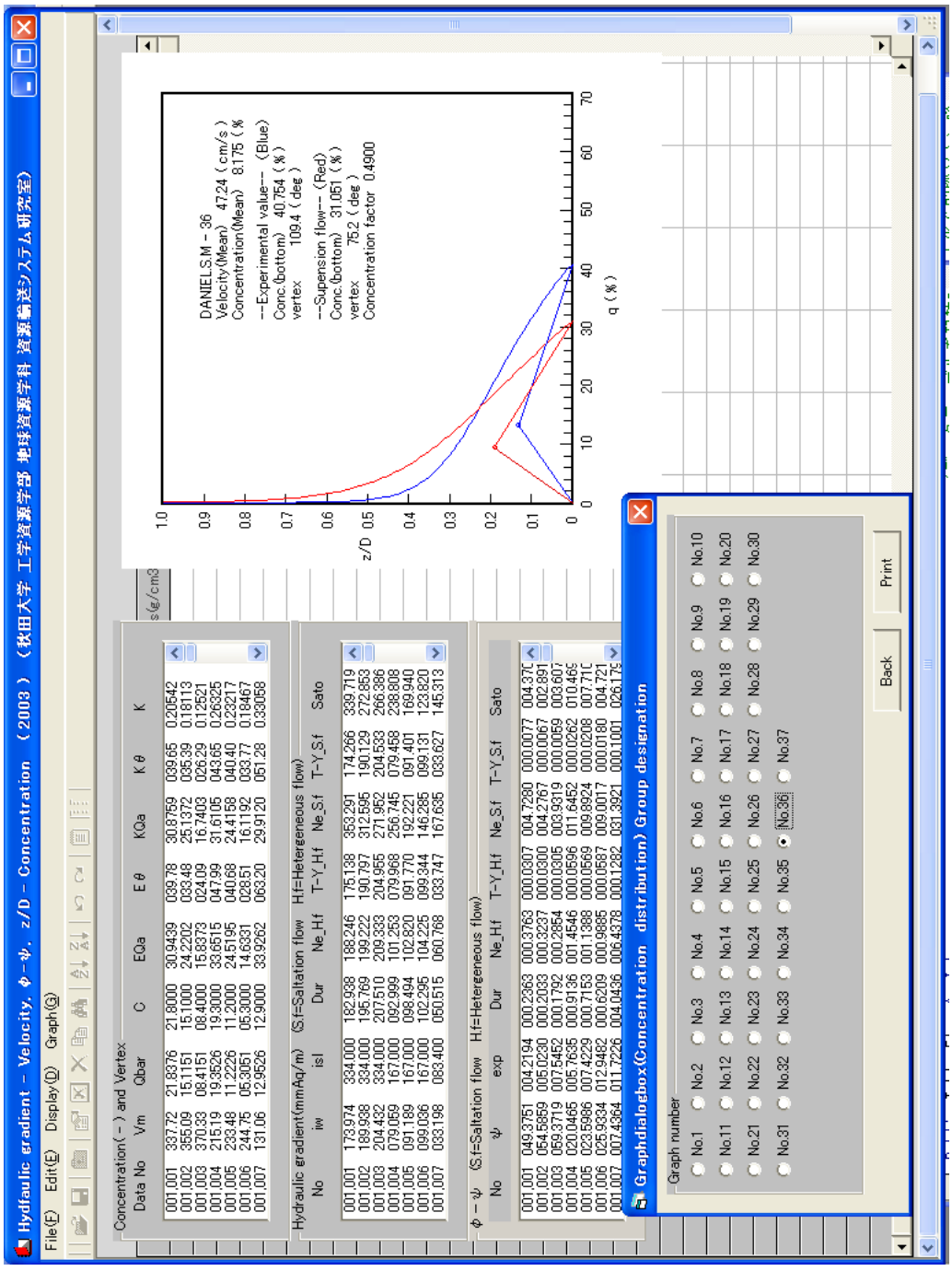

Figure 2. 26 Representative concentration curve of the selected data

Akita University

2.6 Conclusions

The study of Database program was progressed in this chapter and it reached the following conclusions:

1) The slurry transport database program equipped with the fundamental functions such as input, edit and save was developed.
2) The Data Table for input ensured accurate data processing.
3) For compiling published data, careful attention should be paid for lack of information and the unit conversion of the data, especially in U.S. customary units.
4) The graphical representations of estimated results with representative correlations of hydraulic gradient were effective for the comparison with experimental data.
5) The analysis of over three thousand data resulted in the star graphs with six axes, which could describe the characteristics of the researchers' data.

Akita University

2.7 References

[1] Jacobs, B. E. A.: Design of Slurry Transport Systems, Elsevier Science Publisher L.T.D., England, p. 3, (1991).

[2] Schneider, D. I.: An Introduction to Programming Using Visual Basic 6.0, Pearson Education Publishers, USA, pp. 1-28, (2004).

[3] Morris, P. J.: Relational Database Design and Implementation for Biodiversity Informatics, *Phyloinformatics; J. for Taxonomists*, Philadelphia, USA, 1-2, (2005).

[4] Fujita, S.: Database Sekkei Nyumon, Kinokumiya-Shoten Publishers, Japan, pp.29-37, (1992).

[5] Elmasri, R. and Navathe, S. B.: Fundamentals of Database Systems, Third Edition, Addison–Wesley Publishers, USA, pp.24-25, (2000).

[6] Sato, H., Otsuka, K., and Cui, Y.: A Model for the Settling Slurry Flow with a Stationary Bed in a Pipe, Proc. 4th Int. Symp. in Liquid-Solid Flows, Portland, Oregon, USA, **FED-118**, 54-55, (1991).

[7] Sato, H., Otsuka, K., and Cui, Y.: General Correlations of In Situ Concentration and Slip Velocity-Theoretical Considerations on the Mechanism of Slurry Flow with the Stationary Bed in a Pipe, *J. of Min. and Metall. Inst. Of Japan*, **105**, No. 6; 457-463, (1989).

[8] Wasp, E. J., Kenny, J. P., and Gandhi, R. I.: Solid-Liquid Flow, Slurry Pipeline Transportation, Trans. Tech. Publications, Germany, pp. 85-102, (1977).

Akita University

[9] Sato, H., Cui, Y., Sugimoto, F., and Tozawa, Y.: Determination of Distributions of Velocity and Concentration of Solids in a Horizontal Slurry Pipeline with a Digital Video Camera System, *Int. Society of Offshore and Polar Engineers*, **1**, 44-51, (1998).

[10] Sato, H., Takemura, S., Takamatsu, H., and Cui, Y.: An Improved Wasp Method for the Hydraulic Gradient of Slurry Flow with Size Distribution in a Horizontal Pipe, Proc. ASME Fluids Engng. Div. Summer Meeting FEDSM'97, Vancouver, British Columbia, Canada, No. 1400CD, 1-11, (1997).

[11] Sato, H., and Kawahara, M.: Critical Deposit Velocity of Slurry Flow Including Single-size Solid particles, Proc. 2nd Int. Conf. on Multiphase Flow, Kyoto, Japan, 23-30, (1995).

[12] Shook, C. A., Schriek, W., Smith, L. G., Haas, D. B., and Husband, W. H. W.: Experimental Studies on the Transport of Sands in Liquids of Varying Properties in 2 and 4 inch Pipelines, Saskatchewan Research Council, **VI**, 1-158, (1973).

[13] Gillies, R. G.: PhD Thesis, University of Saskatchewan, (1993).

[14] Acaroglu, E. R.: PhD Thesis, Cornell University, (1968).

[15] Daniel, S. M.: PhD Thesis, University of Saskatchewan, (1965).

[16] Yagi, T., Okude, T., Miyazaki, S. and Koreishi, A.: An Analysis of the Hydraulic Transport of Solids in Horizontal Pipelines, Port and Harbour Research Institute, **11**, No. 3, 3-35, (1972).

Akita University

[17] Link, J. M., Faddick, R. R., Pouska, G. A. and Gusek, J. J.: The Hydraulic Transportation of Oil Shale, Colorado School of Mines Research Institute, Report No. BuMines OFR 160-77, (1977).

Akita University

CHAPTER 3

Verification and Application of Design Model for Settling Slurry Transport in Pipes

The application of most empirical correlations for hydraulic gradient of settling slurry are generally limited to the experimental region in which four different flow patterns can be observed: stationary bed flow, saltation flow, heterogeneous flow, and pseudo-homogeneous flow. Therefore, the reliable design model independent on not only the flow regimes but also pipe diameter is imperative for pipeline engineers.

By using the condition factor introduced by Sato et al., which represents the situation of solids movement in a pipe and calculated from the concentration profiles, an equation was derived for hydraulic gradient of settling slurry flow in horizontal circular pipes. With the slurry database, it was also assured that the equation was valid for practical pipeline design under the condition of settling slurry flow. Hence, the effect of pipe diameter and concentration on the Specific Energy Consumption and pipeline design procedure were discussed based on the analytical results.

Akita University

3.1 Introduction

The particle size of solids in slurry affects the transport cost of pipelines. It is reported that coarse coal slurry - a representative settling slurry - becomes more economical than fine coal slurry (non-settling slurry) in horizontal pipelines where the distance is 40 km or lesser at a throughput level of 2.27 million tonne per year, if the transport cost includes preparation and dewatering charges [1]. In all cases of designing slurry transport systems, the prediction of hydraulic gradient as well as critical deposit velocity of slurry is vital for pipeline engineers. A number of correlations for the hydraulic gradient or pressure drop of settling slurry have been proposed: Refer to the reviews by Kazanskij [2], Abulnaga [3], and King [4]. Since most of the correlations were however derived at different flow regimes which depend on the mean velocity of the flow, the boundaries between the regimes should be determined whereas it is not easy to clearly distinguish one regime to another by observation.

The objective of this chapter is to demonstrate the applicability of an analytical model [5] to the settling slurry flow in horizontal pipes by using the Slurry Flow Database developed by Seitshiro et al. [6] and to clarify the design procedure for the optimum operation condition. It is shown that both a condition factor indicating concentration profiles and

Akita University

a generalized particle Reynolds number are vital to predict the energy needed for transporting the slurry.

3.2 Theoretical analysis

3.2.1 Digitisation of Flow patterns

The hydraulic gradient, or head loss per unit distance, of settling slurry flow in a horizontal pipe varies with the mean velocity and concentration, as shown schematically in Figure 3.1. As the velocity increases, the flow pattern of the slurry changes from the flow with stationary bed to saltation, heterogeneous, and pseudo-homogeneous flows. These flow patterns can be characterised by typical in-situ concentration profiles and flow behaviours, as shown in Figure 3.2.

For analysing the hydraulic gradient of slurry from fully suspended to fully saltation flow, a condition factor k for solids movements was introduced. Intermediate flow pattern can be represented by the value of k between 0 to 1.

3.2.1.1 Flow with Stationary bed

If the slurry flow speed is too low to move the solids, the particles begin to settle on the bottom of the pipe. Continuing the transport at the same conditions could lead to accumulation of the solids, resulting in blockage of the pipe. In this regime, the concentration is rather higher at the bottom of the pipe.

Akita University

3.2.1.2 Saltation flow

As the velocity of the slurry flow is increased, a portion of the solids begin rolling and jumping on the surface of the bed. The upper layers of the bed move with higher velocity. A series of the change of the movement could bear an analogy with the mechanical phenomena of sand dunes in a desert. The concentration of the solids in this regime can be essentially restricted to lower parts of the pipe.

3.2.1.3 Heterogeneous flow

At increased flow velocities most solids are suspended by turbulence in pipes. However, the flow velocity is not sufficient to maintain the solids in full suspension. All particles move in an asymmetric concentration profile. This regime can be encountered in slurry transport systems of dredging and tailings disposal in the weight concentration below 35 % [7].

3.2.1.4 Pseudo-homogeneous flow

In this regime, transport velocities are higher and all solids are uniformly distributed throughout the pipe. The flow turbulence is highly sufficient to lift and keep all the particles in suspension. If the velocity is increased further, the risk of pipe erosion rises.

It should be noted that the flow behaviour depends on not only velocity but the size and density of solids. In commercial slurry

Akita University

pipelines, a combination of the heterogeneous-homogeneous regimes is often observed due to complex mixtures of coarse and fine solids [8]. Detailed explanations of the regimes are described elsewhere [4], [7], [8], [9].

For a two dimensional steady and uniform flow in a horizontal pipe, the profile of solids can be represented by [5], [10]:

$$\xi\varepsilon_m \frac{dq}{dz} + (1-q)^n V_t \cdot q = 0 \qquad \text{.....(3.1)}$$

where:

$$\xi = 0.451\psi^{0.281} \qquad \text{.....(3.2)}$$

$$\varepsilon_m = 0.0395 \cdot D \cdot V_t \qquad \text{.....(3.3)}$$

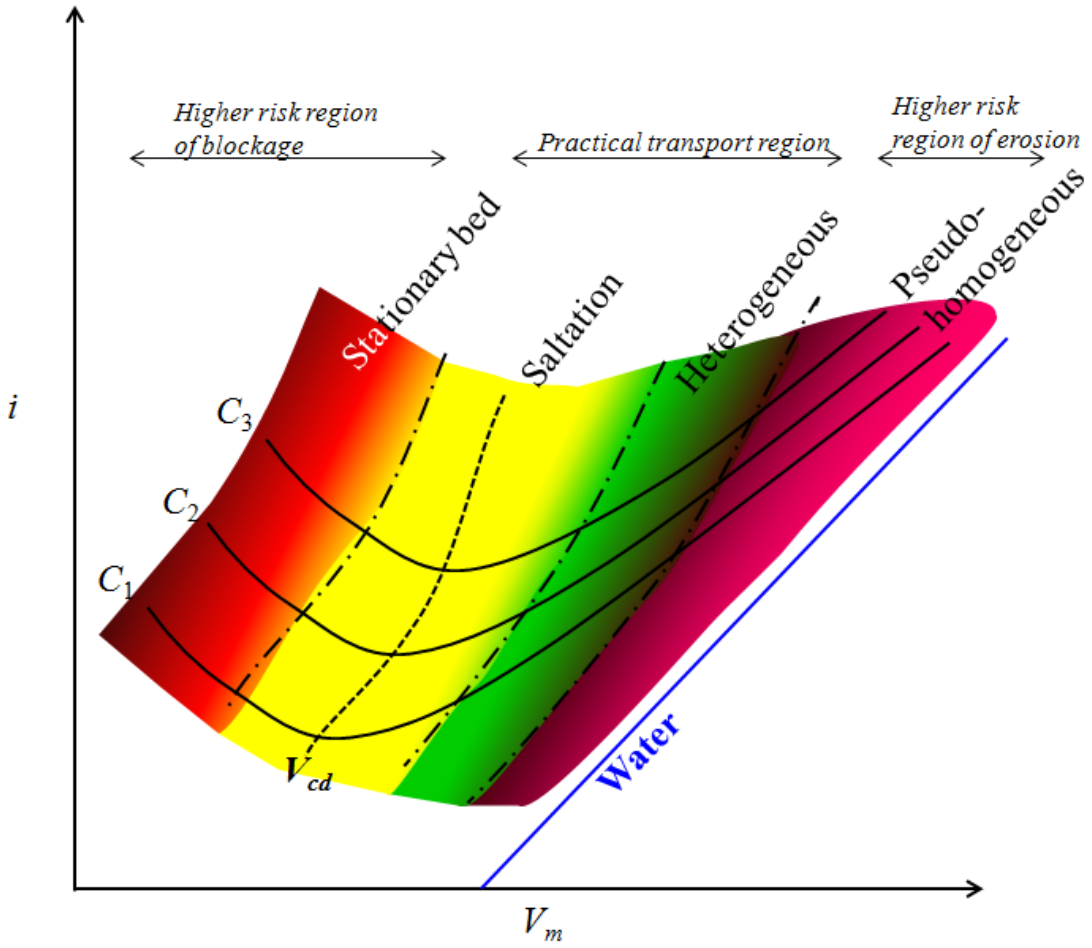

Figure 3. 1 Schematic variation of flow regimes with increasing velocity and concentration of slurry flow

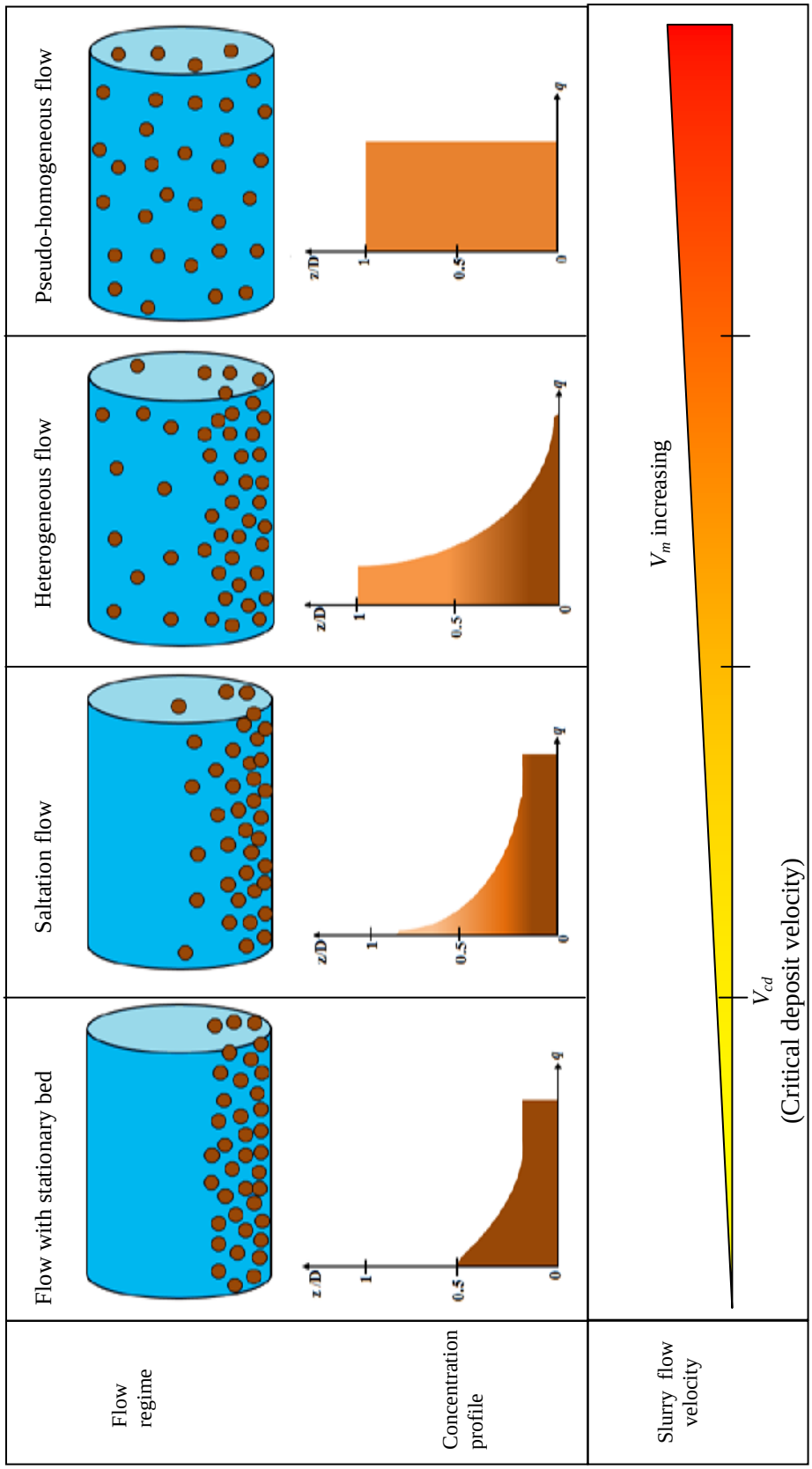

Figure 3. 2 Flow pattern and solids concentration distributions for four regimes

Figure 3. 2 Flow patterns and solids concentration distributions depending on slurry flow velocities

Akita University

For an arbitrary value of n, the concentration q at the distance z from the bottom is given by:

$$\log \frac{q}{q_a} + \sum_{j=1}^{\infty}\left[\left\{\prod_{k=1}^{j}(n+k-1)\right\}\frac{(q^j - {q_a}^j)}{j \cdot j!}\right] = -\frac{(z-a)/D}{0.03953}\frac{V_t}{V_*} \qquad \text{.....(3. 4)}$$

in which the value of n can be estimated by the relationship [10]:

$$n = 2.33\left|\frac{1}{1-\frac{\frac{2\sqrt{48}\alpha\beta}{Re_p}}{Re_p{}^{+}\left(\alpha + Re_p{}^{+}\right)}}\right| \qquad \text{.....(3. 5)}$$

where;

$$Re_p{}^{+} = \sqrt{\alpha^2 + 4\sqrt{48}\alpha\beta/Re_p} \qquad \text{.....(3. 6)}$$

The characteristic plane which can be produced with coordinate axes sides and the concentration distribution curve predicted by using Eq. (3. 1) has the geometrical centre of gravity, G (q_m, $z^*{}_m$), as shown in Figure 3. 3. On the practical transport conditions that all solids in the pipe are in motion, the vertex θ in Figure 3. 3 depends on the flow pattern of the slurry. It varies between θ_B to θ_0 which corresponds to full

Akita University

saltation flow without deposit at low velocity to full homogeneous flow at higher velocity respectively, as illustrated in Figure 3. 4:

$$\theta_B = 2\,tan^{-1}(q_{aB}{}^2/\overline{q}) \qquad \text{……...……(3. 7)}$$

$$\theta_0 = 2\,tan^{-1}\,q_a \qquad \text{……...(3. 8)}$$

in which q_{aB} and q_a represent the concentrations at the bottom of the pipe in saltation and pseudo-homogeneous flows of the average in-situ concentration $\overline{q}$.

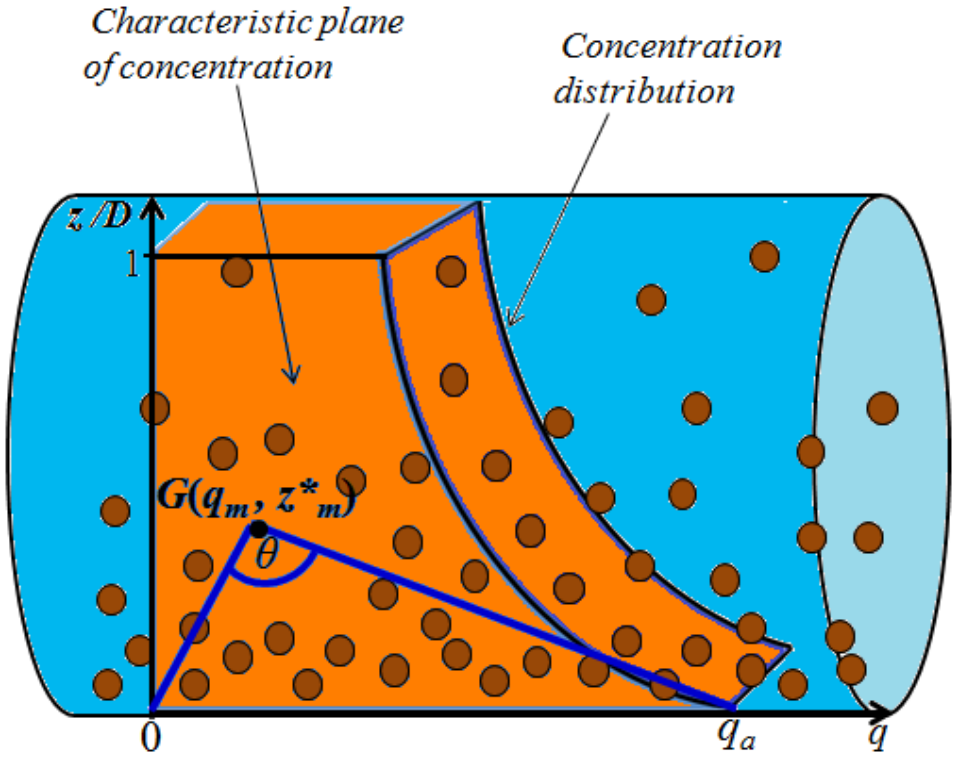

Figure 3. 3 Characterisation of concentration distribution curve

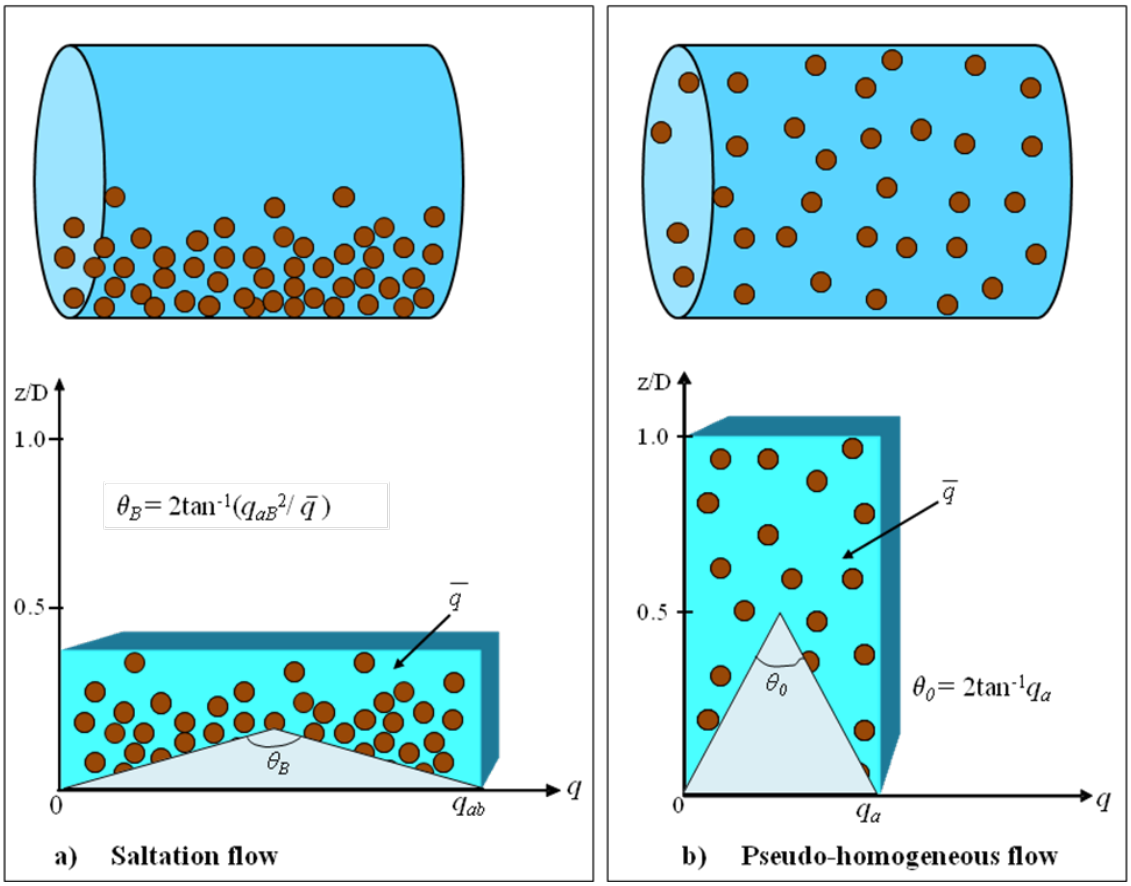

Figure 3. 4 Extreme flow patterns of saltation and pseudo-homogeneous flow

Akita University

Based on the Pappus-Guldins theorem [11], the coordinate G(q_m,z^*_m) in Figure 3. 3, the centroid of the characteristic plane can be computed numerically as illustrated in Figure 3. 5, by the following equations;

$$q_m = \frac{\sum_{i=1}^{n}\left\{\left(\frac{q_i + q_{i+1}}{2}\right)\left(\frac{z^*_i + z^*_{i+1}}{2}\right)(q_i - q_{i+1})\right\}}{\sum_{i=1}^{n}(q_i \cdot \square\ z^*)} \qquad \text{……..…....(3. 9)}$$

$$z^*_m = \frac{\sum_{i=1}^{n}(q_i \cdot z^*_i \cdot \square\ z^*)}{\sum_{i=1}^{n}(q_i \cdot \square\ z^*)} \qquad \text{…….……..……....(3. 10)}$$

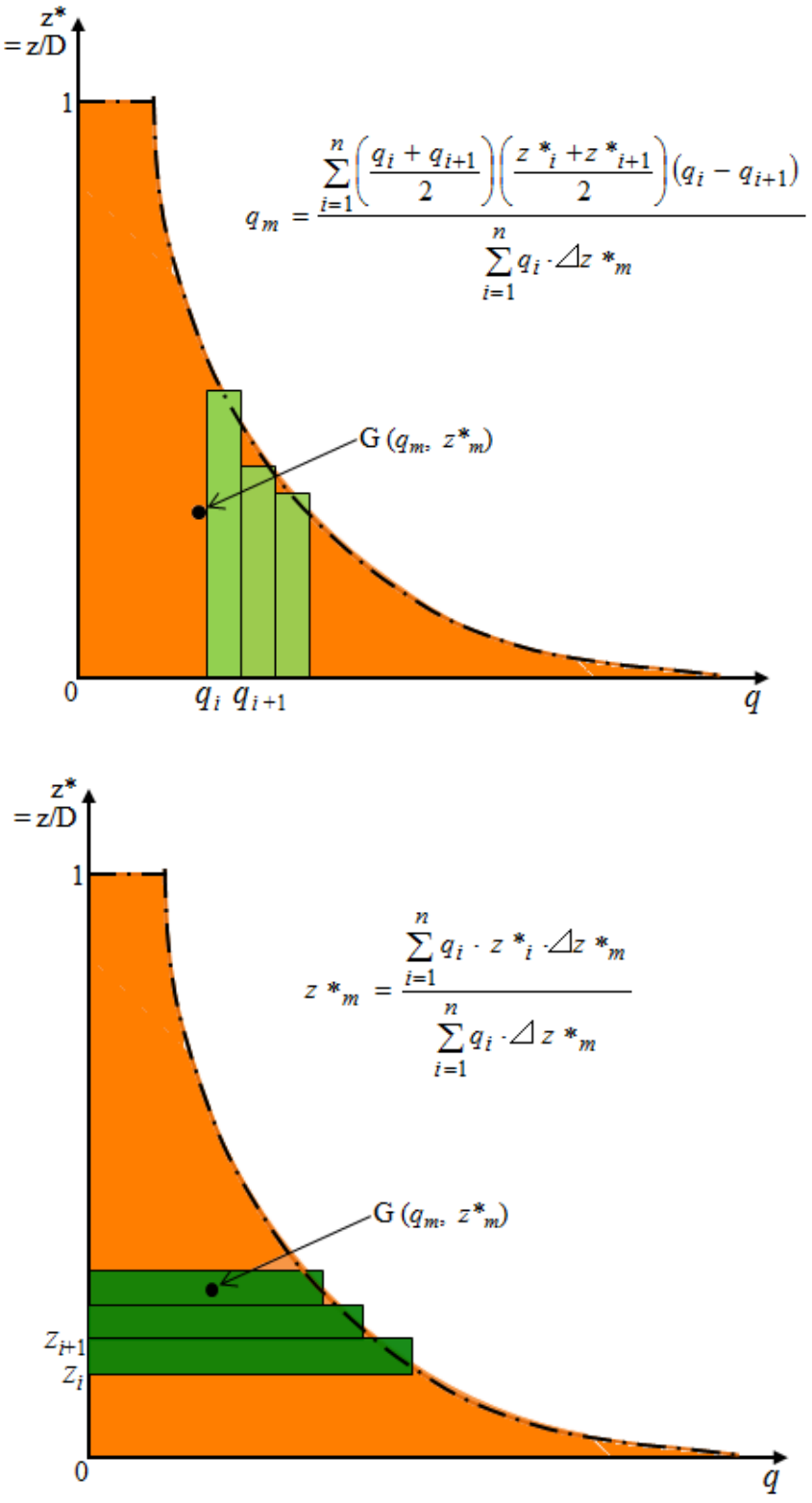

Figure 3. 5 The integral determination of the centre of the characteristic plane

On the other hand, the vertex θ can be calculated by:

$$\cos\theta = \frac{\mathrm{OG}^2 + \mathrm{GQ}^2 - \mathrm{OQ}^2}{2 \cdot \mathrm{OG} \cdot \mathrm{GQ}} \qquad \text{…..…….(3. 11)}$$

where each of the triangle segments, in Figure 3. 6 can be represented as follows:

$$\begin{aligned} \mathrm{OG} &= \sqrt{{q_m}^2 + {z*_m}^2} \\ \mathrm{GQ} &= \sqrt{({q_a}^2 - {q_m}^2) + {z*_m}^2} \\ \mathrm{OQ} &= q_a \end{aligned} \qquad \text{…….……..(3. 12)}$$

Substituting Eq. (3. 12) into Eq. (3. 11), vertex θ can then be estimated by:

$$\cos\theta = \frac{({q_m}^2 + {z^*_m}^2) + \left\{(q_a - q_m)^2 + {z^*_m}^2\right\} - {q_a}^2}{2\sqrt{{q_m}^2 + {z^*_m}^2} + \sqrt{(q_a - q_m)^2 + {z^*_m}^2}}$$

$$\theta = \cos^{-1}\left[\frac{({q_m}^2 + {z^*_m}^2) + \left\{(q_a - q_m)^2 + {z^*_m}^2\right\} - {q_a}^2}{2\sqrt{{q_m}^2 + {z^*_m}^2} + \sqrt{(q_a - q_m)^2 + {z^*_m}^2}}\right] \qquad \text{…....(3. 13)}$$

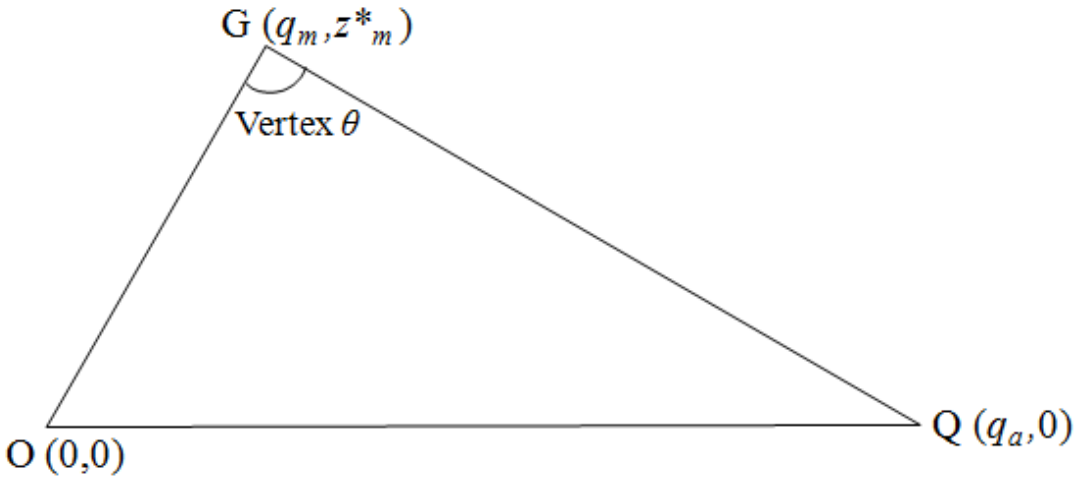

Figure 3. 6 Calculation procedure of the vertex θ

Akita University

Introducing a condition factor *k*, the priority parameter of saltation, with the assumption of a linear correlation between *k* and the vertex θ, the *k* factor can be represented by the following function:

$$k = \frac{\theta - \theta_O}{\theta_B - \theta_O} \qquad \text{.....(3. 14)}$$

It means that as the velocity of slurry flow decreases from the pseudo-homogeneous flow to the saltation, the value of *k* increases and approaches unity, as shown Figure 3. 7.

For practical slurry transport, the heterogeneous flow pattern can mostly be observed, with values of θ ($\theta_0 < \theta < \theta_B$) and *k* ($0 < k < 1$).

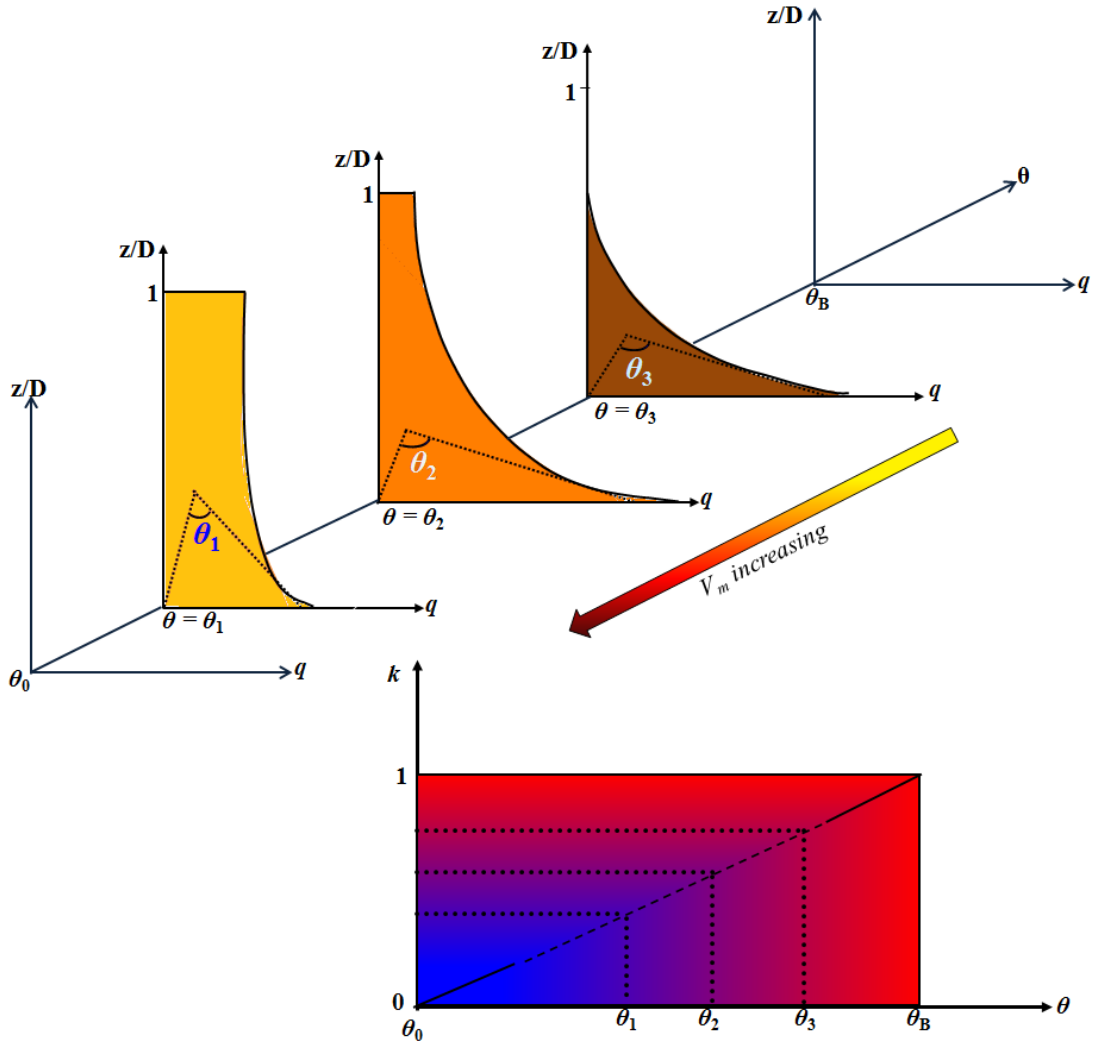

Figure 3. 7 The relationship between *k* and *θ* with the change of concentration profiles

Akita University

3.2.2 Energy losses in Settling Slurry Flow

3.2.2.1 Energy required for pipe flows

In pipe flows, it is assumed that water could exert a normal force F on an imaginary circular plate, as shown in Figure 3. 8(a). The energy required to move the object through the pipe of distance l in time T, the work done per unit time, can be calculated by:

$$E = \frac{F \cdot l}{T} \qquad \text{.....(3. 15)}$$

where the force exerted on the cross-sectional area A, as shown in Figure 3. 8(b) can be calculated by:

$$F = \Delta P \cdot A \qquad \text{.....(3. 16)}$$

The time spent for the work through water of flow rate Q ($=V_m \cdot A$) can be represented by:

$$T = \frac{l}{V_m} = \frac{l}{Q / A} = \frac{A \cdot l}{Q} \qquad \text{.....(3. 17)}$$

Substituting Eqs. (3. 16) and (3. 17) into Eq. (3. 15), the energy to flow water in the pipe can be estimated by:

$$E = \frac{(\Delta P \cdot A) \cdot l}{A \cdot l / Q}$$

$$\therefore \quad E = \Delta P \cdot Q \qquad \text{……(3. 18)}$$

which can be useful for selecting the type of pump and the specifications of pipeline systems for the transport of solids and water.

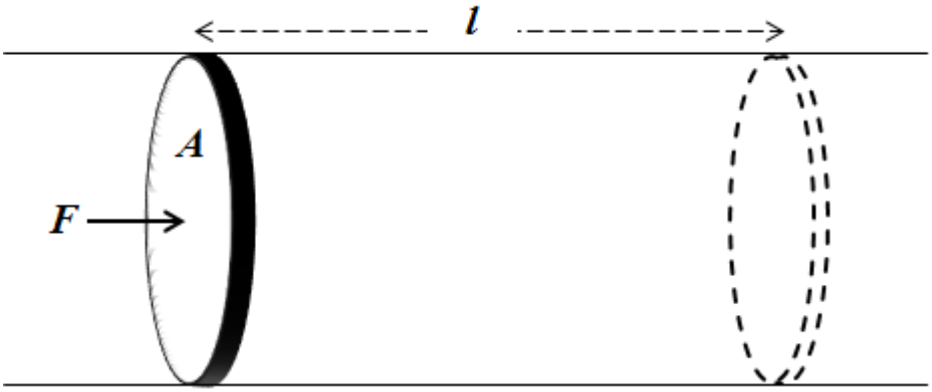

(a) Movement of an imaginary disk

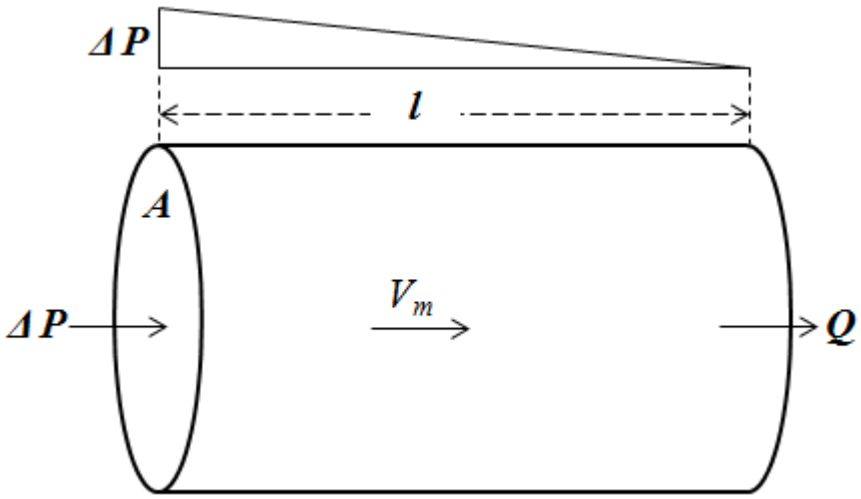

(b) Slurry flow in a pipe

Figure 3. 8 Comparison of slurry flow to the movement of an imaginary disc in a pipe

Akita University

3.2.2.2 Suspended flow of slurry

When the solid particles of slurry are transported in suspension over the length *dl* of the pipe per unit time, the consumed energy *E*, as shown in Figure 3. 9, can be represented by:

$$E = E_w + E_B + E_D \qquad \text{.....(3. 19)}$$

where E_w is the energy loss in flow of clear water as a vehicle at the same velocity as slurry. E_B is the energy loss in maintaining the solids in suspension, and E_D is the energy dissipated for the drag of solid particles.

According to Eq. (3. 18), the component of the energy E_w for water flow with velocity V_w, can be estimated by:

$$E_w = \Delta P_w \cdot A \cdot V_w \qquad \text{.....(3. 20)}$$

Substituting the following ΔP-i_w relationship;

$$i_w = \frac{\Delta P_w}{dl \cdot \gamma} \qquad \text{.....(3. 21)}$$

into Eq. (3. 20), resulting in:

$$E_w = i_w \cdot V_m \cdot A \cdot \gamma \cdot dl \qquad \text{.....(3. 22)}$$

Akita University

The submerged weight of all suspended solids at the interval dl of the pipe in Figure 3. 10 can be represented by:

$$w_{ap} = \overline{q}A \cdot dl \cdot (\rho_s - \rho)g$$

$$= \overline{q}A \cdot dl \cdot (\gamma_s - \gamma) \qquad \text{……..……(3. 23)}$$

In a suspended slurry flow, the energy required to keep the solids in suspension E_B which have the tendency of settling with the velocity V_h, can be calculated by:

$$E_B = w_{ap} \cdot V_h$$

$$= \overline{q}A \cdot dl \cdot (\gamma_s - \gamma)V_h \qquad \text{……...……...……(3. 24)}$$

By using the Richardson-Zaki equation,

$$\frac{V_h}{V_t} = (1 - \overline{q})^n \qquad \text{……...……..……(3. 25)}$$

Eq. (3. 24) can be re-arranged as follows:

$$E_B = (1 - \overline{q})^n V_t (\gamma_s - \gamma) \overline{q} \cdot A \cdot dl$$

$$= \overline{q} (1 - \overline{q})^n V_t A (\gamma_s - \gamma) dl \qquad \text{…… (3. 26)}$$

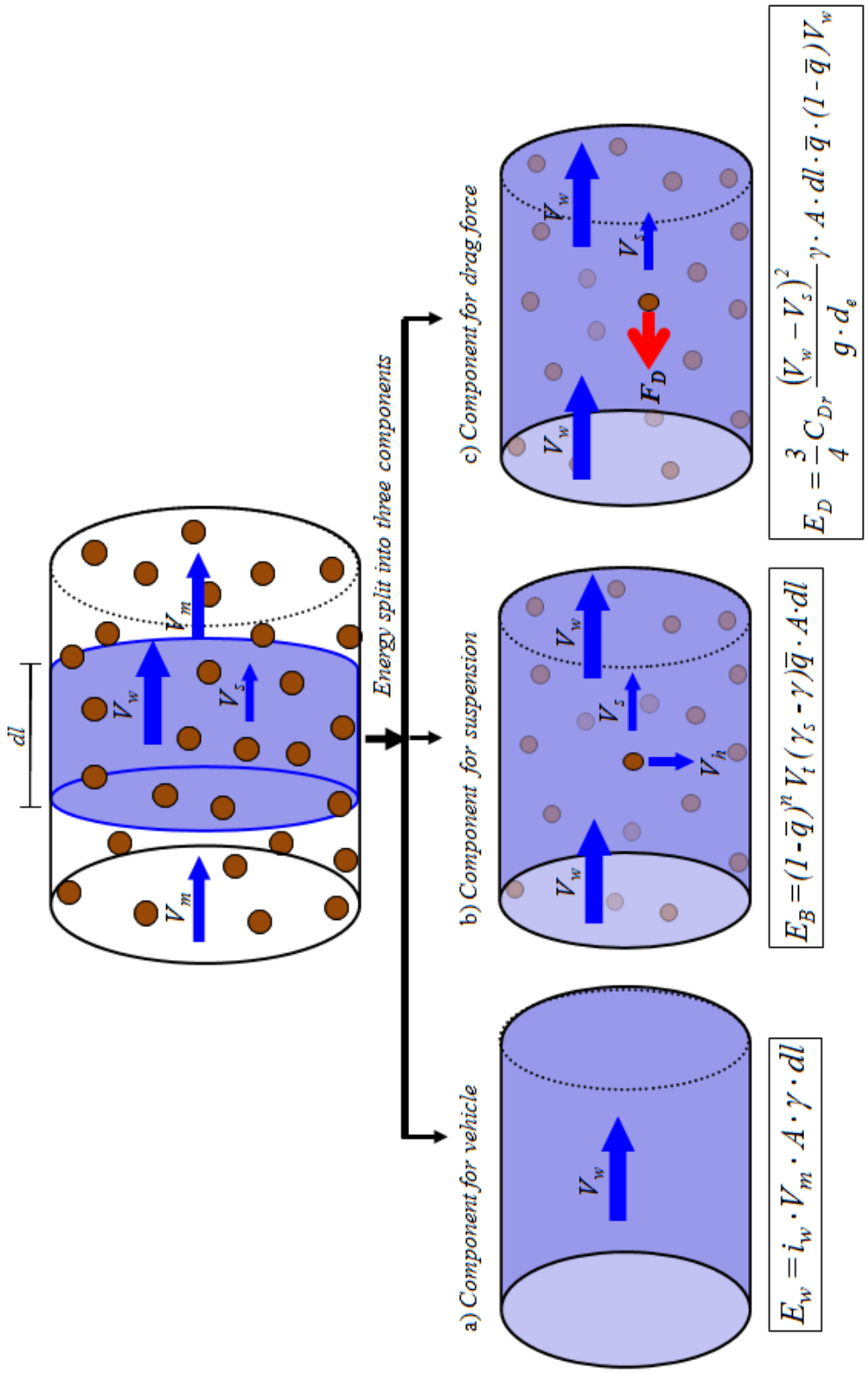

Figure 3. 9 Energy loss consisting of vehicle, suspension and drag force components

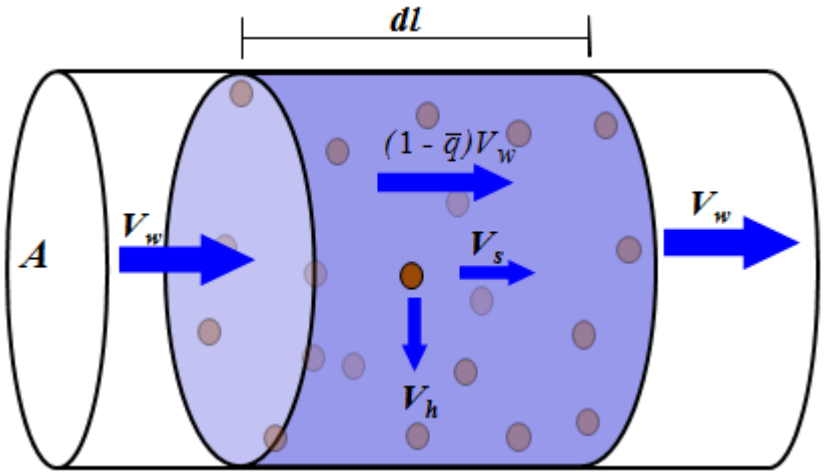

Figure 3. 10 Energy loss due to suspension of solids

Akita University

On the other hand, if clear water flows with velocity V_w could pass through the suspended solids in the small element with volume $A \cdot dl$ in Figure 3.11, it creates the slurry moving with velocities of V_s and $(1-\overline{q})V_w$ for solids and water respectively. The drag force of solid particles in the element can be evaluated by:

$$F_D = \frac{3}{4} C_{Dr} \frac{(V_w - V_s)^2}{g \cdot d_e} \gamma \cdot A \cdot dl \cdot \overline{q} \qquad \text{……..…..…...…..(3. 27)}$$

The energy loss E_D due to the drag force can be estimated by:

$$E_D = (1-\overline{q})V_w \cdot F_D \qquad \text{…….……..……..(3. 28)}$$

Substitution of Eq. (3. 27) into Eq. (3. 28), results in:

$$E_D = \frac{3}{4} C_{Dr} \frac{(V_w - V_s)^2}{g \cdot d_e} \gamma \cdot A \cdot dl \cdot \overline{q} \cdot (1-\overline{q})V_w \qquad \text{……...……(3. 29)}$$

The drag coefficient of solids C_{Dr} in Eq. (3. 29) can be represented by [12]:

$$C_{Dr} = \frac{1}{4}\left(\alpha + \sqrt{\alpha^2 + \frac{4\sqrt{48}\alpha\beta}{Rep_r}}\right)^2 \qquad \text{…….....……(3. 30)}$$

where,

$$Rep_r = \frac{(V_w - V_s)d \cdot \rho}{\mu} \qquad \text{.....(3. 31)}$$

In summary, the total energy E in Eq. (3. 19) can be written by [10]:

$$E = i \cdot V_m \cdot A \cdot \gamma \cdot dl \qquad \text{.....(3. 32)}$$

Substituting Eqs. (3. 22), (3. 26), (3. 29), and (3. 32) into Eq. (3. 19) and dividing by $V_m A \gamma dl$ yields:

$$i = i_w + \frac{\overline{q}(\delta_s - 1)V_h}{V_m} + \frac{3}{16}\left[\alpha + \sqrt{\alpha^2 + \frac{4\sqrt{48}\,\alpha\beta}{\left\{\left(\frac{d V_m \rho}{\mu}\right)\frac{\overline{q} - C}{(1-\overline{q})\overline{q}}\right\}}}\right]^2 \cdot \frac{V_m^{\,2}}{g d}\left\{\frac{\overline{q} - C}{(1-\overline{q})\overline{q}}\right\}^2 \overline{q}(1-C)$$

..... (3. 33)

which can be valid to evaluate the hydraulic gradient of settling slurries in pipes. The relationship between $\overline{q}$ and C can be given by [13]:

$$\left\{\frac{(\overline{q} - C)V_m}{\overline{q}(1-\overline{q})\,V_t}\right\}^2 \frac{\left\{\alpha + \sqrt{\alpha^2 + \dfrac{4\sqrt{48}\alpha\beta}{Re_p \dfrac{V_t}{V_m}\dfrac{\overline{q}(1-\overline{q})}{\overline{q} - C}}}\right\}^2}{\left\{\alpha + \sqrt{\alpha^2 + \dfrac{4\sqrt{48}\alpha\beta}{Re_p}}\right\}^2} + (1-\overline{q})^{2(n-1)} \frac{\left\{\alpha + \sqrt{\dfrac{\alpha^2 + 4\sqrt{48}\alpha\beta}{Re_p(1-\overline{q})^{n-1}}}\right\}^2}{\left\{\alpha + \sqrt{\alpha^2 + \dfrac{4\sqrt{48}\alpha\beta}{Re_p}}\right\}^2} - 1 = 0$$

.....(3. 34)

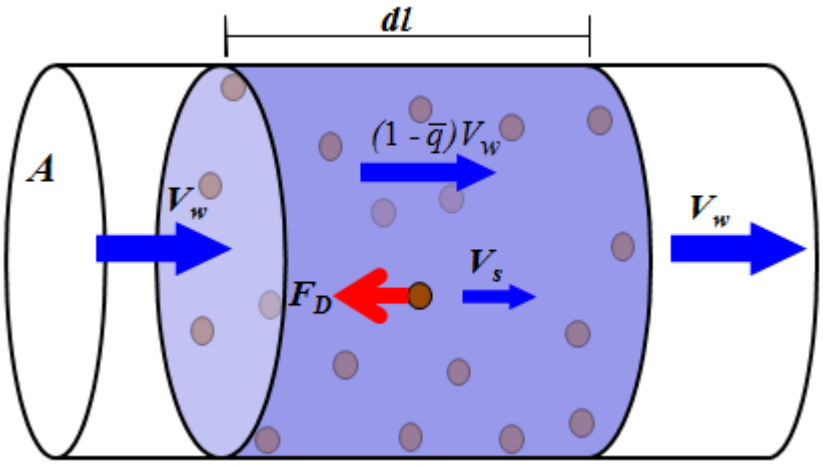

Figure 3. 11 Energy loss due to drag force

Akita University

3.2.2.3 Saltation and Heterogeneous flow of slurry

If the pressure drops of heterogeneous flow in pipes are analysed, the friction factor f between the solids and the pipe decreases with increasing velocity, as reported by Sato et al. [5]. This fact shows that in heterogeneous flow, or intermediate regime between saltation and pseudo-homogeneous flows, some portions of the solids could be assumed to be transported in saltation, or sliding movement and others in suspension.

Transporting the solids in saltation the friction force at the bottom of the pipe, can be represented by:

$$F_f = f \cdot w_{ap}$$

$$= f \cdot \overline{q} \cdot A \cdot dl \cdot (\gamma_s - \gamma) \qquad \text{.....(3. 35)}$$

As a result, the energy lost due to the friction of the solids against the pipe wall can be evaluated by:

$$E_f = F_f \cdot V_s$$

$$= f \cdot \overline{q} \cdot A \cdot dl \cdot (\gamma_s - \gamma) \cdot V_s \qquad \text{.....(3. 36)}$$

For a steady slurry flow, the flow rate Q_{sl} can be represented as:

Akita University

$$Q_{sl} = A \cdot V_m \qquad \text{……...……(3. 37)}$$

Evaluating the discharge flow rate of slurry as the value of Q_{sl},

$$\overline{q} \cdot V_s = C \cdot V_m \qquad \text{…….……(3. 38)}$$

Substituting Eqs. (3. 37) and (3. 38) into Eq. (3. 36) results in:

$$E_f = f \cdot \overline{q} \cdot (\gamma_s - \gamma) \cdot Q_{sl} \qquad \text{…….……(3. 39)}$$

Dividing Eq. (3. 39) by $V_m A \gamma dl$ gives:

$$i_s = f \cdot \overline{q} \cdot (\delta_s - 1) \qquad \text{…...……...…...……... (3. 40)}$$

Lastly, the hydraulic gradient of slurry flow in saltation can be evaluated by [5]:

$$i = i_w + f \cdot \overline{q} \cdot (\delta_s - 1) \qquad \text{…...……... (3. 41)}$$

The condition factor k represented by Eq. (3. 14) could be used to divide the slurry into saltation and suspension portions, as shown in

Akita University

Figure 3. 12. Therefore, the hydraulic gradient due to the solids i_s in slurry can be written as:

$$i_s = k \cdot i_{s1} + (1-k)\, i_{s2} \qquad \text{..... (3. 42)}$$

in which i_{s1} and i_{s2} are excess hydraulic gradients due to sliding particles and suspended particles respectively, as represented by:

$$i_{s1} = f \cdot \overline{q} \cdot (\delta_s - 1) \qquad \text{.....(3. 43)}$$

$$i_{s2} = \frac{\overline{q}\,(\delta_s - 1) V_h}{V_m} + \frac{3}{16}\left[\alpha + \sqrt{\alpha^2 + \frac{4\sqrt{48}\,\alpha\,\beta}{\left\{\left(\frac{d\,V_m\,\rho}{\mu}\right)\frac{\overline{q} - C}{(1-\overline{q})\overline{q}}\right\}}}\right]^2 \cdot \frac{{V_m}^2}{g\,d}\left\{\frac{\overline{q} - C}{(1-\overline{q})\overline{q}}\right\}^2 \overline{q}(1-C)$$

..... (3. 44)

After calculation of i_{s1} and i_{s2}, the hydraulic gradient of slurry flow can be estimated by.

$$i = i_w + i_s \qquad \text{.....} \qquad \text{..... (3. 45)}$$

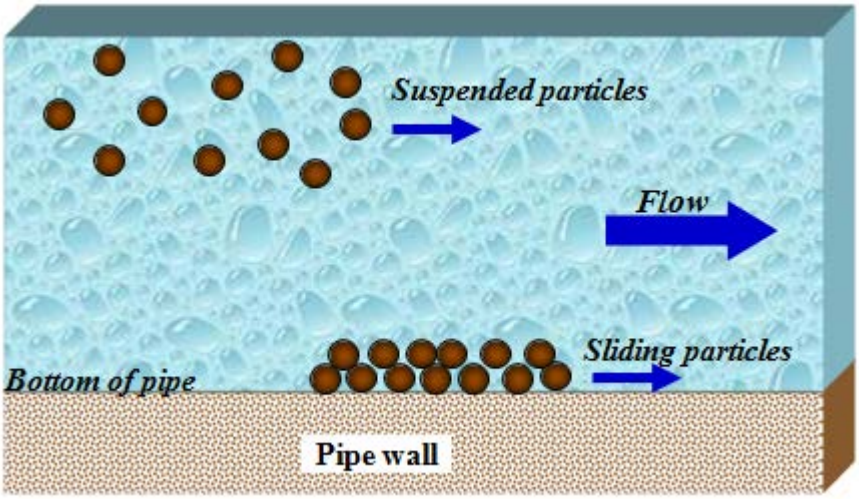

Figure 3. 12 Suspension and sliding of particles in the slurry flow

Akita University

3.3 Verification of the Model with the Database

For confirming the accuracy of evaluating hydraulic gradient of slurry flow with the analytical model, the experimental data (about 3,000 points) in the database reported by Seitshiro et al. [6] were compared with predicted values of *i*, as shown in Figure 3. 13.

It is recognised that the data scattering in a wide range of flow conditions could be found outside the ±20 % boundary (measured in the y-axis). These unsatisfactory predictions could be attributed to not only the application of representative diameter for the solids with a broad size distribution, but of the model for non-settling slurry flow with higher volume concentration than 30 %.

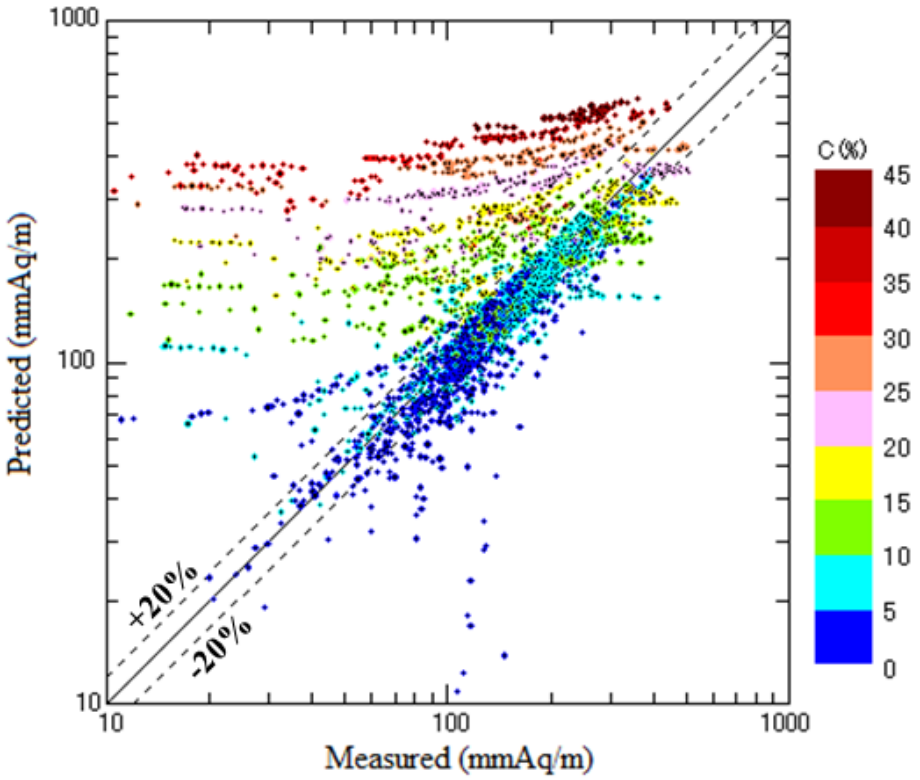

Figure 3. 13 Comparison of predicted hydraulic gradient with the measured (all data in the database)

Akita University

Since the correlations based on heterogeneous flow of suspensions tend to overestimate the hydraulic gradient, as pointed out by Liu **[14]**, the slurry flow should be analysed as the mixture of coarser solids and vehicle, when a larger fraction of fines are especially included in the size distribution. As shown in Figures 3.14 and 3.15, high content of fines in the slurry results in large deviations in comparison of predicted hydraulic gradients against experimentals of Shook et al. [15] and Gillies [16].

If the data are limited to the settling slurry of narrow-sized solids, e.g., for C < 15 % and C < 20 % of experimental results presented by Acaroglu [17] and Sato et al. [10], [18] - [20] respectively, predicted results could be improved, as shown in Figures 3.16 and 3.17.

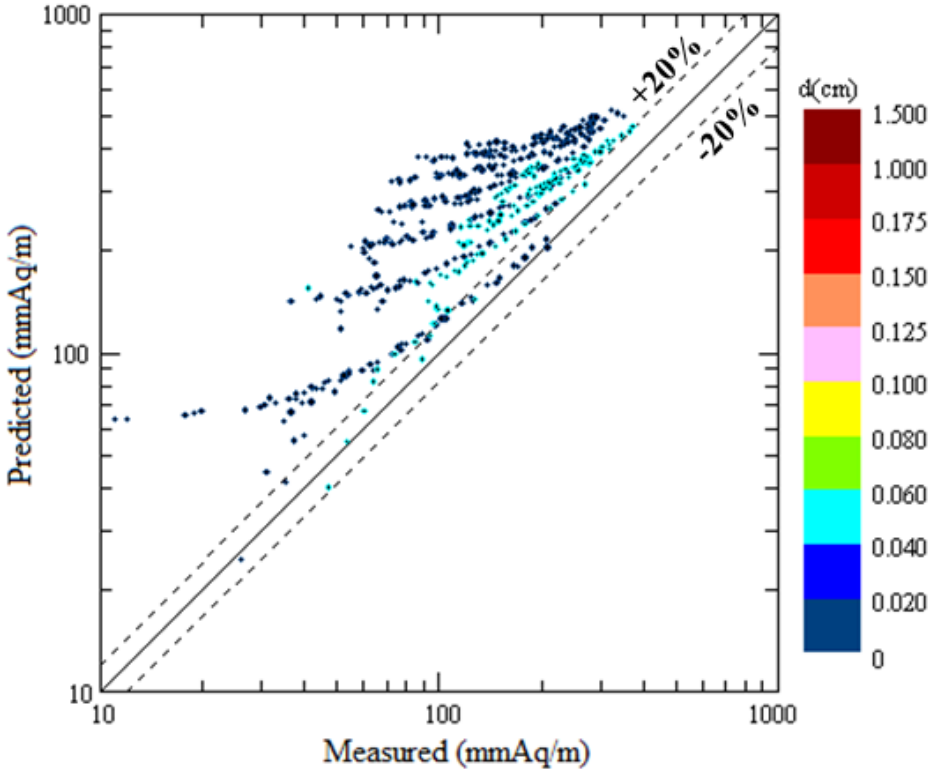

Figure 3. 14 Comparison of predicted hydraulic gradient with the measured data of Shook et al.

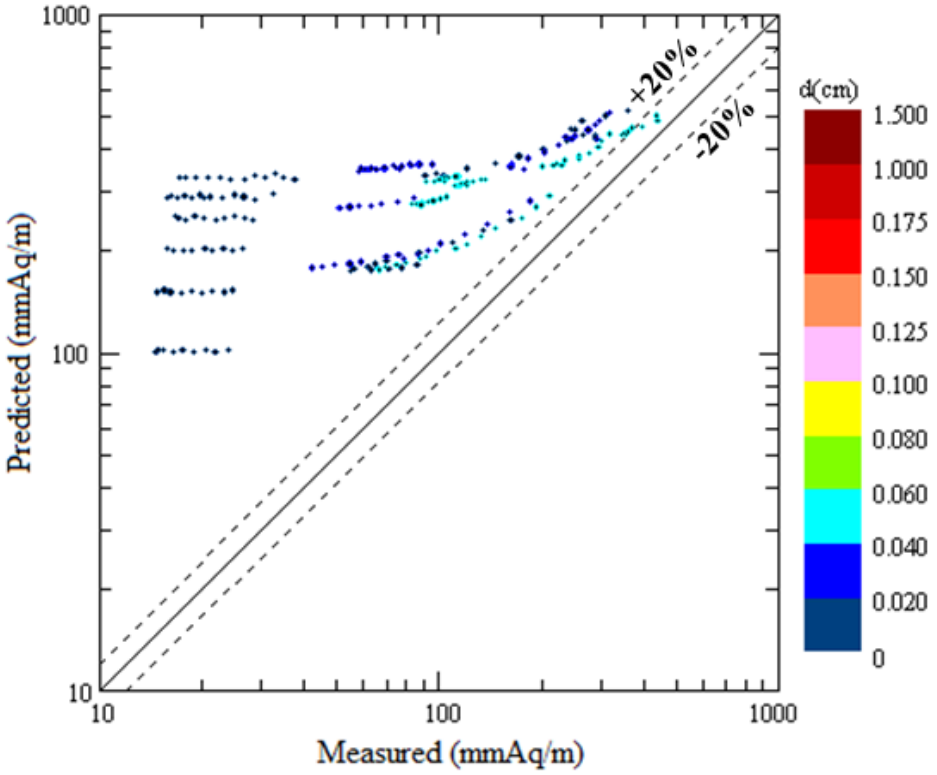

Figure 3. 15 Comparison of predicted hydraulic gradient with the measured data of Gillies

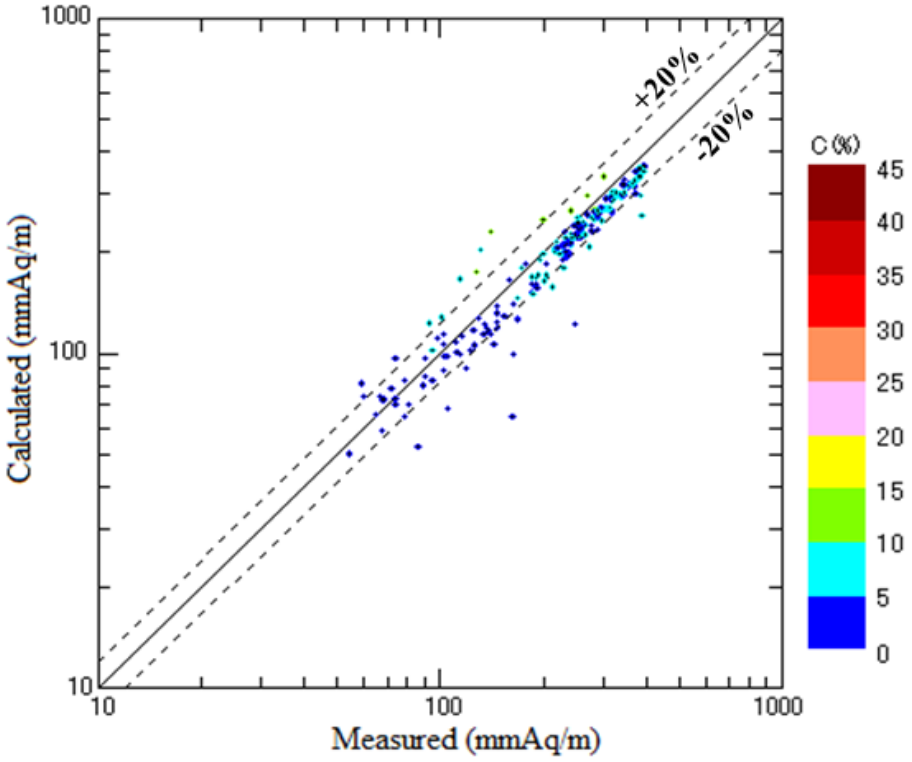

Figure 3. 16 Comparison of predicted hydraulic gradient with the measured data of Acaroglu

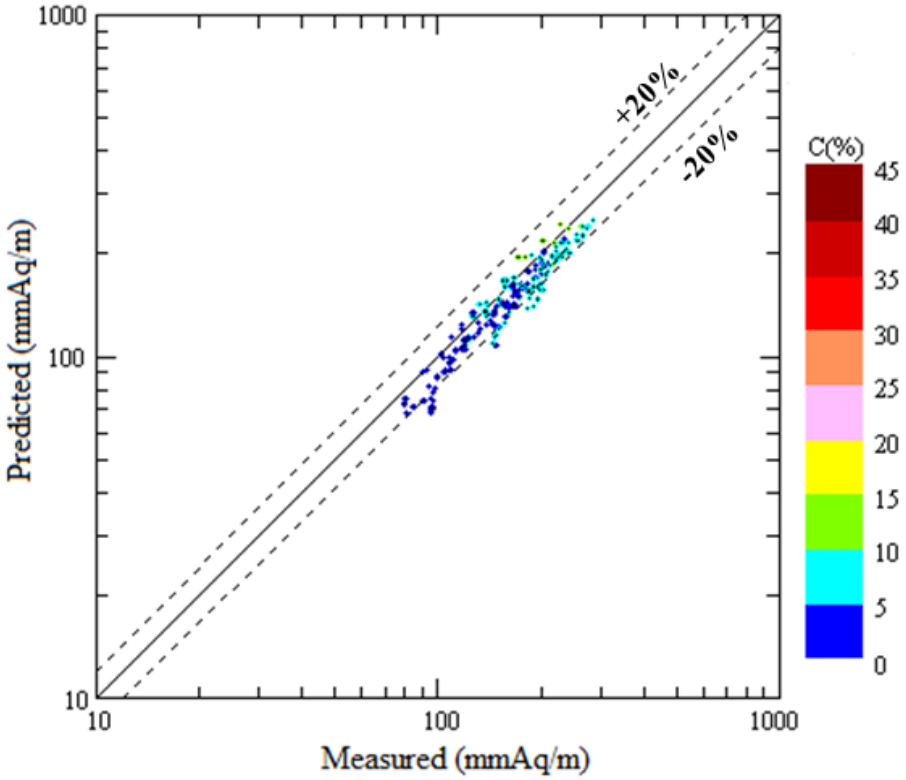

Figure 3. 17 Comparison of predicted hydraulic gradient with the measured data of Sato et al.

Akita University

If the criterion index Re_p*, a generalised particle Reynolds number, can be calculated by;

$$Re_p^* = \frac{d \cdot V_h \cdot \rho}{\mu} \qquad \text{.....(3. 46)}$$

The value of Re_p* coincides approximately with Re_p* = 10, when the solids of sand slurry can be classified into the medium sand in the diameter of 0.25 mm [21] and transported at the limiting lower concentration corresponding to the condition of $V_h = V_t$. Therefore, the following criterion for applicable regime of the settling slurry model is proposed:

$$Re_p^* > 10$$

Figure 3. 18 shows predicted versus measured hydraulic gradient i applying the settling slurry model in the range of Re_p* > 10. Comparison of measured and predicted values of i shows good agreement for slurry transport of solids with relatively broad size distribution in the various sizes of pipes.

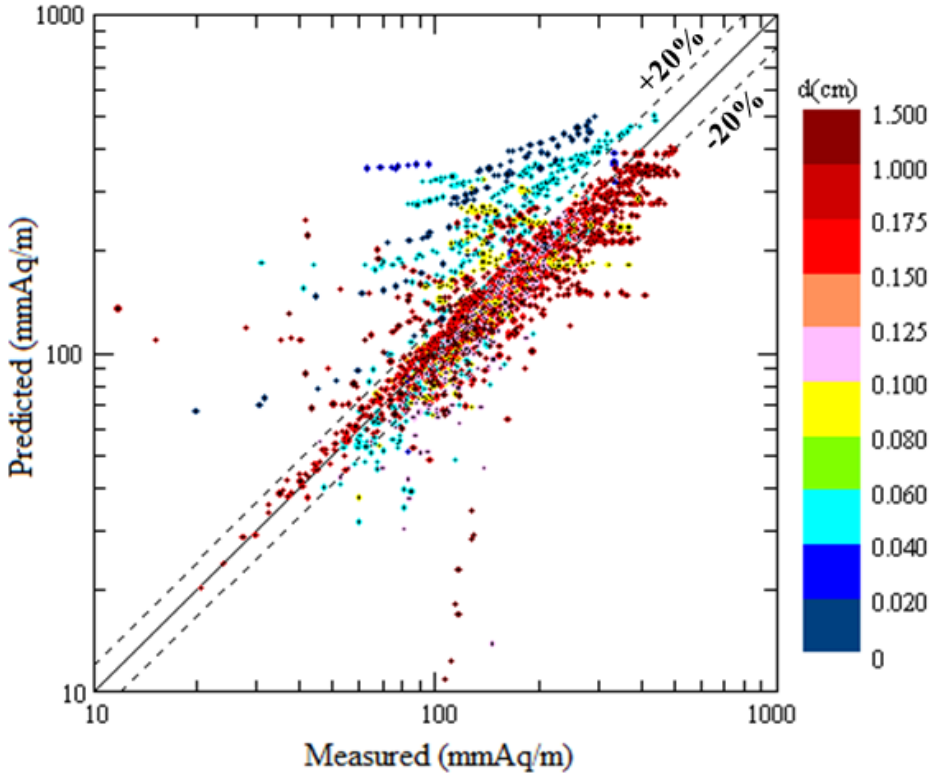

Figure 3. 18 Comparison of measured and predicted hydraulic gradients for slurry transport at the condition of $Re_p^* > 10$

Akita University

3.4 Specific Energy Consumption for Pipeline Design

The design of slurry pipelines involves estimation of the optimum conditions of the transport system. While the minimum part of the curve of the hydraulic gradient versus mean velocity could be chosen as a basic criterion, it is vital to predict the Specific Energy Consumption (*SEC*), the energy required to transport a unit weight of solids over a unit distance, given as:

$$SEC = 9.807 \times 10^{-3} \cdot i \cdot \gamma \cdot Q/M_s \qquad \text{..... (3. 47)}$$

in which M_s (in kg/s) is the solid flow rate through a pipeline, and can be calculated by:

$$M_s = Q \cdot C \cdot \gamma_s \qquad \text{..... (3. 48)}$$

Substituting Eq. (3. 48) into Eq. (3. 47), the *SEC* in kW·h/t·km can be expressed as:

$$SEC = \frac{2.726 \cdot i}{C \cdot \delta_s} \qquad \text{.....(3. 49)}$$

According to the Eq. (3. 49), the design transport velocity should be determined as the velocity at which the *SEC* values reach minima, or

Akita University

$\partial i/\partial V_m = 0$ on the $i - V_m$ curves. Figures 3. 19(a) and (b) show the *SEC* versus mean velocity curves computed for two different pipe sizes of 25 mm and 50 mm diameters at various delivered volume concentrations. Increasing the concentration and the pipe diameter, the *SEC* at the minimum point on the curves decreases. However, Cabrera [22] recommend that the solid concentration of settling slurries with coarse particles should be lower than 20 % to 40 % by weight.

In some commercial pipelines it is rather difficult to keep definite transport conditions such as the mean velocity of slurry V_m, delivered concentration C, and so on. However the volumetric concentration of C = 0.25 is reported as a commonly-used-fraction of solids in the slurry [23]. Therefore, the computed relationship between flow rate Q and pipe diameter D at the optimum transport conditions which exist on the minimum SEC point at C = 0.25 can be shown in Figure 3. 20. Based on the results, the influence of the particle size is almost negligible in the range of d < 2.0 mm.

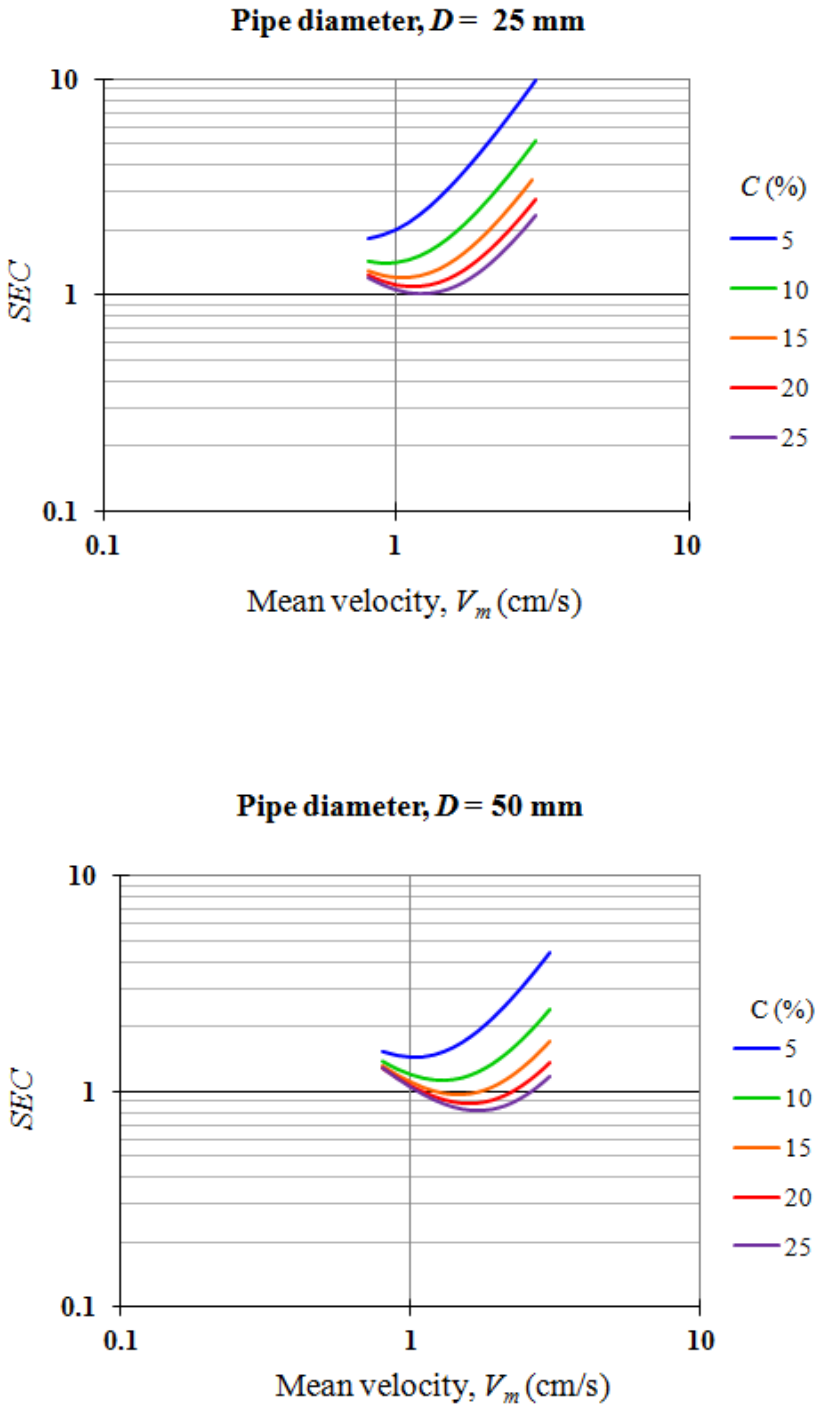

Figure 3. 19 Specific Energy Consumption (*SEC*) versus mean flow velocity at different concentrations of solids: (a) *D* = 25 mm; (b) *D* = 50 mm

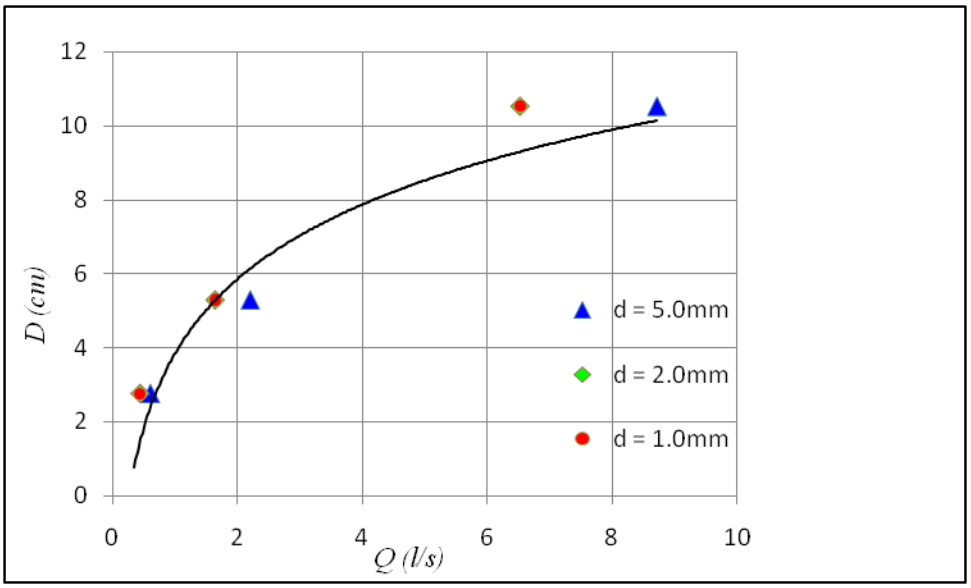

Figure 3. 20 Variation of pipe diameter for minimum values of Specific Energy Consumption (*SEC*) with flow rate

Akita University

In summary, the pipeline design procedure for settling slurry transport is recommended as follows:

1. Determine the particle size of solids in accordance with system requirements.
2. Select the volumetric concentration of $C = 0.25$.
3. Determine the slurry flow rate Q with the solid flow rate M_s.
4. By using Figure 3.20, select the pipe size D which assures the minimum SEC at the flow rate of Q.
5. Determine the mean velocity V_m of slurry flow and the hydraulic gradient at the velocity, based on the analytical model proposed in this chapter.

Akita University

3.5 Conclusions

1) Applying the analytical model of settling slurry flow to practical designs, the settling slurry index Re_p* is useful for the improvement of prediction accuracy.

2) The verification of the proposed model can be proved with the slurry database which includes more than three thousand experimental measurements.

3) The data scattering in the relationship between predicted and measured hydraulic gradients could be due to the broad size distribution of solids and non-settling slurry flow.

4) The minimum *SEC* in the unit of the kilowatt-hour for tonne-kilometre decreases as the delivered concentration and pipe diameter increases.

5) At the optimum conditions of settling slurry transport, the pipe diameter in pipelines is related with the flow rate of the slurry, independent on the particle size in the range of less than 2.0 mm.

6) It appears that the design method proposed in this paper can be applied to the pipeline design without any scale-up, since it is based on the database which covers the practical scales of pipe diameter.

Akita University

3.6 References

[1] Elsibai, N. G., Snoek, P. E., and Pitts, J. D.: How Particle Size Affects the Cost of Short Distance Coal-Slurry Pipelines, *J. of Oil and Gas, Technology,* 253-259, (1982).

[2] Kazanskij, I.: Scale-up Effects in Hydraulic Transport Theory and Practice, Hydrotransport 5, 5th Int. Conf. on the Hydraulic Transport of Solids in Pipes, Germany, Paper B3, 47–79, (1978).

[3] Abulnaga, B: Slurry Systems Handbook, McGraw Hill Publishing, USA, pp. 4.1 - 4.68, (2002).

[4] King, R. P.: Introduction to Practical Fluid Flow, Butterworth-Heinemann Publishers, England, pp. 83-107, (2002).

[5] Sato, H., Cui, Y., Sato, I., Yamaguchi, S., Nakazawa, A., and Adachi, H.: The Effect of Flow Pattern of Slurry Flow on Pressure Loss in Horizontal Pipes, Proc. ASME Fluids Engng. Div. Summer Meeting FEDSM'03, Honolulu, Hawaii, USA, 1-6, (2003).

[6] Seitshiro, I. Sato, I., and Sato, H.: Development and Application of Slurry Transport Database, *J. of Min. and Metall. Inst. of Japan*, **127**, 77-81, (2011).

[7] Abulnaga, B.: pp. 1.15–1.17, from previously cited Ref. [3]

[8] Darby, R: Hydrodynamics of Slurries and Suspensions, Encyclopaedia of Fluid Mechanics, **5**., Slurry Flow Technology, Gulf Publishing Company, USA, pp. 50-87, (1986).

[9] Kazanskij, I.: 50-51, from previously cited Ref. [2]

Akita University

[10] Sato, H., Takemura, S., Takamatsu, H., and Cui, Y.: An Improved Wasp Method for the Hydraulic Gradient of Slurry Flow with Size Distribution in a Horizontal Pipe, Proc. ASME Fluids Engng. Div. Summer Meeting FEDSM'97, Vancouver, British Columbia, Canada, No. 1400CD, 1-11, (1997).

[11] Hibbeler, R. C.: Engineering Mechanics-Statics, 12th Edition, Prentice Hall PTR Publishers, USA, pp. 447-492, (2008).

[12] Sato, H., Otsuka, K., and Cui, Y.: A Model for the Settling Slurry Flow with a Stationary Bed in a Pipe, Proc. 4th Int. Symp. in Liquid-Solid Flows, Portland, Oregon, USA, **FED-118**, 54-55, (1991).

[13] Sato, H., Otsuka, K., and Cui, Y.: General Correlations of In Situ Concentration and Slip Velocity-Theoretical Considerations on the Mechanism of Slurry Flow with the Stationary Bed in a Pipe, *J. of Min. and Metall. Inst. Of Japan*, **105**, No. 6; 457-463, (1989).

[14] Liu, H.: Pipeline Engineering, Lewis Publishers, USA, p. 142, (2003).

[15] Shook, C. A., Schriek, W., Smith, L. G., Haas, D. B., and Husband, W. H. W.: Experimental Studies on the Transport of Sands in Liquids of Varying Properties in 2 and 4 inch Pipelines, Saskatchewan Research Council, **VI**, 1-158, (1973).

[16] Gillies, R. G.: PhD Thesis, University of Saskatchewan, (1993).

[17] Acaroglu, E. R.: PhD Thesis, Cornell University, (1968).

Akita University

[18] Sato, H., Otsuka, K., and Cui, Y.: 53-63, from previously cited Ref. [12].

[19] Sato, H., Cui, Y., Sugimoto, F., and Tozawa, Y.: Determination of Distributions of Velocity and Concentration of Solids in a Horizontal Slurry Pipeline with a Digital Video Camera System, *Int. Society of Offshore and Polar Engineers*, **1**, 44-51, (1998).

[20] Sato, H., and Kawahara, M.: Critical Deposit Velocity of Slurry Flow Including Single-size Solid particles, Proc. 2nd Int. Conf. on Multiphase Flow, Kyoto, Japan, 23-30, (1995).

[21] United States Department of Agriculture: USDA Textural Classification, Soil Mechanics Study Guide, 5-7, (1987).

[22] Cabrera, V. R.: Slurry Pipelines; Theory, Design and Equipment, *J. of World Mining*, 56-65, (1979).

[23] Jacobs, B. E. A.: Design of Slurry Transport Systems, Elsevier Science Publisher L.T.D, England, pp. 1-9, (1991).

Akita University

CHAPTER 4

The Multi-Sized Slurry Flows in Horizontal Pipes: Innovated Models and Verification

In designing pipeline systems for commercial slurries, it is essential to accurately determine the hydraulic gradient at transport velocities. It is crucial to note that the slurries are conveyed as a mixture of multi-sized solids and water. Although many researchers have proposed correlations for the prediction of hydraulic gradient, most have been developed for slurries with uniform sized particles of solids.

By considering two different transport conditions of a mixed-sized slurry, innovated models were proposed and then verified with experimental data. The data was also analysed with the Wasp method and the conventional method by Condolios-Chapus.

Measurements of hydraulic gradient, solids concentration, and flow velocity in a 1-inch pipeline were made in this study. Predictions with the innovated models could be correlated with the data including experimental results from large-scale pipelines, in spite of discrepancies at unstable flow regimes.

Akita University

4.1 Introduction

Although multi-sized particles slurries are transported in practical pipelines, most reported correlations were proposed for single-size slurries. If the average diameter of solids is used to estimate the drag coefficient of multi-sized particles slurries, the hydraulic gradients with these correlations lead to considerable scatter of data [1]. Kazanskij [2], Moro [3], and STSJ (Slurry Transport Society of Japan) [4] summarised some empirical equations of hydraulic gradient of slurry flow with experimental data. The Wasp method [5] recommended by Liu [6] has been used by designers of pipeline systems for predicting hydraulic gradient of compound slurries of homogeneous and heterogeneous flows. However, the range of application of the method is limited. Kaushal et al. [7] also discussed the limitations and attempted to modify the method. They concluded that the Wasp method provided reasonable accurate results at limited low concentrations.

This chapter discusses the limitations of application of other researchers' correlations and to develop innovated models, based on the single size slurry model of Seitshiro et al. [8]. The analytical models depend on particle size distribution: (1) coarse-coarse model; for a slurry consisting of two different coarse solids flowing in water, and (2) coarse-fine model; for coarse solids being transported in a modified vehicle containing fine particles in high concentration. The fine solids

Akita University

are defined as particles with sizes smaller than the critical diameter [9] in this study. For both models, it is assumed that the coarse solids in the slurry do not hinder each other's movements.

Experiments were performed in a 1-inch transparent pipe with sand-bakelite mixed slurries. The data of Shook et al. [10], Boothroyde et al. [11], and that of this study were used to verify the application of the models. The analytical results suggest that the innovated models can be effective for designing slurry pipelines.

4.2 Experimental

For verifying the applicability of the models, a wide range of data from three different systems is used: a 1-inch pipeline system of the authors, closed and open loop systems of Shook et al. [10], and prototype systems of Boothroyde et al. [11]

4.2.1 Experimental techniques

The experiments were conducted in a closed-loop, horizontal transparent perspex pipe of diameter 2.62 cm and length 25.7 m, presented schematically in Figure 4.1. For clarifying the solids behaviours, two different kinds of solids, sand and coloured bakelite were used for the mixed-sized slurry flow experiments: particle sizes

Akita University

ranging from 1.21 mm to 2.18 mm; maximum concentration of 25 %. Details of the transport conditions are summarised in Table 4.1.

For the mixed-sized slurry flow, solids were fed into the mixing tank and transported through the pipeline by the centrifugal Warman pump. Delivered concentration was adjusted by varying the volume of the solids and the speed of the motor that drove the pump with the flow control panel. The range of transport velocities was 70 cm/s to 230 cm/s. At half-hour intervals, the movement of solids was visually monitored at the illuminated observation section, and digital and video cameras captured images for confirming flow patterns. After the slurry flow stabilised, the pressure drops at the interval of 1.89 m were measured with the differential pressure transducer. A weighing cage was used to collect solids at the outlet of the loop and determine the delivered concentrations from the values of the weight.

4.2.2 Characteristics of reported data

4.2.2.1 Boothroyde et al. data

Boothroyde et al. carried out field tests to find the correlations for predicting hydraulic gradient of colliery spoil flow in pipes. It consists of a 200 mm diameter- primary circuit of 100 m length, and 250 mm and 150 mm subsidiary loops conveying granite particles of 12 mm diameter and Markham coal fines of 0.2 mm. For the analysis of the correlations,

Akita University

the data of the 200 mm circuit was used in the report. Summary of the data is displayed in Table 4.2.

4.2.2.2 Shook et al. data

The data of Shook et al. represented a range of practical pipeline transport conditions and solids flow phenomena. Two horizontal systems of 2-inch-closed and 4-inch-open loops were used in the experimental research with sand particles of 0.198 mm to 0.54 mm sizes and specific gravity of 2.65. The slurries were transported at mean velocities of 55 cm/s to 378 cm/s, and concentration by volume of up to 42 %. Full contents of the experiments can be found in Table 4.3.

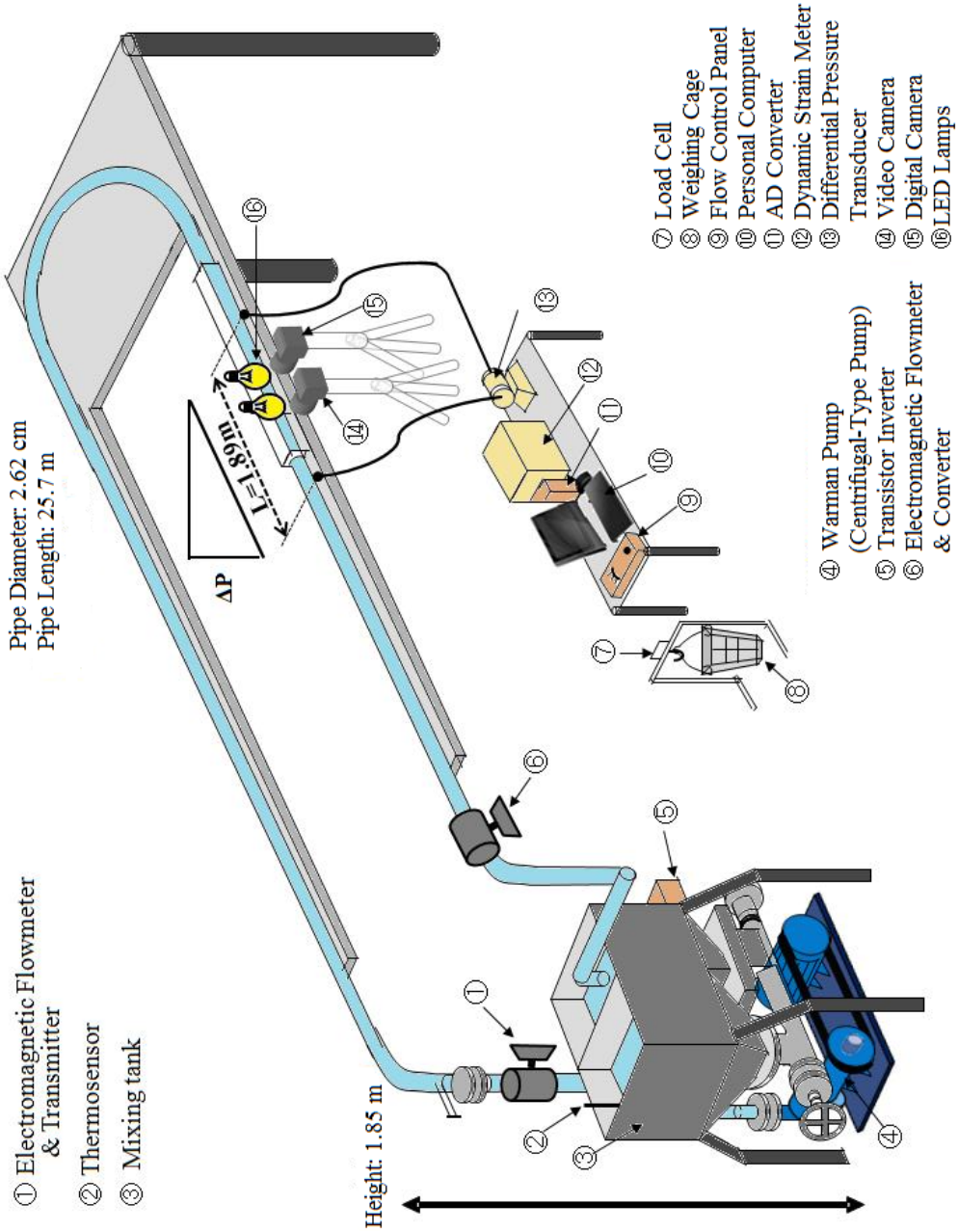

Figure 4.1 Schematic diagram of the experimental apparatus

Akita University

Table 4.1 Slurry transport conditions of the laboratory experiments

Solids	Sand	Bakelite
Particle diameter, d (mm)	1.21 ~ 1.71	1.71 ~ 2.18
Specific gravity of solids, δ_s (-)	2.67	1.40
Pipe diameter, D (cm)	2.62	
Loop length, l (m)	25.7	
Terminal velocity, V_t (cm/s)	16.63	7.24
Mean flow velocity, V_m (cm/s)	70 ~ 230	
Delivered concentration, C (%)	2 ~ 25	

Table 4.2 Summarised characteristics of Boothroyde et al. data

Solids	Granite	Markham coal fines
Particle diameter, d (mm)	12	0.2
Specific gravity of solids, δ_s (-)	2.8	1.5
Pipe diameter, D (cm)	20.3	
Mean flow velocity, V_m (cm/s)	206.9 ~ 672.3	
Delivered concentration, C (%)	27.3 ~ 50	

Table 4.3 Slurry transport conditions of the representative data of Shook et al.

Pipeline loop	Closed			Open
Carrier	Water			
Pipe diameter, D (cm)	5.25			10.30
Particle diameter, d (mm)	Mixture of solids in : $\begin{pmatrix} 0.198 \\ 0.210 \\ 0.297 \\ 0.540 \end{pmatrix}$			Mixture of solids in : $\begin{pmatrix} 0.198 \\ 0.210 \\ 0.540 \end{pmatrix}$
Mean flow velocity, V_m (cm/s)	55.8 ~ 378.0			86.0 ~ 374.0
Delivered concentration, C (%)	5 ~ 42			1.4 ~ 41.9
Temperature, t (°C)	60.0	21.1	10.0	21.1

Akita University

4. 3 Analysis of reported correlations

4.3.1 The Wasp method

The model developed by Wasp et al., has been used satisfactorily for compound slurries, homogeneous-heterogeneous slurries [5]),[6],[7]. The procedure is composed of calculation blocks as illustrated in Figure 4.2. When a mixed-sized slurry of different sizes of $d_{1,}$ d_2, ···, d_n with corresponding volume concentration q_1, q_2, ···, q_n flows in a horizontal pipe, each size fraction of slurry can be divided into the homogeneous and heterogeneous parts, q_{vi} and q_{Hi} respectively, as shown in Figure 4.3, according to Wasp method. This method has analytical restrictions for application to multi-sized slurries:

(1) the criteria for splitting the multi-sized slurry into vehicle and heterogeneous portions;

$$log\frac{q_w}{q_0} = -1.8\frac{V_t}{\beta\cdot\kappa\cdot V_*} \qquad \text{.....(4.1)}$$

(2) applicability of the Durand-Condolios equation;

$$\phi = 82\psi^{-1.5} \qquad \text{.....(4. 2)}$$

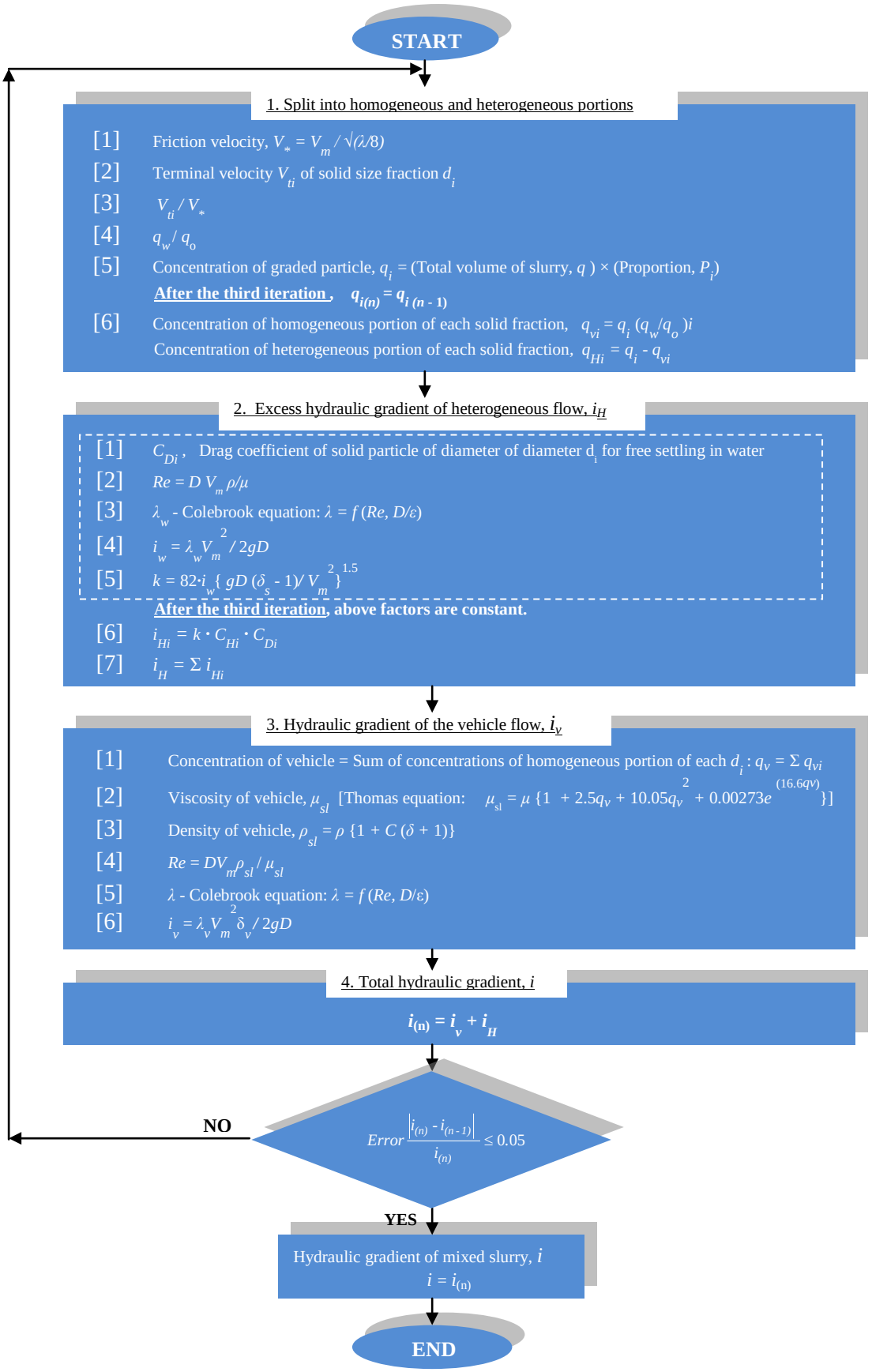

Figure 4.2 Flowchart of the calculation procedure of the Wasp method

Akita University

4.3.1.1 Criteria for splitting the slurry into two flows

Wasp et al. [5], [12] discussed multi-sized slurry flows containing solids of different sizes d_1, d_2, ..., d_n. Each portion of the solids is then split into vehicle and heterogeneous parts depending on transport conditions, as shown in Figure 4.3, by using the Eq. (4.1) as a criteria; where β = 1 and κ = 0.35 for slurry flow [12]; q_w and q_0 are the in-situ concentrations of solids at the point 92 % from the bottom and at the centre of the pipe respectively; V_t is the terminal velocity of the solids, and V_* is friction velocity. Eq. (4.1) could be derived from the O'Brien equation [13] which is only valid for low concentration slurries [14].

4.3.1.2 Hydraulic gradient of homogeneous portion

The homogeneous portions of the slurry should be assumed to be Newtonian flow under volume concentration of 30 % approximately [15]. In this region, the hydraulic gradient of the homogeneous portion is calculated by the modified Darcy-Weisbach equation:

$$i_v = \frac{\lambda_v \cdot V_m{}^2 \cdot \delta_v}{2 \cdot g \cdot D} \qquad \text{.....(4.3)}$$

with the vehicle's values of ρ_{sl} evaluated by:

$$\rho_{sl} = \rho\{1 + C \cdot (\delta - 1)\} \qquad \text{.....(4.4)}$$

Akita University

where λ is friction factor calculated by the Colebrook equation [16]. As concentration increases, the slurry viscosity μ_{sl} increases. The value of μ_{sl} depends, however, not only on concentration but particle size distribution, shape, size, and kinds of solids of suspension [17]. Wasp et al. [12] recommended an experimental correlation to estimate the viscosity in his report:

$$\mu_{sl} = (\mu + A)e^{B \cdot V_R} \qquad \text{.....(4.5)}$$

where A and B are constants depending on the characteristics of the solids and fluid, and V_R is volumetric ratio of solids to water, $\{V_R = C/(1-C)\}$.

If rheological characteristics could not be determined experimentally, the Thomas equation [18] should be recommended as an alternative to predict the value of μ_{sl}:

$$\mu_{sl} = \mu\left\{1 + 2.5\,C + 10.05\,C^2 + 0.00273\,e^{(16.6C)}\right\} \qquad \text{.....(4.6)}$$

because Eq. (4.6) has been applied in the slurry industry to characterise Newtonian rheology of mixtures with higher volume concentrations [19].

Akita University

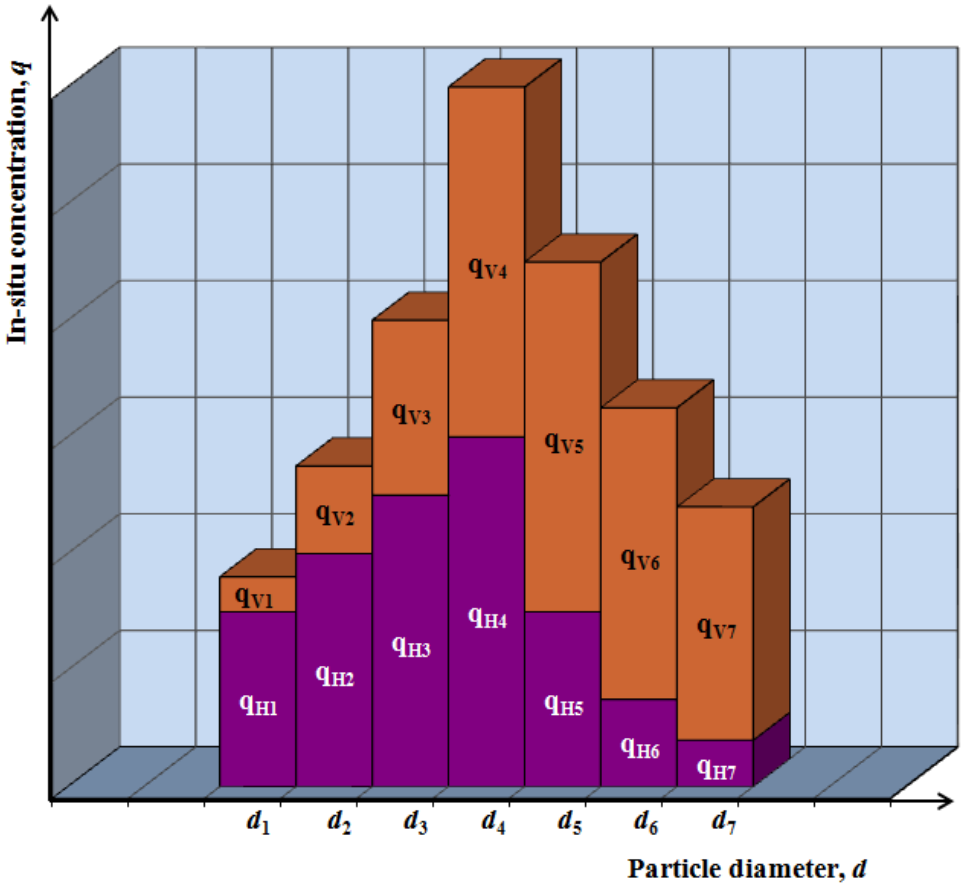

Figure 4.3 The split portions of vehicle and heterogeneous flows based on the Wasp method

Akita University

4.3.1.3 Hydraulic gradient of heterogeneous portions; applicability of the Durand-Condolios equation

For each heterogeneous portion of the solids in Figure 4.3, excess hydraulic gradient i_{Hi} can be estimated by the Durand-Condolios equation (4.2),

where; $$\phi = \frac{i - i_w}{i_w \cdot C} \qquad \text{.....(4.7)}$$

and $$\psi = \frac{V_m{}^2 \cdot \sqrt{C_{Dm}}}{g \cdot D \cdot (\delta - 1)} \qquad \text{.....(4.8)}$$

Wasp et al. [5] recommended K_D = 82 as the constant value in the Eq. (4.2), although the coefficient and the index of the correlation depend on transport conditions, as shown in Table 4.4 [2]. Figure 4.4 shows representative analytical results of K_D for the slurry flow in the 2.54 cm diameter pipeline based on the settling slurry model [8]. As concentration and particle size (in the range of d < 2 mm) decrease, the value of K_D increases. However, the analysis of representative data of single-size slurry of sand and bakelite, and sand-bakelite mixed slurries in this study does not coincide with the Durand-Condolios correlation, as shown in Figure 4.5.

Nevertheless, according to the Wasp method, the hydraulic gradient of each heterogeneous portion can be calculated by:

$$i_{Hi} = 82 \cdot (i_w \cdot C_{Hi}) \cdot \left\{ \frac{V_m{}^2 \sqrt{C_{Di}}}{gD(\delta_s - 1)} \right\}^{-1.5} \qquad \text{.....(4.9)}$$

Akita University

Table 4.4 Coefficients and indices of the Durand-type equation for heterogeneous slurries

Researcher	Published year	K_D	n
1. Durand & Condolios	1954	81	1.5
2. Condolios & Chapus	1963	85	1.5
3. Bonnington	1961	71	1.5
4. Chaskelberg & Karlin	1962	78	1.4
5. Ellis et al.	1963	385	1.5
6. Kazanskij	1967	134	1.4
7. Zandi & Govatos	1962	6.3	0.354
		280	1.93
8. Babcock	1970	6.3	0.254
9. Welte	1971	36	1.37

NOTE: Summarised after Kazanskij [2]

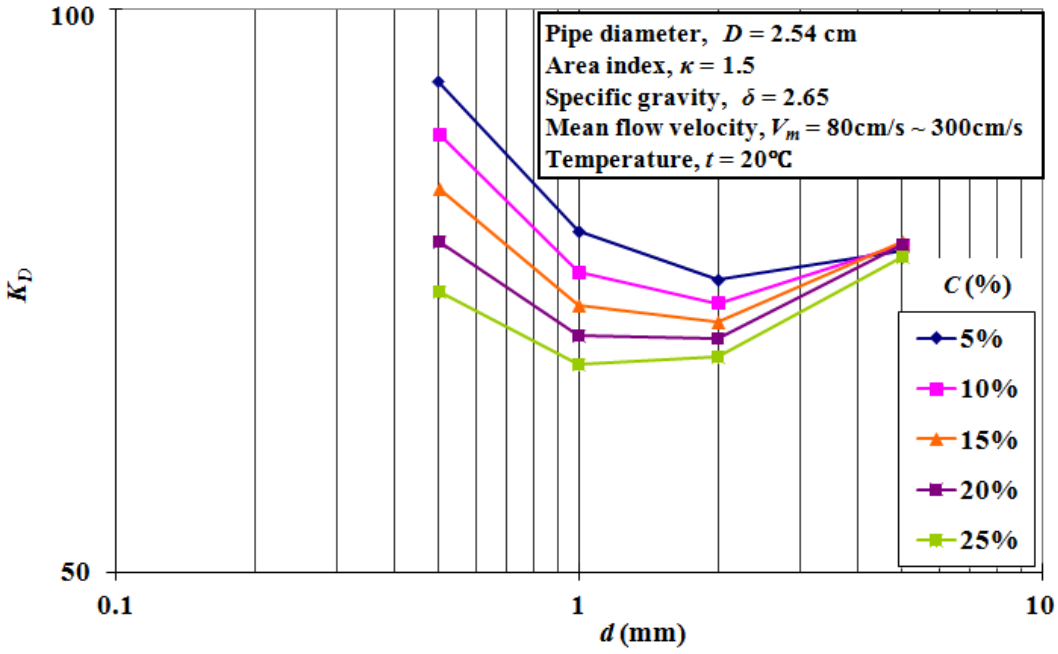

Figure 4.4 Effects of transport conditions on the value of K_D in the Durand-Condolios equation

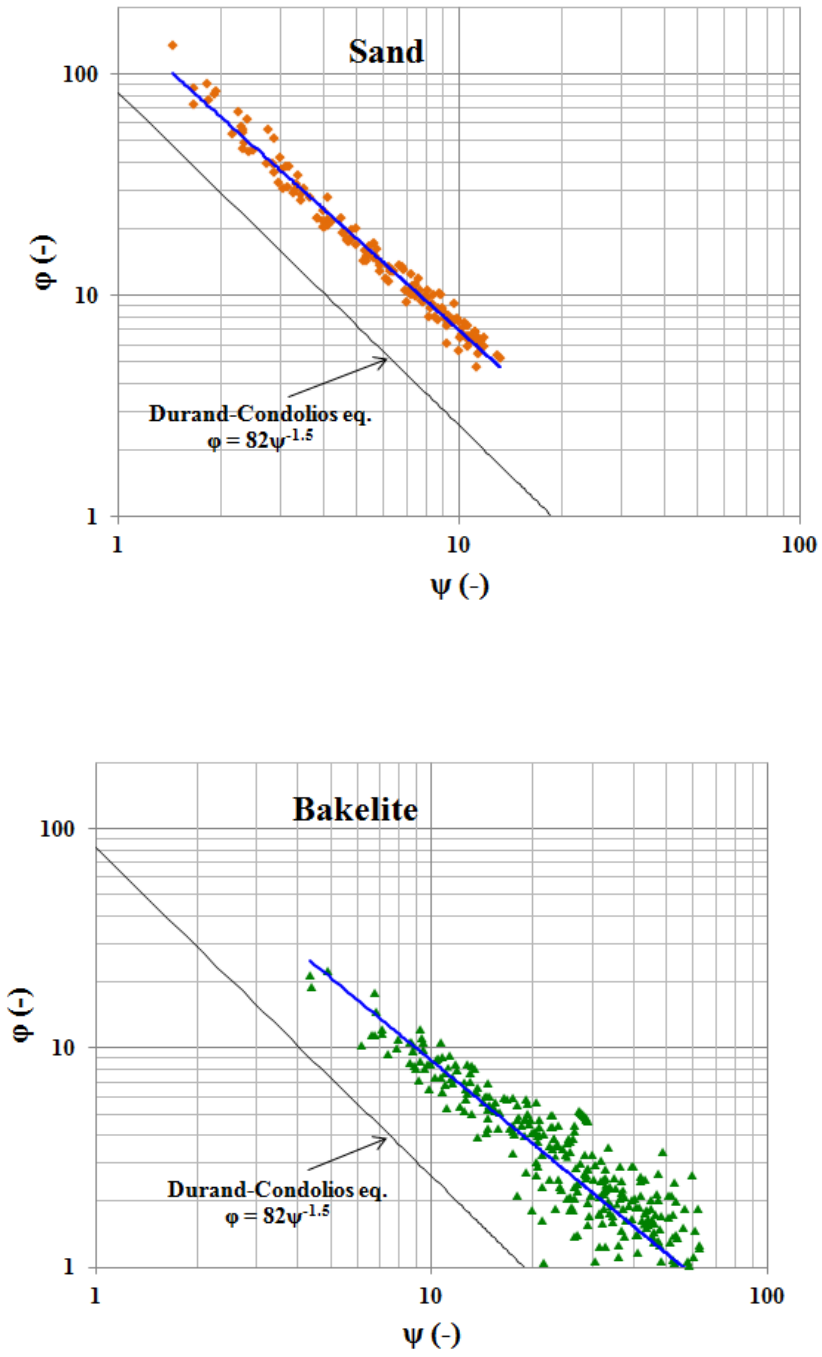

Figure 4.5(a) Comparison of representative results of single-size slurries of sand and bakelite against calculated results with Durand-Condolios equation.

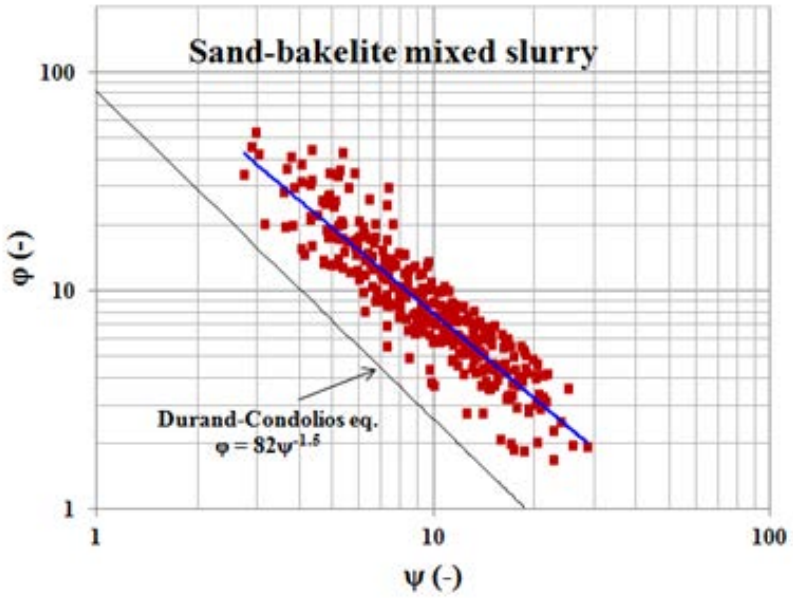

Figure 4.5(b) Comparison of representative results of the sand-bakelite mixed slurry against calculated results with Durand-Condolios equation.

Akita University

4.3.1.4 Total hydraulic gradient of slurry

The hydraulic gradient of the multi-sized slurry can lastly be represented as the sum of vehicle and heterogeneous components, as follows:

$$i = \sum i_v + \sum i_{Hi} \qquad \text{.....(4.10)}$$

The Wasp method for mixed slurries flows was developed based on experiment data of coal pipelines [12].

4.3.2 Condolios-Chapus method

To predict the hydraulic gradients of mixed-sized slurries including a wide size distribution of solids, the following Durand-type equation has been used [1]:

$$\phi = \frac{i - i_w}{i_w \cdot C} = K_D \left[\frac{V_m{}^2 \sqrt{C_{Dm}}}{g \cdot D \cdot (\delta - 1)} \right]^{-n} \qquad \text{.....(4.11)}$$

According to the Condolios-Chapus method, the drag coefficient of the solids C_{Dm} in the Eq. (4.11) can be calculated by [20]:

$$\sqrt{C_{Dm}} = x_1\sqrt{C_{D1}} + x_2\sqrt{C_{D2}} + x_3\sqrt{C_{D3}} + ... + x_n\sqrt{C_{Dn}} \qquad \text{.....(4.12)}$$

$$\sqrt{C_{Dm}} = \sum \left(x_i \sqrt{C_{Di}} \right) \qquad \text{.....(4.13)}$$

Akita University

where x_i is a proportion of the solids and C_{Di} represents the drag coefficient of each proportion. The method can be schematically shown in Figure 4.6. It should also be noted that no limitations of the application range have been reported.

If the slurry contains a wide range of sizes of solids, as shown in Figure 4.7, it should be split into two parts of vehicle and coarser solids flows. In these commercial slurries, the Eq. (4.12) cannot be valid for calculation of C_{Dm} of vehicle flows.

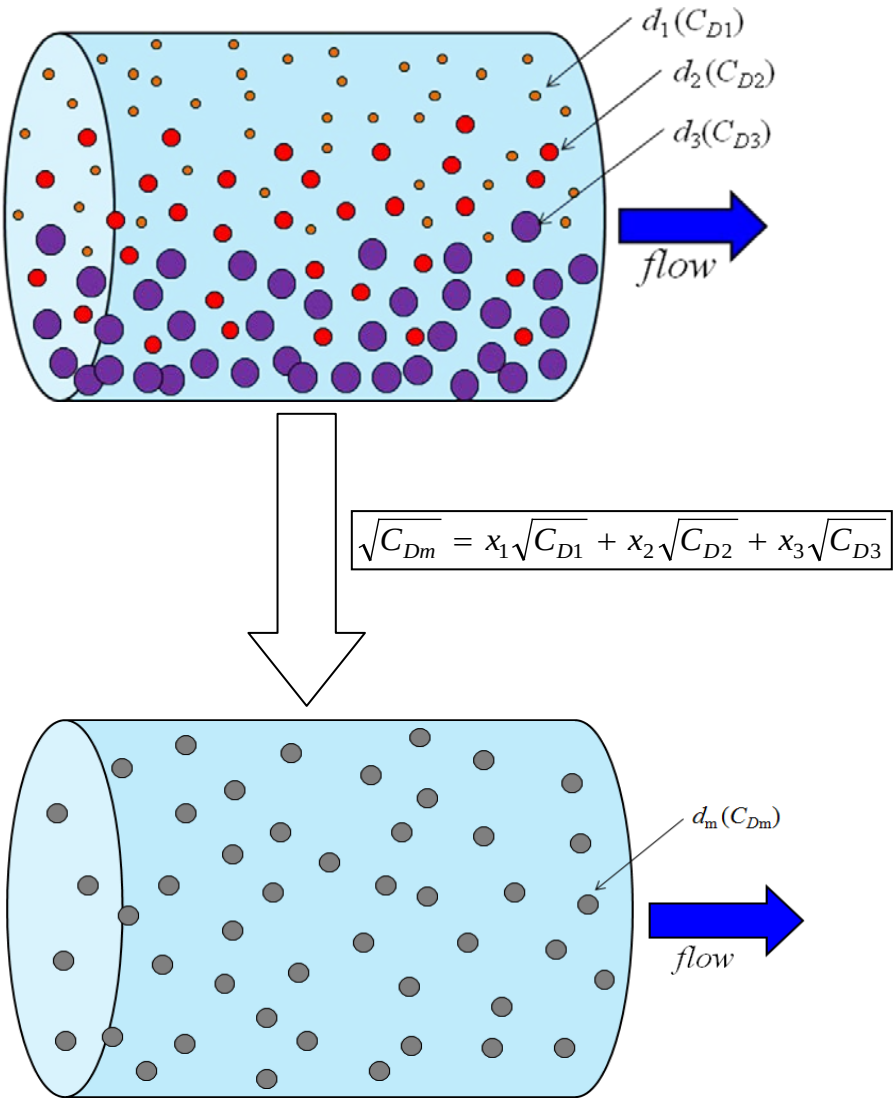

Figure 4. 6 The calculation procedure of representative drag coefficient proportions in a mixed-sized slurry

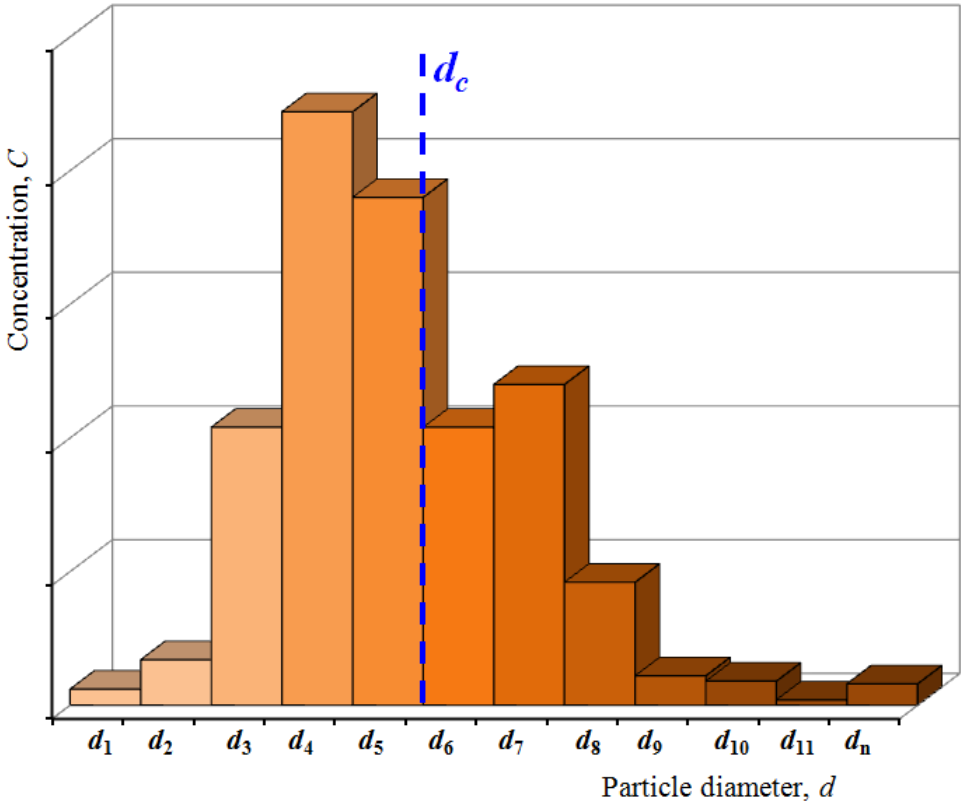

Figure 4. 7 Typical sieve analysis of a multi-sized slurry solids distribution

Akita University

4.4 Theoretical consideration of the innovated models

The behaviour of slurry in pipes is dependent on not only flow velocity, concentration, pipe diameter, and solids density, but also particle size distribution. Fines portion of the slurry affects its rheology. In practical pipelines, two representative types of the size distribution could exist: type-1; all solids are larger than the critical diameter, $d_i > d_c$, and type-2; the slurry contains large portion of fines, as shown in Figure 4.8.

4.4.1 Coarse-coarse particles slurry model

This model can be applied to the slurry with type-1-solids distribution, in which the sieve analysis results can be schematically represented by Figure 4.9. Average diameter d_m has been conventionally used as a representative diameter of the solids for predicting hydraulic gradients of slurry. However, if the slurry contains a wide range of solid particle sizes larger than d_c, the use of d_m leads to the scatter of the predicted results [1].

In this study, the analytical model applicable to practical design of coarse-coarse slurry flow was proposed: based on the sieve analysis, shown in Figure 4.9, the contributes of each size solids portion to the

Akita University

slurry flow could be summarised to calculate the hydraulic gradient for solids i_s, as follows:

$$i_s = \sum i_{si} \qquad \text{..... (4.14)}$$

where i_{si} = contributed value of particle size d_i.

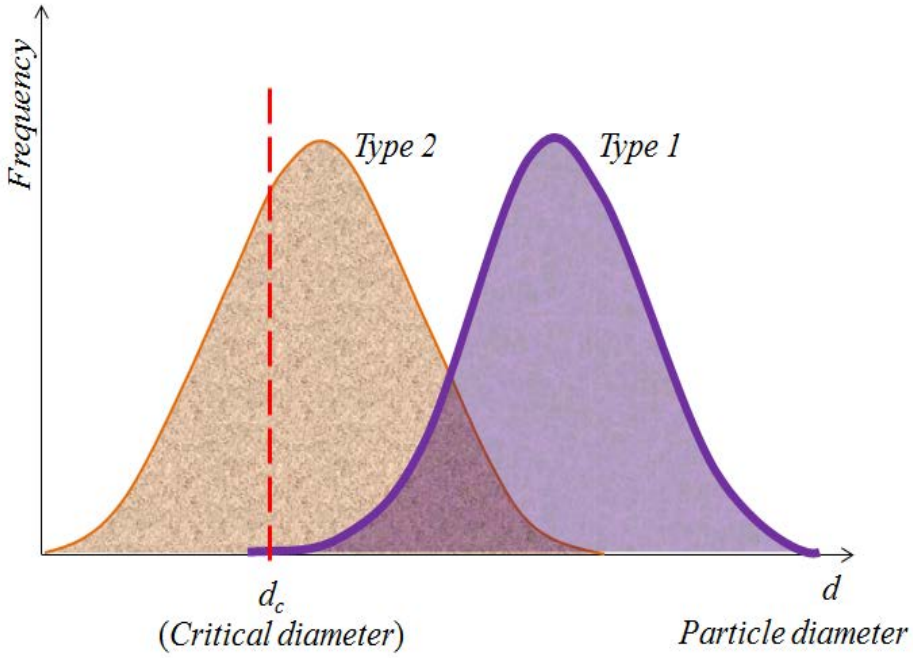

Figure 4. 8 Two types of the size distribution for the innovated models

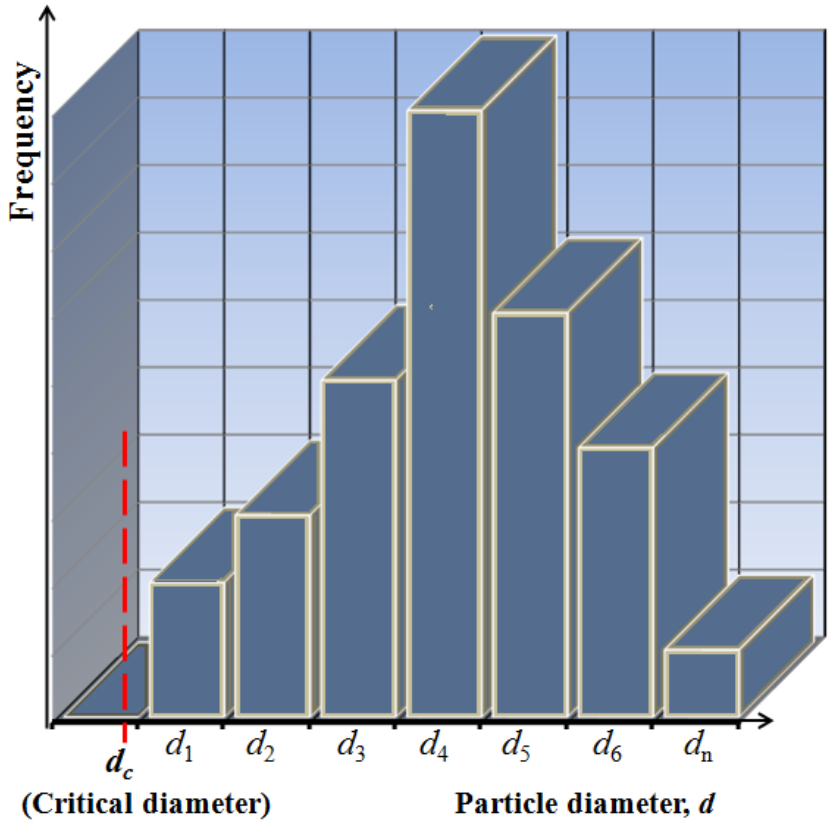

Figure 4. 9 Typical sieve analysis of type-1 solids distribution

Akita University

If the solids consist of two different-sized coarse particles of d_1 and d_2, concentration profiles and flow behaviour models can be schematically represented by Figures 4.10 and 4.11 respectively. Supposing that each solid flow does not hinder the other, the hydraulic gradient of the slurry i, as shown in Figure 4.11 is given as the sum of all the components, as follows:

$$i = i_w + i_{s1} + i_{s2} \qquad \text{.....(4.15)}$$

where i_w is the hydraulic gradient consumed for the flow of water flowing alone at the same velocity as slurry. The values of i_{s1} and i_{s2} due to the coarse solids can be calculated by using the single-size-settling slurry model of Seitshiro et al. [8]

Akita University

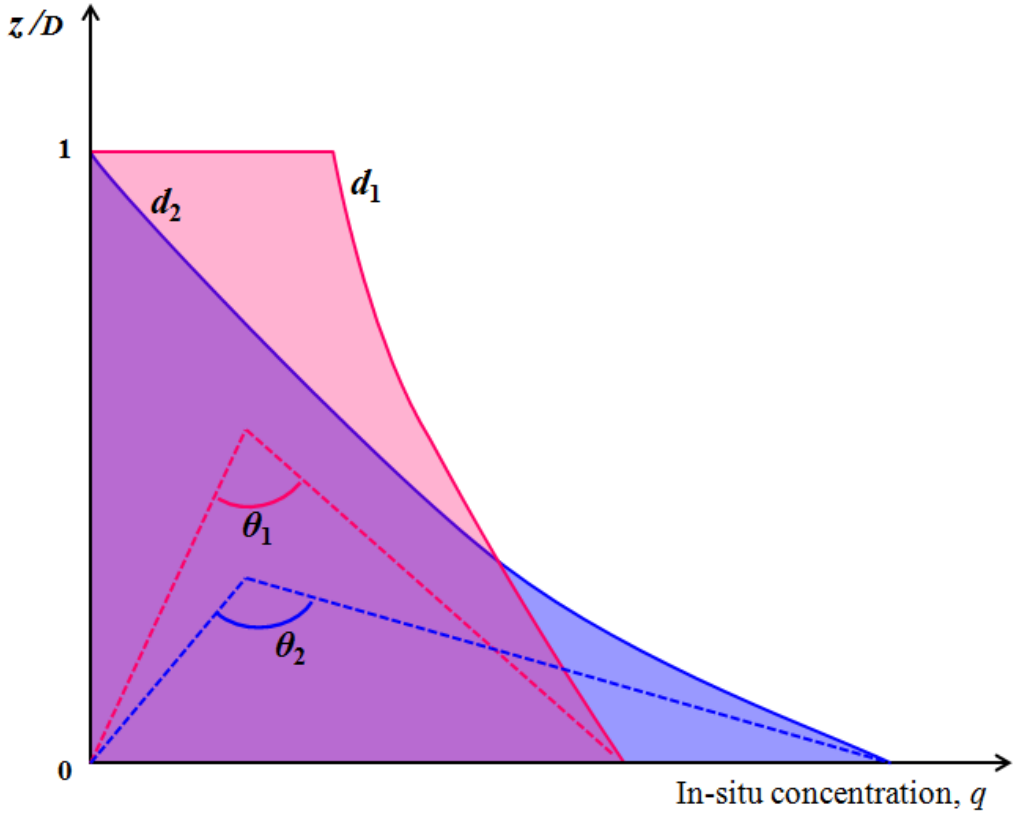

Figure 4.10 Representative in-situ concentration profiles of coarse-coarse particles slurry containing two different sizes of solids

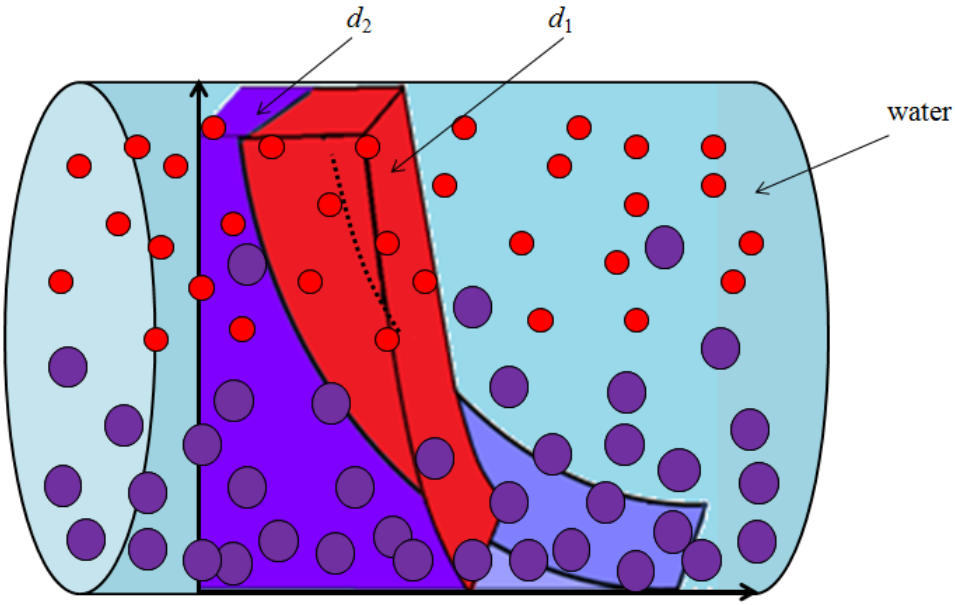

Figure 4.11 Schematic flow behaviour of coarse-coarse slurry containing two different sizes of solids

Akita University

Figure 4.12 shows the i-V_m relationships of the experimental data of single size slurries of sand and bakelite. For analysing the data approximately, the $\varphi-\psi$ relationships can be calculated as aforementioned in Sect. 4.3.1.3 and compared with the Durand-Condolios correlation as shown in Figure 4.5. By using the least-square method, a linear curve can be drawn in the range of the data to determine the values of K_D and n.

The calculated results show good agreement against the experimental data, as shown in Figures 4.13. As a result, a reasonable i-V_m relationships can be drawn as shown in Figure 4.14, which illustrates an application of the coarse-coarse model to the slurry as represented by Eq. (4.15).

Akita University

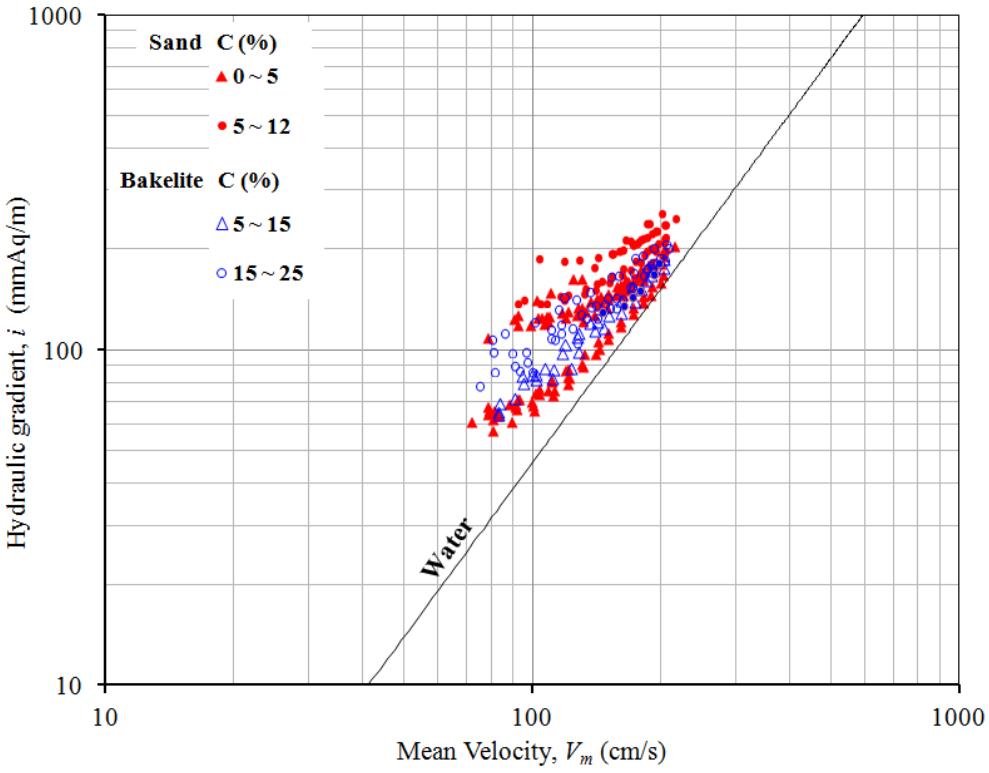

Figure 4.12 ***i*-V_m relationships of the experimental data of single size slurries of sand and bakelite**

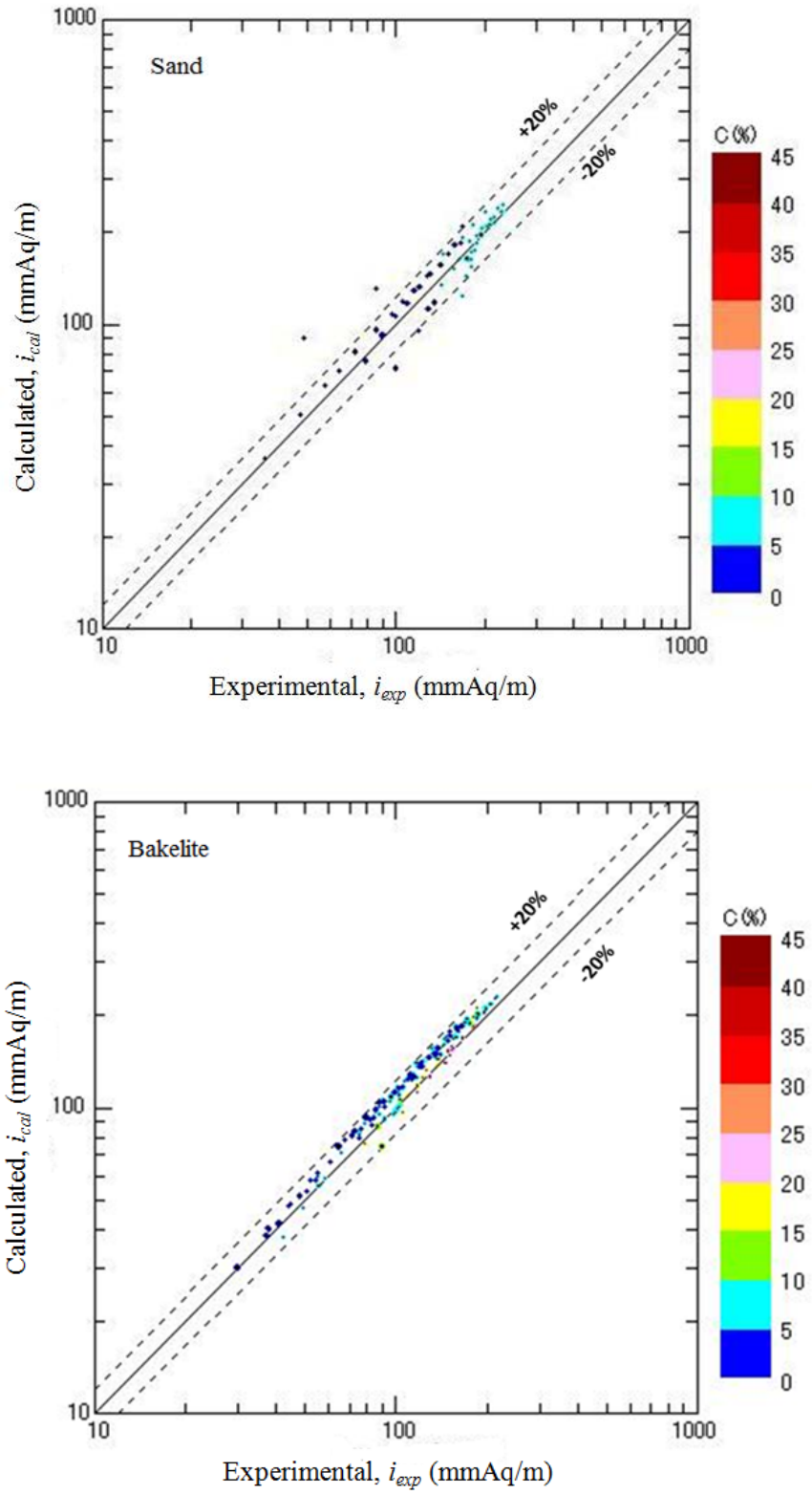

Figure 4.13 Analytical results based on the single size settling slurry model with sand and bakelite experimental data

Akita University

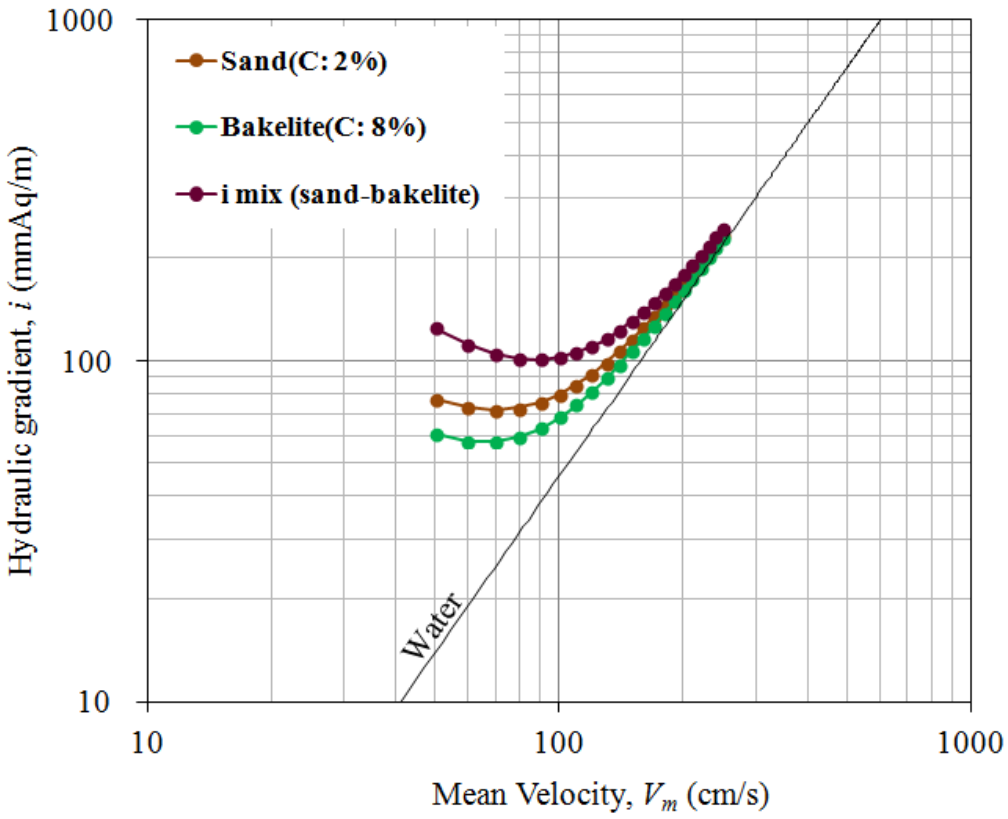

Figure 4.14 ***i*-V_m relationships from the summarised data of the laboratory (delivered concentration of sand and bakelite: 2 %, 8 %)**

Akita University

Figure 4.15 shows analytical results against experimental data of sand-bakelite slurry flow. Most of the data are in good agreement with the predicted within ±20 % accuracy.

Akita University

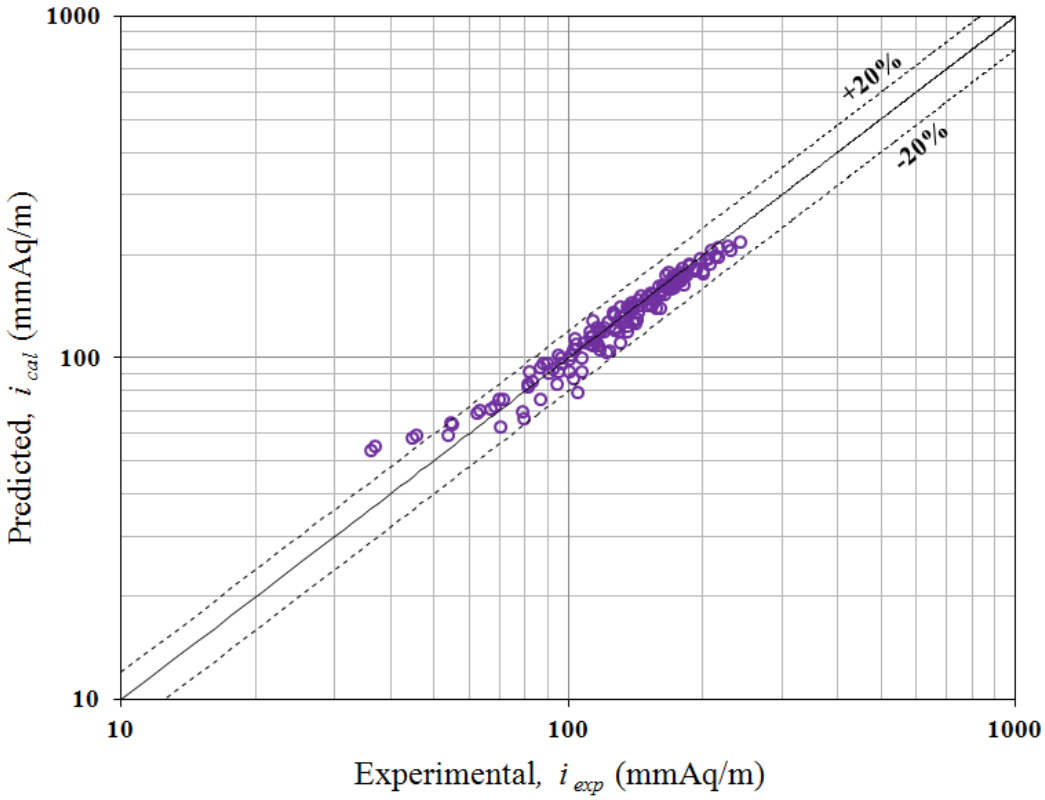

Figure 4.15 Experiment data of sand-bakelite mixed slurry against the predicted based on the coarse-coarse model

Akita University

4.4.2 Coarse-fine particles slurry model

According to the USDA soil textural classification system, fine sand should be separated from coarser solids of sizes larger than 0.25 mm [21]. If the slurry contains large volume of fine solids of diameter smaller than d_c (= 0.25 mm), as shown in Figure 4.16, the physical characteristics of the vehicle as a carrier fluid could be altered. The behaviour of the modified vehicle can be characterised as a Newtonian flow of values ρ_{sl} and μ_{sl}, which can be estimated by Eqs. (4.4) and (4.6). Therefore, it can be presumed that the modified vehicle transports the coarse solids of arbitrarily selected size of d_a in the coarse-fine slurry flow, as illustrated in Figure 4.17. The hydraulic gradient of the slurry i is represented by:

$$i = i_v + i_s \qquad \text{.....(4.16)}$$

where hydraulic gradients i_v for modified vehicle and i_s for all coarse solid portions, represented by Eq. (4.14), are estimated by using the modified Darcy-Weisbach equation and settling slurry model [8] respectively.

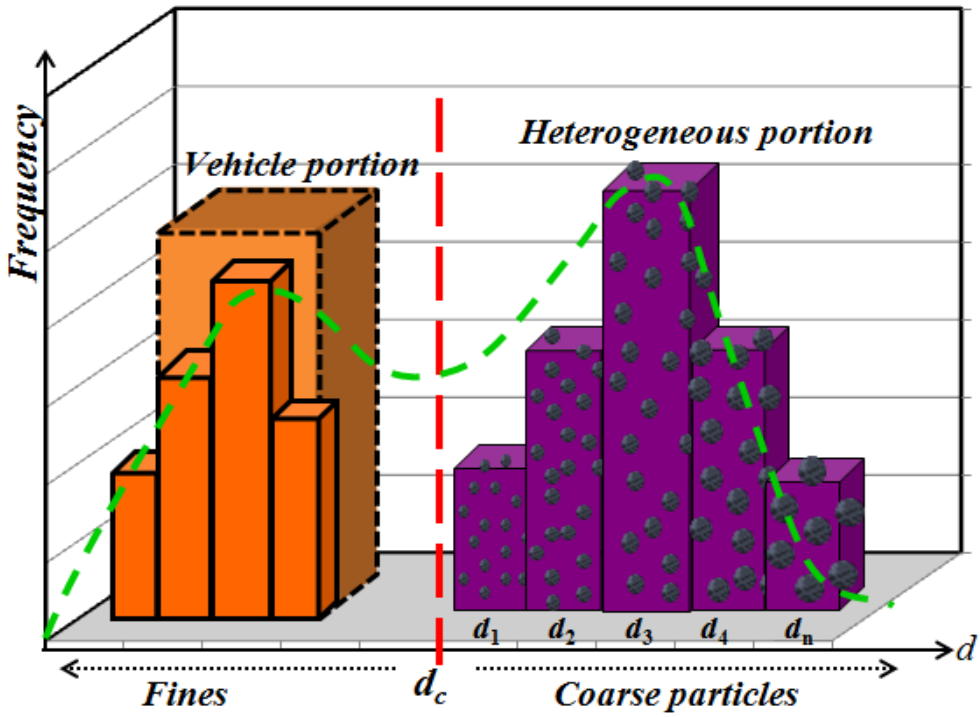

Figure 4.16 Typical sieve analysis of type-2 solids distribution

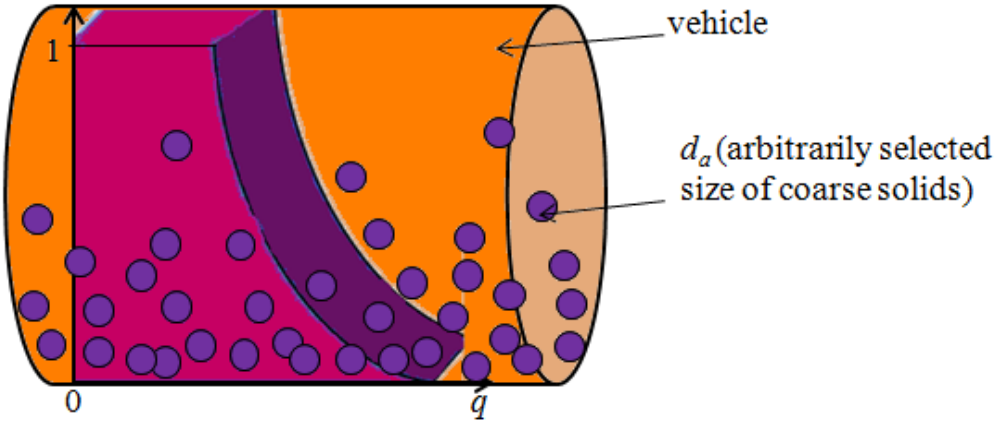

Figure 4.17 The schematic flow behaviour of coarse-fine slurry

Akita University

4.5 Verification of the models with experimental data

4.5.1 The Wasp method

Figure 4.18 shows the comparison of calculated hydraulic gradients i_{cal} with the Wasp method against the experimentals i_{exp} of sand-bakelite mixed slurries in this study, and of Boothroyde et al. and Shook et al. As concentration increases, the data tend to deviate from the predicted values. As a result, it can be confirmed that the application of the Wasp method could be restricted to the range of lower concentrations of slurry, as pointed by Kaushal et al. [7]

4.5.2 The Innovated models

Application of the single size model with average diameter d_m to the wide range-size distribution data of Shook et al. leads to large scatter, as shown in Figure 4.19. However, the analysis of the same data based on the innovated analytical models discussed in Sect. 4.4 results in improved agreement, as shown in Figure 4.20 against five different particle size distributions; 50-50 mixture to Mixture 4, although some data are overestimated from the ±20 % accuracy limit. It can be assumed that the deviation is related with the unstable flow at low velocities reported by Shook et al., as illustrated graphically in Figure 4.21. Figure 4.22 shows the analytical results limited to stable regions according to the records of Shook et al.

Akita University

To verify the scale-up of the models, Boothroyde et al. data of large size diameter and long pipeline was used. Figure 4.23 shows the analytical results in a good agreement with the experimental data.

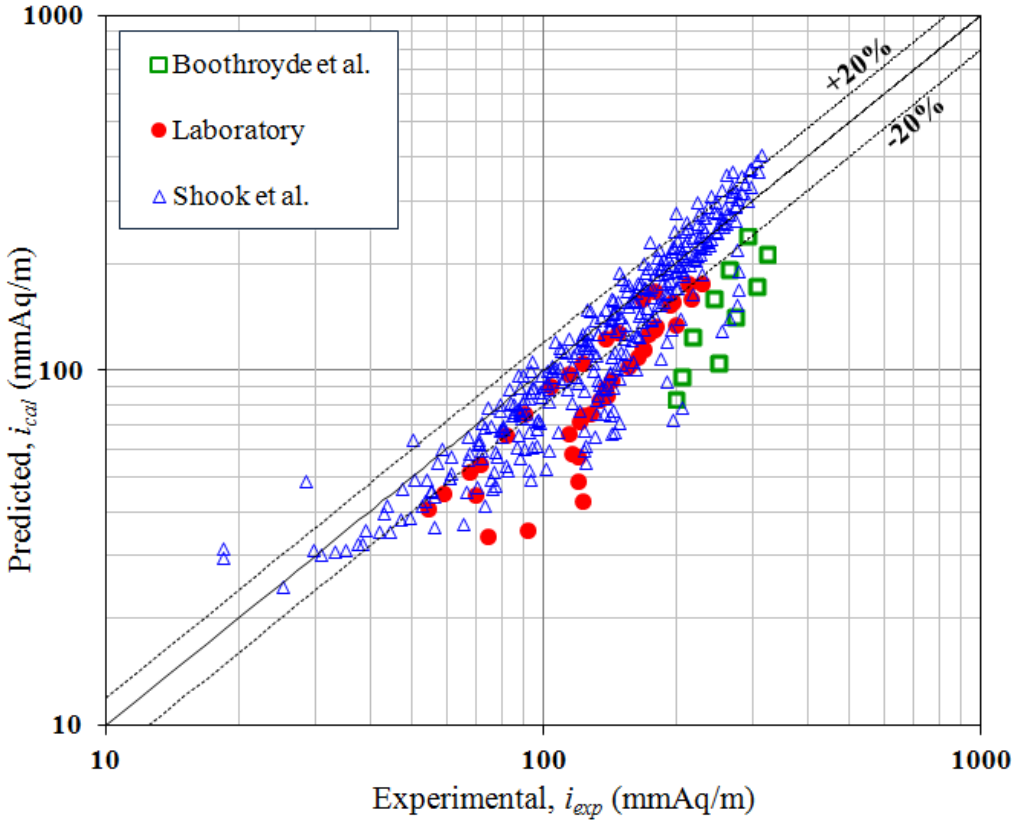

Figure 4.18 Predicted results of *i* against the experimental data of the laboratory, Boothroyde et al. and Shook et al. by using the Wasp method

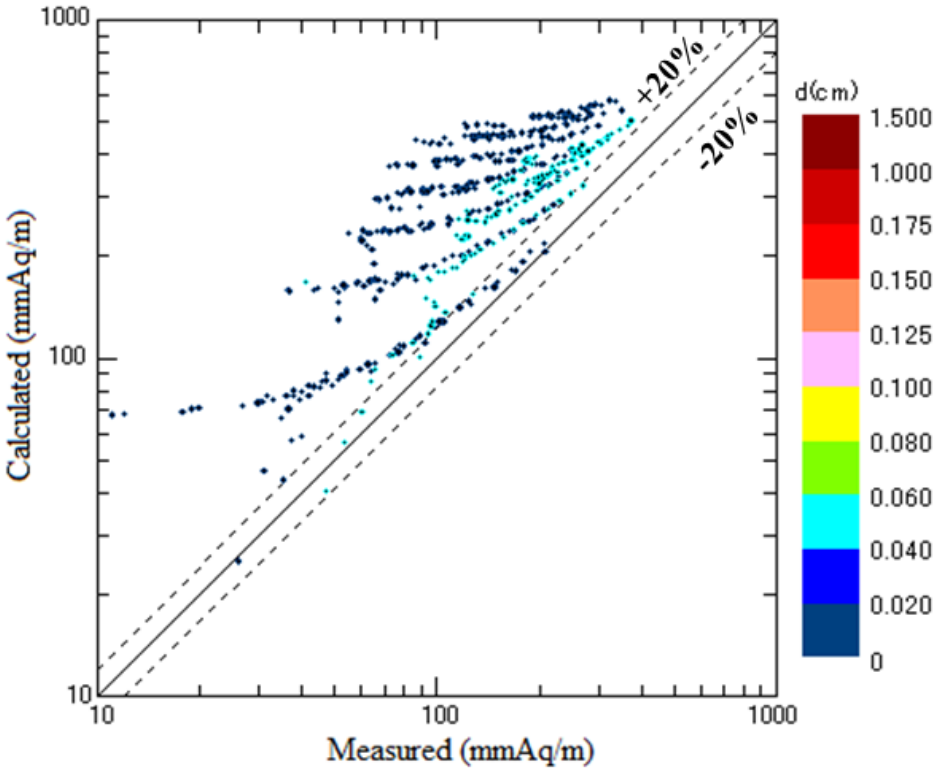

Figure 4.19 Analytical results of hydraulic gradient based on the single size settling slurry model with Shook et al. data

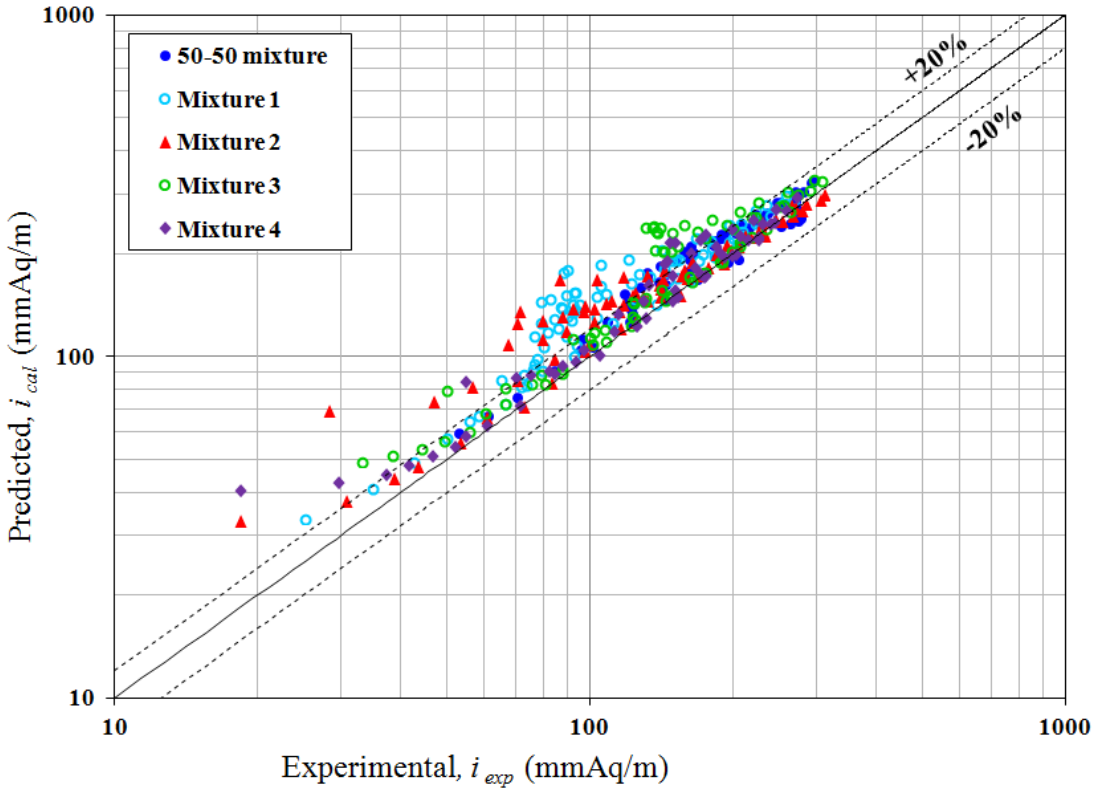

Figure 4.20 Predicted results of *i* against Shook et al. data by using the innovated models

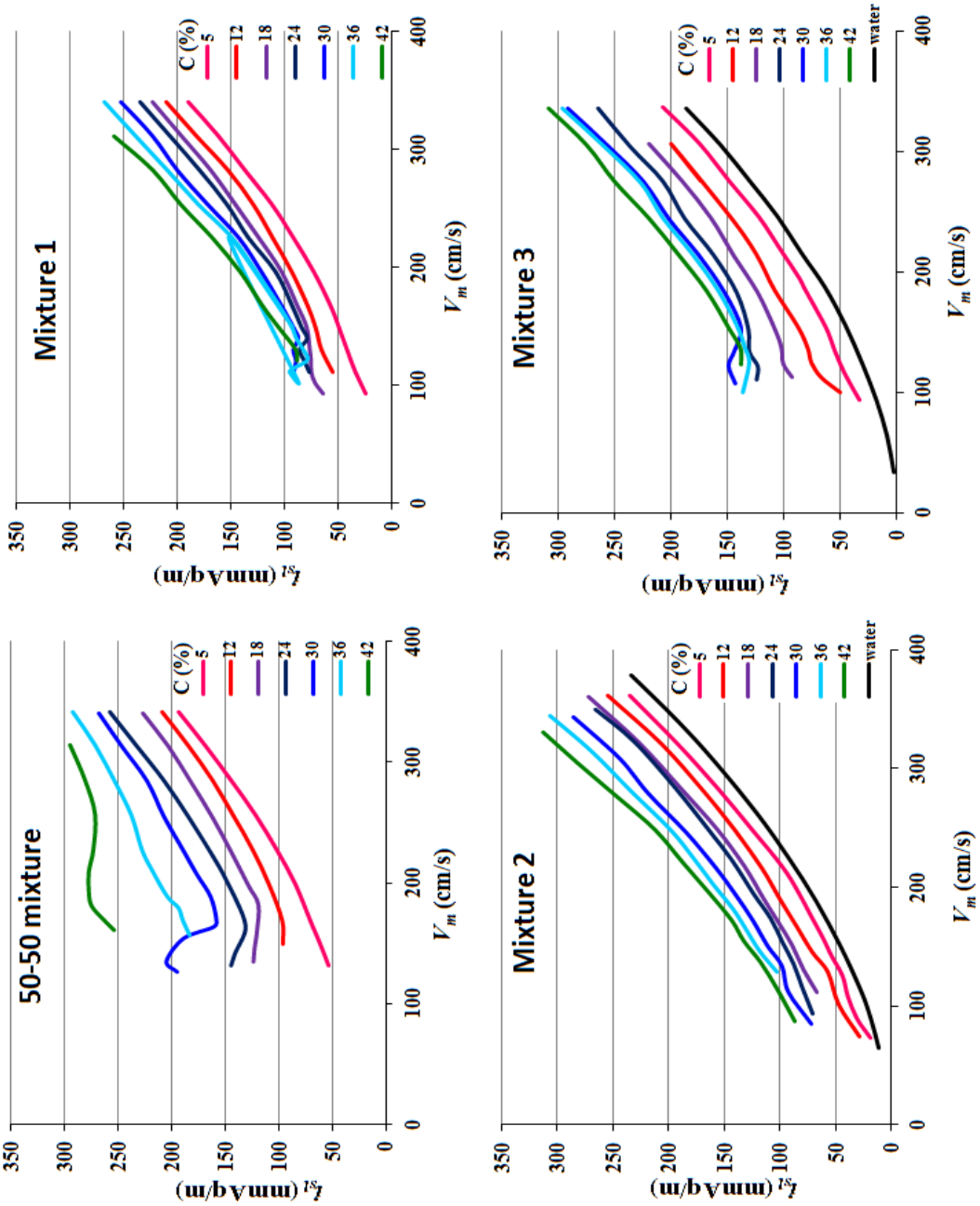

Figure 4.21 The graphic *i*-V_m relationships of Shook et al. data

Akita University

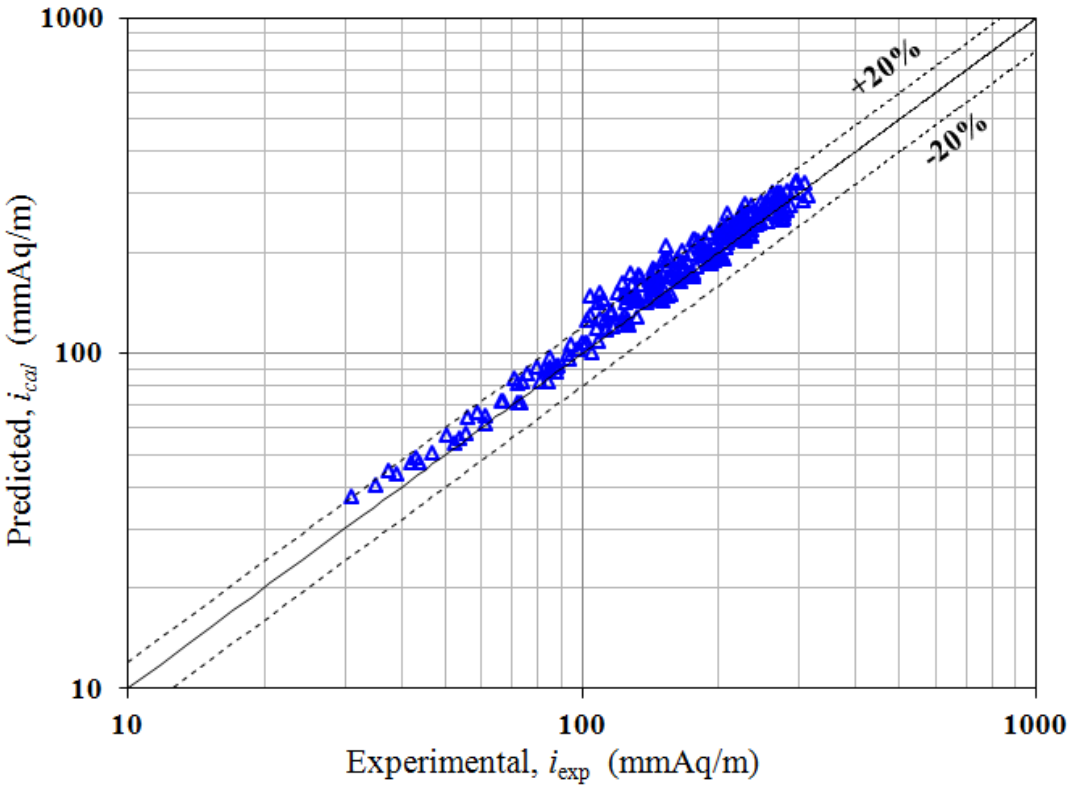

Figure 4.22 Predicted results of *i* against Shook et al. data in the stable regions

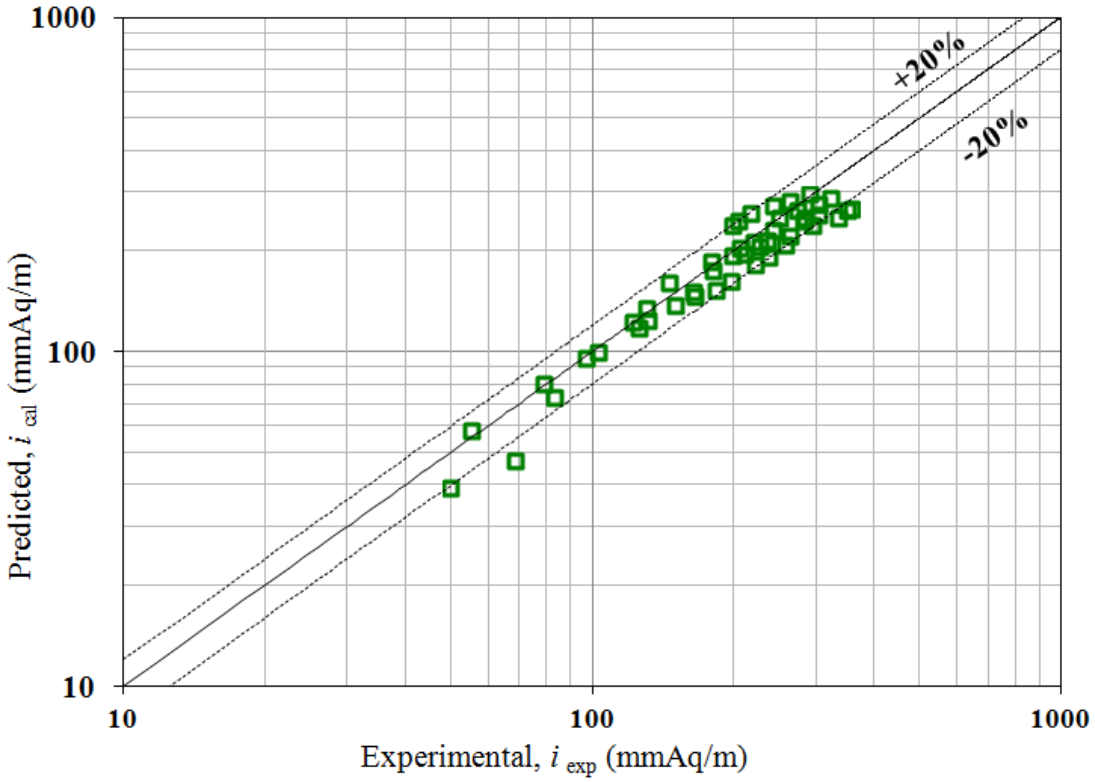

Figure 4.23 Predicted results of *i* against the large-scale data of Boothroyde et al. by using the innovated models

Akita University

4.6 Conclusions

In this chapter, conclusions are summarised briefly as follows:

1) The analysis of single size and mixed-sized data with the Condolios-Chapus method results in large deviations from the Durand-Condolios correlation.
2) The Wasp method can only be applied to slurry flows in the range of low concentrations.
3) Two types of analytical models for mixed-sized slurry, depending on the size distribution of solids, were developed for practical pipeline design.
4) The application of the settling slurry model with average diameter of solids to the multi-sized slurry flows leads to the greater scatter in hydraulic gradient.
5) The mixed-sized experimental data of sand slurries shows the applicability of the models in the stable regions.
6) The scale-up of the innovated models was confirmed with data of granite-Markham fines from prototype systems and sand-bakelite mixed slurries.
7) The innovated slurry models proved to satisfy the accuracy of ±20 % relative error.

Akita University

4.7 References

[1] Kao, D. T. Y. and Hwang, A. L. Y.: Determination of Particle Settling Velocity in Heterogeneous Suspensions and its Effects on Energy Loss Prediction in Solid-Liquid Freight Pipelines, *J. of Powder and Bulk Solids Technology*, **4**, No. 1, 31–40, (1980).

[2] Kazanskij, I.: Scale-up Effects in Hydraulic Transport Theory and Practice, Hydrotransport 5, 5th Int. Conf. on the Hydraulic Transport of Solids in Pipes, Paper B3, 47–79, (1978).

[3] Moro, T.: Pressure Losses in Slurry Transport (Two-phase Flow), Proc. Symp. Multiphase Flow, 209–232, (1982).

[4] STSJ (Slurry Transport Society of Japan): The Sub-Committee Report on Flow Behaviour of Fine-Coarse Mixed Slurries in Pipes (in Japanese), (1983).

[5] Wasp, E.J., Kenny, J.P., and Gandhi, R.L.: Solid-Liquid Flow, Slurry Pipeline Transportation, Trans. Tech. Publications, Germany, pp. 93–94, (1977).

[6] Liu, H.: Pipeline Engineering, Lewis Publishers, USA, pp. 131–143, (2003).

[7] Kaushal, D. R. and Tomita, Y.: Solids Concentrations Profiles and Pressure Drops in Pipeline Flow of Multisized Particulate Slurries, *Int. J. Multiphase Flow.*, **28**, 1697–1717, (2002).

Akita University

[8] Seitshiro, I., Sato, I., and Sato, H.: Verification and Application of Design Model for Settling Slurry Transport in Pipes, *Int. J. Soc. Mater. Eng. Resour.*, **18**, No. 2, 44–50, (2012).

[9] Seitshiro, I., Fujii, S., Yokoyama, N., Sato, I., and Sato, H.: Data Analysis of Mixed-sized Flows in Pipes with Innovated Models, Proc. MMIJ Fall Meeting, 161–162, (2012).

[10] Shook, C. A., Schriek, W., Smith, L. G., Haas, D. B., and Husband, W. H. W.: Experimental Studies on the Transport of Sands in Liquids of Varying Properties in 2 and 4 inch Pipelines, Saskatchewan Research Council, **VI**, 1–158, (1973).

[11] Boothroyde, J., Jacobs, B. E. A., and Jenkins, P.: Coarse Particle Hydraulic Transport, Hydrotransport 6, 6th Int. Conf. on the Hydraulic Transport of Solids in Pipes, 405–428, (1979).

[12] Wasp, E. J., Regan, T. J., Withers, J., Cook, P. A. C., and Clancey, J. T.: Cross Country Coal Pipeline, Texas Eastern Transmission Corp, Shreveport, La., Pipeline News, **35**, 20–28, (1963).

[13] O'Brien, M. P.: Review of the Theory of Turbulent Flow and its Relation to Sediment-Transportation, Trans. Am. Geophysical Union, **14**, 487–491, (1933).

[14] Sato, H., Otsuka, K., and Cui, Y.: A Model for the Settling Slurry Flow with a Stationary Bed in a Pipe, Proc. 4th Int. Symp. in Liquid-Solid Flows, Portland, Oregon, **FED-118**, 53–63, (1991).

Akita University

[15] Darby, R: Hydrodynamics of Slurries and Suspensions, Encyclopaedia of Fluid Mechanics, **5**, Slurry Flow Technology, Gulf Publishing Company, USA, p. 53, (1986).

[16] Abulnaga, B.: Slurry Systems Handbook, McGraw-Hill Publishing, USA, pp. 2.9–2.18, (2002).

[17] Krieger, I. M.: Rheology of Monodisperse Latices, *J. Advanc. Colloid Interface Sci.*, **3**, 111–136, (1972).

[18] Thomas, D. G.: Transport Characteristics of Suspension; Part VII-A Note on the Viscosity of Newtonian Suspensions of Uniform Spherical Particles, *J. of Colloid Science.*, **20**, 267–277, (1965).

[19] Abulnaga, B.: pp. 1.21–1.22 from previously cited Ref. [16]

[20] Condolios, E. and Chapus, E. E.: Designing Solids-Handling Pipelines, Solids Pipelines 2, *J. Chemical Eng.*, 131–138, (1963).

[21] United States Department of Agriculture: USDA Textural Classification, Soil Mechanics Study Guide, pp. 5–7, (1987).

Akita University

CHAPTER 5

Conclusions and Further Research

With continued research projects, the conclusions and recommendations of this study can be summarised as follows.

5.1 Conclusions

Reviewing reported papers in chapter 1, this study was progressed to develop analytical models for not only settling slurry flow but also mixed-sized slurry flows. After discussion of the theoretical analyses with slurry flow database, the following conclusions were reached.

Extensive experimental data was useful to confirm the limits of application of correlations for slurry design. However, it should be noted that availability of reliable data has been limited because of lack of some transport conditions, such as pipe friction factor, and so on. In chapter 2, over three thousand data was successfully accumulated from different researchers for the development of a database program. The database program could be also beneficial in editing and storing different kinds of experimental data.

Due to diverse transport conditions of the researchers, it was essential to standardise the units of measurements. Graphical representation was also applied to analyse and compare correlations. The

Akita University

data was also typified by using star graphs, which clearly categorised researchers' transport conditions.

The object of chapter 3 was to develop the settling slurry model of single size flows in horizontal pipes. The applicability of the model was verified by using the Slurry Flow Database developed by Seitshiro et al., and the design procedure for the optimum operation condition was clarified.

Although the settling slurry model produced large scattering when compared to wide-range data, the introduction of the general particles Reynolds number Re_p* resulted in improved agreement. Specific energy consumption was vital to determine the most favourable conditions of transport.

In chapter 4, the innovated models for mixed-sized slurry flow were discussed. The models which depend on particle size distributions, were developed based on the single size slurry model. Furthermore, other reported methods for evaluating hydraulic gradient were discussed.

Even though the Wasp method has been used for estimating hydraulic gradient of mixed-sized slurries, it was shown that good results could be attained only in lower concentrations. The two innovated models in this study were satisfactorily proved to be indispensable for the design of slurry pipeline systems, with verification of experimental data in prototype systems. The innovated models could

Akita University

be also applied to evaluate critical deposit velocity, which can be helpful for determining the optimal transport conditions.

5.2 Remarks on application of the innovated models to pipeline design

Hydraulic gradient i is one of the important parameters used in the design of slurry pipelines. The fundamental concept of pipeline design is to evaluate the relationship between i and mean velocity V_m for specific transport conditions. Based on the relationship, the optimum transport velocity could be calculated.

By using the predicted values of hydraulic gradient or pressure drop of transport line, the required energy for conveying slurry can be determined; it could be essential to select the pump size, pipe material and thickness, valves, and so on. More concrete details of the procedure for the design will be discussed at the Seventh International Conference on Materials Engineering for Resources, ICMR 2013 AKITA, held on November 20-22, 2013, in Akita, Japan.

Akita University

ACKNOWLEDGEMENTS

It is with great pleasure that I express my sincerest gratitude to Professor Hiroshi Sato for his continued guidance throughout my research. In my pursuit of career diversification, the Professor provided me an opportunity to study in his Slurry Transport Technology Laboratory. His vision in my potential, continuous faith in my capabilities, and the words, ‘‘Your success depends on your effort’’, have kept me motivated for the past four years. Moreover, I am grateful for his support with not only my academic but also campus life.

I wish to thank Professor Fumio Sugimoto of the Rock Mechanics Laboratory, Professor Takaho Otomo of the Water Resources and Environmental Engineering Laboratory, and Professor Masahide Nakamura of Fluid Mechanics Laboratory, Akita University, who reviewed and provided useful comments for improving my thesis.

I wish to extend my appreciation to the fellow students of the Slurry Transport Technology Laboratory from 2009 to 2013 for supporting my work. Many thanks go to Mr. Isamu Sato, Engineering Staff, whose technical abilities helped me immensely in my research.

My greatest gratitude goes to Professor Noboru Yoshimura, President of Akita University, and Professor Nobuaki Ogawa, Dean of the Faculty of Engineering and Resource Science, for affording me the opportunity to study in Akita.

Akita University

Last, I would like to thank my family for believing in me and for their continuous encouragement and support throughout my stay in Japan.